Identification and characterization of the novel mKSR1 phosphorylation site Tyr728 and its role in MAPK signaling

Dissertation zur Erlangung des naturwissenschaftlichen Doktorgrades

der Julius-Maximilians-Universität Würzburg (Fakultät für Biologie)

vorgelegt von

Claudia Sibilski

geboren in Rudolstadt (Deutschland)

Würzburg, 2014

Eingereicht am: _____

Mitglieder der Promotionskommission:

Vorsitzender: Prof. Dr. Markus Engstler

1. Gutachter: Prof. Dr. Thomas Rudel

2. Gutachter: Prof. Dr. Antje Gohla

Tag des Promotionskolloquiums: _____

Doktorurkunde ausgehändigt am: _____

I dedicate this thesis to my lovely parents.

Science knows no country,
because knowledge belongs to humanity,
and is the torch which illuminates the world.

Science is the highest personification of the nation
because that nation will remain the first
which carries the furthest the works of thought and intelligence.

LOUIS PASTEUR

TABLE OF CONTENTS

1 SUMMARY

In mammals, KSR1 functions as an essential scaffold that coordinates the assembly of RAF/MEK/ERK complexes and regulates intracellular signal transduction upon extracellular stimulation. Aberrant activation of the equivalent MAPK signaling pathway has been implicated in multiple human cancers and some developmental disorders. The mechanism of KSR1 regulation is highly complex and involves several phosphorylation/dephosphorylation steps. In the present study, a number of novel *in vivo* phosphorylation sites were detected in mKSR1 by use of mass spectrometry analysis. Among others, Tyr728 was identified as a unique regulatory residue phosphorylated by LCK, a Src kinase family member. To understand how phosphorylation of Tyr728 may regulate the function of KSR1 in signal transduction and cellular processes, structural modeling and biochemical studies were integrated in this work.

Computational modeling of the mKSR1(KD) protein structure revealed strong hydrogen bonding between phospho-Tyr728 and the residues surrounding Arg649. Remarkably, this pattern was altered when Tyr728 was non-phosphorylated or substituted. As confirmed by biochemical analysis, Arg649 may serve as a major anchor point for phospho-Tyr728 in order to stabilize internal structures of KSR1. In line with the protein modeling results, mutational studies revealed that substitution of Tyr728 by phenylalanine leads to a less compact interaction between KSR1 and MEK, a facilitated KSR1/B-RAF binding and an increased phosphorylation of MEK in complex with KSR1. From these findings it can be concluded that phospho-Tyr728 is involved in tightening the KSR1/MEK interaction interface and in regulating the phosphorylation of KSR1-bound MEK by either RAF or KSR1 kinases.

Beside the Tyr728, Ser722 was identified as a novel regulatory phosphorylation site. Amino acid exchanges at the relevant position demonstrated that Ser722 regulates KSR1-bound MEK phosphorylation without affecting KSR1/MEK binding *per se*. Due to its localization, Ser722 might consequently control the catalytic activity of KSR1 by interfering with the access of substrate (possibly MEK) to the active site of KSR1 kinase. Together with Ser722, phosphorylated Tyr728 may further positively affect the kinase activity of KSR1 as a consequence of its vicinity to the activation and catalytic loop in the KSR1(KD). As revealed by structural modeling, phospho-Tyr728 builds a hydrogen bond with the highly conserved Lys685.

Consequently, phospho-Tyr728 has a stabilizing effect on internal structures involved in the catalytic reaction and possibly enhances the phosphate transfer within the catalytic cleft in KSR1. Considering these facts, it seems very likely that the LCK-dependent phosphorylation of Tyr728 plays a crucial role in the regulation of KSR1 catalytic activity.

Results of fractionation and morphology analyses revealed that KSR1 recruits LCK to cytoskeleton for its phosphorylation at Tyr728 suggesting that this residue may regulate cytoskeleton dynamics and, consequently, cell motility. Beside that, phosphorylation of Tyr728 is involved in the regulation of cell proliferation, as shown by a significantly reduced population doubling time of KSR1-Y728F cells compared to cells expressing wild type KSR1.

Taken together, tyrosine phosphorylation in KSR1 uncovers a new link between Src family kinases and MAPK signaling. Tyr728, the novel regulatory phosphorylation site in murine KSR1, may coordinate the transition between the scaffolding and the catalytic function of KSR1 serving as a control point used to fine-tune cellular responses.

2 ZUSAMMENFASSUNG

KSR1 fungiert bei Säugetieren als zentrales Gerüstprotein, welches die Anordnung von RAF/MEK/ERK-Komplexen koordiniert und die intrazelluläre Signalweiterleitung nach extrazellulärer Stimulation reguliert. Eine abweichende Aktivierung des entsprechenden MAPK-Signalwegs wurde mit vielen humanen Krebsformen und einigen Entwicklungsstörungen in Verbindung gebracht. Der Mechanismus der KSR1-Regulierung ist hochgradig komplex und involviert mehrfach Schritte der Phosphorylierung/Dephosphorylierung. In der vorliegenden Studie wurden etliche neue *in-vivo*-Phosphorylierungsstellen in mKSR1 mittels massenspektrometrischer Analyse entdeckt. Neben anderen wurde Tyr728 als besonderer regulatorischer Rest identifiziert, welcher durch LCK, einem Mitglied der Src-Kinase-Familie, phosphoryliert wird. Um zu verstehen wie die Phosphorylierung von Tyr728 die Funktion von KSR1 innerhalb der Signalweiterleitung und zellulärer Prozesse regulieren könnte, wurden strukturelle Modellierungen und biochemische Untersuchungen in diese Arbeit integriert.

Die Computermodellierung der mKSR1(KD)-Proteinstruktur zeigte starke Wasserstoff-brückenbindungen zwischen Phospho-Tyr728 und den Resten in der Umgebung von Arg649 auf. Dieses Muster war auffällig verändert, wenn Tyr728 nicht phosphoryliert oder substituiert war. Wie anhand biochemischer Analyse untermauert wurde, könnte Arg649 für phospho-Tyr728 als Hauptankerpunkt dienen, um interne Strukturen in KSR1 zu stabilisieren. In Übereinstimmung mit den Ergebnissen der Proteinmodellierung enthüllten die Mutationsstudien, dass die Substitution von Tyr728 mit Phenylalanin zu einer weniger kompakten Interaktion zwischen KSR1 und MEK, einer erleichterten KSR1/B-RAF-Bindung und einer ansteigenden Phosphorylierung von MEK im Komplex mit KSR1 führt. Anhand dieser Erkenntnisse kann man rückschließen, dass Phospho-Tyr728 in die Verstärkung der Interaktionen innerhalb der KSR1/MEK-Grenzfläche und in die Regulierung der Phosphorylierung von KSR1-gebundenem MEK durch entweder RAF- oder KSR1-Kinasen involviert ist.

Neben Tyr728 wurde Ser722 als eine neuartige regulatorische Phosphorylierungsstelle identifiziert. Aminosäureaustausche an der betreffenden Position demonstrierten, dass Ser722 die Phosphorylierung von KSR1-gebundenem MEK reguliert ohne die KSR1/MEK-Bindung selbst zu beeinträchtigen. Bedingt durch seine Lokalisierung könnte Ser722 folglich die katalytische

Aktivität von KSR1 kontrollieren, indem es den Zugang des Substrates (möglicherweise MEK) zur aktiven Seite der KSR1-Kinase behindert. Zusammen mit Ser722 könnte phosphoryliertes Tyr728 ferner die Kinaseaktivität von KSR1 positiv beeinflussen, infolge von dessen Nähe zur Aktivierungs- und katalytischen Schleife in der KSR1(KD). Wie mittels Strukturmodellierung offengelegt wurde, bildet Phospho-Tyr728 eine Wasserstoffbrücke mit dem hochgradig konservierten Lys685 aus. Folglich hat Phospho-Tyr728 einen stabilisierenden Effekt auf interne Strukturen, welche in die katalytische Reaktion involviert sind, und erleichtert möglicherweise den Phosphattransfer innerhalb der katalytischen Spalte in KSR1. In Anbetracht dieser Fakten scheint es sehr wahrscheinlich, dass die LCK-abhängige Phosphorylierung von Tyr728 eine äußerst wichtige Rolle in der Regulierung der katalytischen Aktivität von KSR1 spielt.

Die Ergebnisse der Fraktionierungs- und Morphologieanalysen enthüllten, dass KSR1 für die Phosphorylierung an Tyr728 LCK zum Zytoskelett rekrutiert, was darauf hindeutet, dass dieser Rest die Dynamik des Zytoskeletts und folglich Zellmotilität regulieren könnte. Darüber hinaus ist die Phosphorylierung von Tyr728 in die Regulierung der Zellproliferation involviert, wie anhand einer bedeutend reduzierten Populationsverdopplungszeit von KSR1-Y728F-Zellen im Vergleich zu Zellen, welche wildtypisches KSR1 exprimieren, gezeigt wurde.

Zusammenfassend lässt sich sagen, dass die Tyrosin-Phosphorylierung in KSR1 eine neue Verknüpfung zwischen Kinasen der Src-Familie und der MAPK-Signalwirkung enthüllt. Tyr728, die neuartige regulatorische Phosphorylierungsstelle in Maus-KSR1, könnte den Übergang zwischen der Gerüst- und der katalytischen Funktion von KSR1 koordinieren und damit als Kontrollpunkt dienen, um zelluläre Reaktionen fein abzustimmen.

3 INTRODUCTION

3.1 Certain disorders of cellular processes lead to cancer development

Cells are the smallest unity of all living organisms or rather the base unit of life. In multi-cellular systems, they form networks and communicate with each other via various stimuli like growth factors, mitogens, cytokines, and hormones in order to induce response-regulated cell fate. Upon binding of such a small molecule to the extracellular part of the appropriate receptor incorporated into the plasma membrane of the cell, the signal is transferred to the cytoplasmic site of the membrane. The interconnection of numerous proteins, involved in the signal transmission, amplifies the initial signal to a complex cellular process. Although these mechanisms are highly controlled, disorders occasionally occur and result in a variety of diseases including brain injury, cardiac hypertrophy, diabetes, inflammation, and cancer (1–6). Dynamic changes in the genome – translating proteins that are involved in multistep cell division or proliferative events – have the potential to cause cancer in two different ways: in form of oncogenes gaining of function or tumor suppressors loosing their function. The classical hallmarks of cancer comprise six biological capabilities acquired for tumorigenesis: self-sufficiency in growth signals, insensitivity to antigrowth signals, apoptosis evasion, unlimited replicative potential, sustained angiogenesis, and tissue invasion and metastasis (7). Of note, Hanahan and Weinberg (8) themselves defined the next generation of cancer hallmarks. In addition to the six known ones, deregulation of cellular energetics and avoidance of immune destruction are emerging hallmarks. Moreover, the acquisition of different tumor types is enabled by two characteristics: tumor-promoting inflammation as well as genome instability and mutation. Actually, one in four humans dies due to cancer highlighting this disease as the second most common cause of death. For affecting the development of uncontrolled cell fate, we have to learn more about and understand better the regular signaling situation.

3.2 Protein phosphorylation by kinases – an indispensable event for intracellular signal transduction

Regulation of cellular behavior in response to extracellular stimuli requires dynamic intracellular changes, which are effectively mediated by post-translational protein modifications. Phosphorylation and dephosphorylation are the most common post-translational modifications used for signal transduction that take a pivotal role in almost every issue of cell biology (9). Enzyme activity, cellular localization, and protein degradation are processes highly controlled by this interplay. For substrate recognition, consensus sequences surrounding the regulatory site are required and peripheral interaction motifs are occasionally needed to guarantee substrate specificity.

Phosphorylation, which represents the most intensely studied post-translational modification, is mediated by protein kinases. In humans, the protein kinase family is one of the largest gene families comprising 518 members, which are classified as serine/threonine kinases (385 members), tyrosine kinases (90 members), and tyrosine-kinase like proteins (43 members) (10). Kinases constitutionally catalyze the transfer of the γ-phosphate group from the embedded adenosine-5'-triphosphate (ATP) molecule onto a hydroxyl residue of their bound substrate. Thereby, protein alcohol groups (on serines and threonines) as well as protein phenolic groups (on tyrosines) serve as phosphate acceptors. In contrast, protein phosphatases catalyze dephosphorylation events by the highly regulated hydrolytic mechanism of removing the phosphate moiety from a protein substrate (11, 12). Hanks and Hunter (13) characterized the eukaryotic kinase superfamily and discovered three separate roles for the protein kinase domain in order to serve catalytic activity: *i)* binding and orientation of the ATP molecule in complex with a cation (usually magnesium), *ii)* binding and orientation of the substrate, and *iii)* transfer of the γ-phosphate from the ATP onto the substrate according to a common mechanism. Therefore, twelve smaller subdomains, which are defined as (highly) conserved regions with characteristic patterns, form the kinase domain structure. Moreover, twelve amino acids are (nearly) invariant throughout the superfamily, conserved in more than 95% of the kinases, and are essential for catalytic function. Protein kinase domains exhibit a two-lobed structure: a smaller N-terminal lobe (subdomains I-IV) adjusts anchoring and orientation of the ATP molecule and a larger C-terminal lobe (subdomains VIA-XI) coordinates substrate binding and initiates the

phosphotransfer reaction. A deep cleft between these two lobes specifies the site of catalysis. By neutralizing the negative charge of the γ-phosphate moiety, a highly conserved lysine in the catalytic loop of the kinase domain enhances the phosphotransfer. Thereby, a side chain stabilizes the magnesium ion and the catalytic loop that bridges the α- and γ-phosphates of the bound ATP molecule inside the protein core. Similarly, the highly conserved aspartate-phenylalanine-glycine (DFG) motif acts to stabilize the magnesium ion bridging the β- and γ-phosphates of the embedded ATP in order to orient the γ-phosphate group for subsequent phosphotransfer reaction.

Dependent on the function of the regulatory site, activation as well as inhibition of proteins is mediated by both phosphorylation and dephosphorylation. This interplay is fundamental in order to proceed signaling transduction within numerous pathways, like the MAPK cascade, regulating different types of cell behavior. Particularly with regard to the treatment of cancer, protein kinases represent efficient targets for drug development. Since the launch of a monoclonal anti-HER2 antibody (trastuzumab) in 1998, which is used for the treatment of mamma carcinoma, more than seventeen drugs in the form of kinase inhibitors and kinase-blocking antibodies were released for cancer therapy (14). In contrast, phosphatase-targeted drugs are currently used for immune suppression preventing rejection of transplanted organs as well as for therapy of autoimmune diseases, but not for the treatment of cancer.

3.3   RAF/MEK/ERK signaling cascade

One of the pathways being critical for cancer development is the MAPK signaling cascade due to its key role in the regulation of different cellular functions (15). Mitogen-activated protein kinases (MAPKs) are evolutionarily conserved in all eukaryotes (16–18). In mammals, they can be grouped into four classical families named after their MAPK tier component; ERK1/2 (extracellular signal-regulated kinases), JNK1-3 (Jun amino-terminal kinases), p38α-δ (SAPKs, stress-activated protein kinases), and ERK5 (also known as Big MAPK) link extracellular signals to the machinery, which controls fundamental cellular behavior (19). The stepwise signal transduction (sequential phosphorylation and activation of proteins) allows a fine-tune regulation of signal strength and duration on the one hand and amplifies simple signals to complex biological responses on the other hand.

The best studied mammalian MAPK signaling cascade is the RAF/MEK/ERK pathway (also named ERK1/2 cascade as described above) (for reviews see (20, 21)) (Fig. 1). It plays a remarkable role in the control of various cellular processes, such as proliferation, differentiation, development, motility, migration, and apoptosis. Deregulation of this pathway is observed in approximately one-third of all human cancers (21). The RAF/MEK/ERK signaling cascade is initiated by the interaction of small extracellular ligands with their respective cell surface receptors (e.g. receptor tyrosine kinases (RTKs) and G-protein-coupled receptors (GPCRs) as well as integrin/receptor binding) that terminates in the activation of RAF proteins – one of the major serine/threonine kinases of the pathway. Subsequently, with the focus on growth factor-regulated signaling, the intrinsic kinase function of RTKs induces autophosphorylation upon dimerization of their monomers. Sequences of phosphorylated tyrosines, located in the cytoplasmic domain, serve as docking site for the Src homology 2 (SH2) domain of adaptor proteins, like Grb2 (growth factor receptor-binding protein 2). Grb2 further contains two SH3 domains to bind constitutively to a proline-rich region of the guanine nucleotide exchange protein SOS (son of sevenless). Consequently, membrane-bound SOS catalyzes the GDP/GTP exchange in the small GTPase RAS resulting in its activation, which then translocates RAF to the plasma membrane. The initiated canonical MAPK module comprises three serine/threonine kinases: RAF (MAPK kinase kinase, MAPKKK or MAP3K) phosphorylates and activates MEK (MAPK kinase, MAPKK or MAP2K) that, in turn, activates ERK (MAPK) by phosphorylation (22–24).
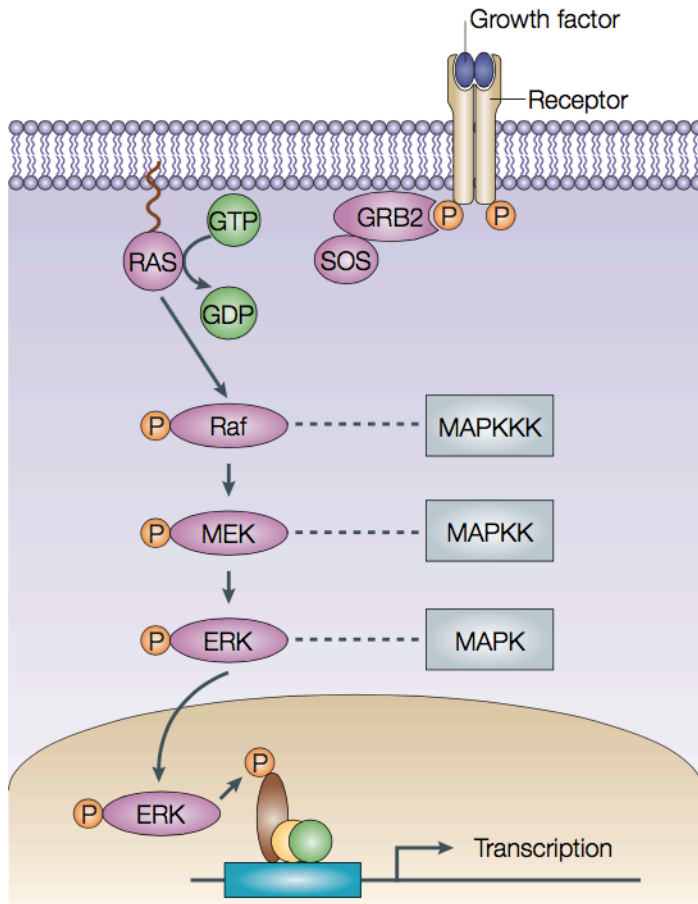
FIGURE 1: Signal transduction of the RAF/MEK/ERK cascade (25). Growth factor-induced receptor dimerization and intracellular tyrosine autophosphorylation initiate the recruitment of the adaptor protein Grb2 in complex with the guanine nucleotide exchange protein SOS. Activated SOS catalyzes the exchange of GDP to GTP in membrane-anchored RAS (a small GTPase). This mechanism results in the activation of RAS, which translocates RAF to the plasma membrane. A multistage process regulates the activation of RAF, which involves phosphorylation and dephosphorylation events. Once activated RAF phosphorylates and activates its substrate MEK, which, in turn, activates ERK by phosphorylation on several sites. Generally, ERK plays an important role in the control of gene expression by phosphorylation and activation of transcription factors within the nucleus directing various cellular processes.

The specificity of numerous cellular responses includes temporal and spatial control of signaling components, which is mediated by scaffold proteins (see Fig. 2). Scaffold proteins bind components of the pathway to bring interacting partners into close proximity, assemble multiprotein signaling platforms (signalosomes), and facilitate efficient propagation of signals. One of the best characterized scaffolds of the MAPK pathway is kinase suppressor of RAS (KSR). Membrane-located KSR brings RAF, MEK, and ERK in close proximity for facilitating their syndetic activation and subsequent intracellular signal transmission. Therefore, scaffold proteins play a fundamental role in the regulation of physiological processes by both signal intensity and time course modulation of pathways (26).
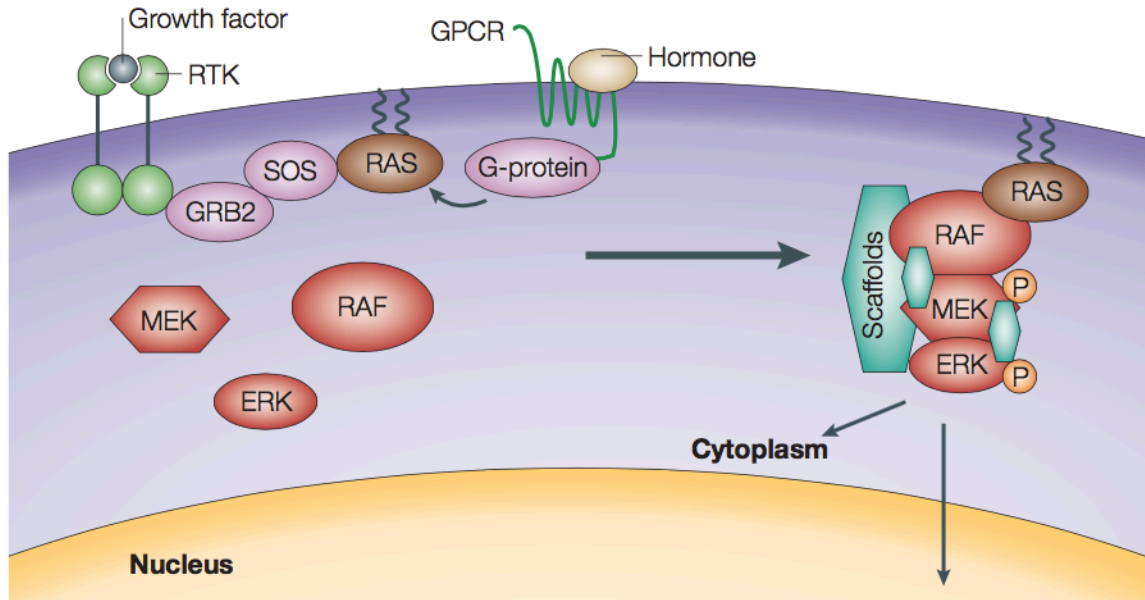
FIGURE 2: **Facilitation of the MAPK signal transmission by molecular scaffolds** (23)**.** Numerous cellular responses are temporally and spatially controlled by scaffold proteins. KSR, which is one of the best characterized scaffolds, mainly bridges the MAPK module of the RAF/MEK/ERK pathway. Thereby, it assembles proteins in signalosomes for facilitating the general signal propagation.

3.3.1 Intracellular initiators of the MAPK pathway

3.3.1.1 *RAS, a membrane-bound small GTPase*

The name RAS (abbreviation of 'rat sarcoma') refers to its origin in 1964, when sarcoma development in new-born rodents induced by murine leukemia virus was observed (27). In quiescent cells, RAS is guanosine diphosphate(GDP)-bound and inactive. Extracellular stimulation induces the nucleotide exchange of GDP for guanosine triphosphate (GTP), which results in the activation of RAS mediated by the guanine nucleotide exchange factor SOS at the plasma membrane (28, 29).

In humans, the RAS protein family consists of at least 35 members; H-, N-, and K-RAS are the most prominent and best characterized members (30, 31). RAS proteins translocate to membranes with their C-terminal hypervariable region (HVR), which consists of a lipid anchor (the most C-terminal region) and a preceding linker domain. Post-translational modifications of the HVR are mainly responsible for the intracellular trafficking of RAS proteins. Thereby, farnesylation (directed to the CAAX motif) and subsequent carboxylmethylation mediate endoplasmic reticulum (ER) localization (32). Moreover, the HVRs of H-RAS and N-RAS are

additionally palmitoylated (33). K-RAS primarily targets to the plasma membrane, but can also localize to other endomembrane compartments including the Golgi, ER, and mitochondria (34, 35), whereas H-RAS and N-RAS constantly shuttle between the Golgi apparatus and the plasma membrane depending on their palmitoylation level (36, 37).

Single amino-acid substitutions of RAS (primarily at residues Gly12 or Gln61) lead to constitutive GTP binding and attendant activation of this small GTPase, remarkably present in 30% of all human cancers. Especially in pancreatic (90%), papillary thyroid (60%), colon (50%), and non-small cell lung cancer (30%) as well as in melanoma (25%) active RAS mutations are stimulus-independent and, hence, promote persistent activation of downstream effectors (38). To reason, RAS is the most commonly mutated oncogene in human cancer. Therefore, blocking of RAS membrane association as a consequence of impaired post-translational modifications is an important target for drug development (39). Of note, using cytosolic farnesyltransferase (FTase) inhibitors (FTIs), the treatment of hematologic cancers was successful, but K-RAS and N-RAS, which are commonly mutated in cancer, underwent alternative prenylation in this case (40, 41). Prenylation is mediated by geranylgeranyltransferase I (GGTaseI). Hence, inhibitors of GGTaseI that block K-RAS and N-RAS activity (combined with FTIs) were further considered as potent inhibitors.

3.3.1.2 *LCK, a tyrosine kinase located at the plasma membrane*

In T cells, the MAPK signaling cascade can be alternatively initiated. Here, activation of T cell receptors as well as interleukin-2 (IL-2)/receptor binding leads to the activation of LCK (lymphocyte-specific kinase). LCK, in turn, actives RAF kinases resulting directly or indirectly in consecutive MAPK signaling, which induces T cell proliferation and differentiation (42, 43).

LCK (also named p56[Lck]) is a member of the Src family kinase (SFK) group, which comprises nine non-receptor tyrosine kinases in mammals. All members (Src, Fyn, Yes, Fgr, Lyn, Hck, Blk, Yrk, and LCK) trigger numerous cellular responses, e.g. cell survival, proliferation, differentiation, angiogenesis, cell motility, adhesion, and invasion initiated by cell surface receptor activation due to growth factor, cytokine or ligand binding (for review, see (44, 45)). Src kinases are closely related and possess a common protein structure: that comprises an SH4 domain (a short N-terminal membrane anchor), an SH3 domain (to interact with specific

proline-rich sequences of the substrate), an SH2 domain (in order to bind to a specific phospho-tyrosine motif located in the substrate), a poorly conserved 'unique' region, a kinase domain (or SH1; for catalytic function), and a short C-terminal regulatory region containing a conserved tyrosine residue (Tyr505 in LCK; for negative regulation) (45–47). LCK is (highly) expressed in all T cells, in some B cells, and in natural killer cells, but it shows weak expression in other cell types (48–50).

In resting, non-stimulated cells, membrane-localized SFKs are conformationally closed and enzymatically inactive as a result of intramolecular interactions (Fig. 3) (51). The conformation and interrelated catalytic function of LCK is regulated by both the phosphorylation level of Tyr394 (an autophosphorylation site within the activation loop of the kinase domain) and the inhibitory Tyr505 (52, 53). When Tyr505 is phosphorylated, LCK kinase activity is blocked as a consequence of induced intramolecular association of Tyr505 with the SH2 domain. This mechanism leads to a closed, inactive, and substrate inaccessible conformation (54, 55). The dephosphorylation of Tyr505 and ligand binding to the SH2 and SH3 domains of LCK generate an opened and primed conformation contributing a relatively low kinase activity (56). Additional phosphorylation of the positive regulatory Tyr394 leads to full catalytic activity possibly as a result of *trans*-autophosphorylation of coreceptor-bound LCK in a ligand-dependent manner (57). Interestingly, Nika *et al.* (58) revealed that phosphorylation of Tyr394 is also present in unstimulated naïve T cells and thymocytes. Furthermore, a complete removal of Tyr394-phosphorylated LCK resulted in a loss of approximately 50% of the phosphorylation on Tyr505 and vice versa.
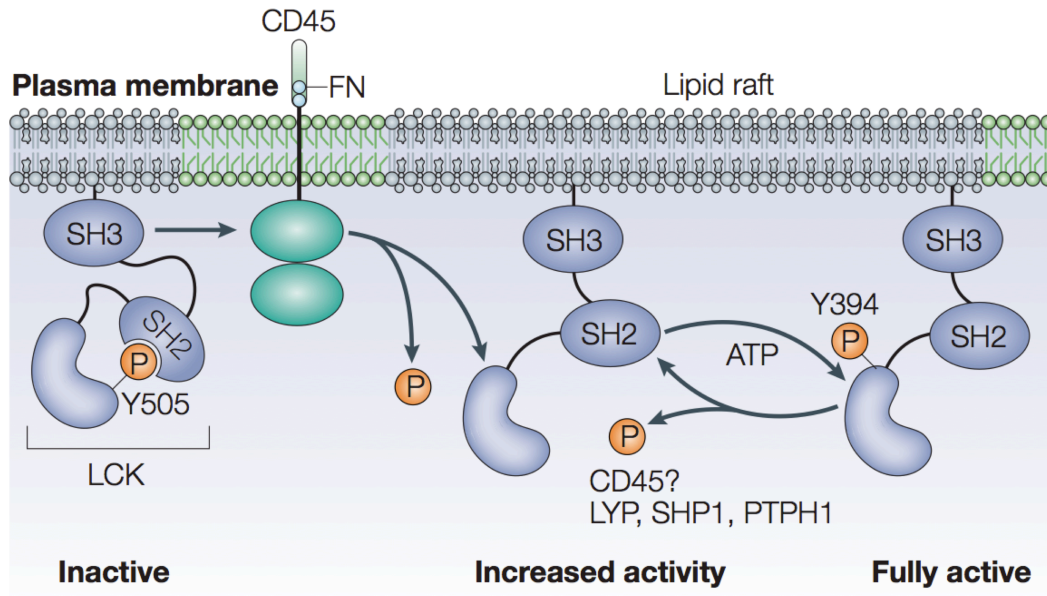
FIGURE 3: Activation mechanism of the Src family member LCK (59). Membrane-bound LCK is activated by conformational changes in a two-step manner. Upon dephosphorylation of Tyr505 low kinase activity is reached. The additional phosphorylation of Tyr394 results in full enzymatic activity of the tyrosine kinase LCK.

The conformation and activation level of SFKs generally mediate their cellular localization. Therefore, the SH4 domain contains a myristoylation site and, within some members (in all SFKs but Src and Blk), an additional palmitoylation site for the translocation either to the plasma membrane or further to intracellular membranes, such as ER and endosomes (60, 61). At the plasma membrane, LCK associates non-covalently with the cytoplasmic domains of the cell surface glycoproteins CD4 and CD8 (57, 62). These coreceptors aggregate with the T cell receptor (TCR) for enhancing the interaction of T cells with class I or class II peptide-loaded major histocompatibility complex (MHC) molecules on the surface of antigen-presenting cells (APCs) to initiate an antigen-dependent T cell response (Fig. 4) (63, 64). The mechanism of TCR activation further comprises the phosphorylation of immunoreceptor tyrosine-based activation motifs (ITAMs), present in the cytosolic tail of TCRs, by colocalized active LCK (52). This effect leads to the recruitment of the tyrosine kinase ZAP-70 to the TCR as well as its phosphorylation and activation by LCK. In turn, ZAP-70 phosphorylates and activates LAT, a transmembrane adaptor protein that initiates multiple signaling cascades in order to regulate T cell activation and proliferation (65–68). Accordingly, it was demonstrated that LCK-deficient cells exhibit severely impaired T cell development (69). Moreover, it was reported that LCK further activates directly the RAF/MEK/ERK pathway to regulate T lymphocyte growth by

phosphorylating C-RAF on Tyr340/341 (70–72). However, the mechanism of RAF protein activation by Src kinases is so far poorly understood.
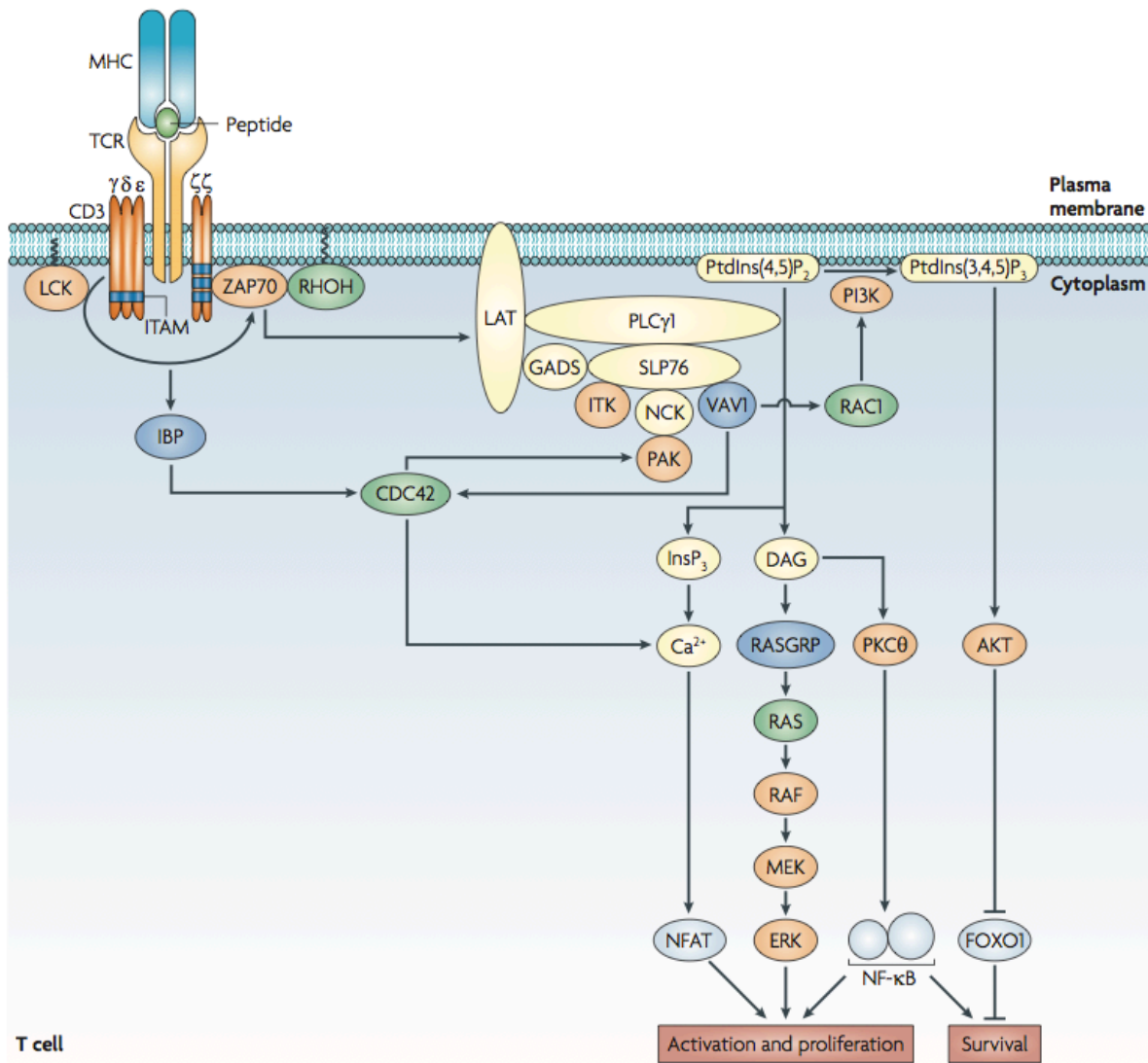
FIGURE 4: Activation of the RAF/MEK/ERK signaling pathway by LCK (73)**.** The interaction of T cells with peptide-loaded major histocompatibility complex (MHC) molecules on the surface of antigen-presenting cells (APCs) induces an antigen-dependent T cell response. Therefore, active, membrane-bound LCK triggers the T cell receptor (TCR) by phosphorylation of immunoreceptor tyrosine-based activation motifs (ITAMs) present in the cytosolic tail of TCRs. Recruited ZAP-70 becomes phosphorylated and activated by LCK at the plasma membrane. In turn, LAT, a transmembrane adaptor protein that initiates multiple signaling cascades in order to regulate T cell activation, proliferation, and survival, is phosphorylated and activated by ZAP-70.

3.3.2 Main components of MAPK signaling

3.3.2.1 *MAP3Ks – RAF protein kinases*

One of the key components of the RAF/MEK/ERK signaling cascade is the serine/threonine-specific RAF kinase. RAF is an abbreviation for 'rapidly accelerated fibrosarcoma', which is based on its first description by Rapp *et al.* (74) in 1983. They transduced a unique acutely transforming replication-defective mouse retrovirus in NIH 3T3 cells and characterized its acquired oncogene (named *v-RAF*), which induced tumors in mice, regarding its structure and biological activity. Equivalent homologs are present in multicellular eukaryotes, such as *Arabidopsis* (CTR1) (75), *Caenorhabditis* (lin-45) (76), and *Drosophila* (D-RAF) (77) as well as humans (C-RAF; cellular RAF or RAF-1) (78). In mammals, two additional isoforms with varied cellular localization and function exist (A-RAF and B-RAF).

All RAF isoforms consist of three highly conserved regions (CRs): CR1 to CR3 (Fig. 5). The CR1 is composed of a RAS-binding domain (RBD) and a cysteine rich domain (CRD). By interaction of the RBD with the effector domain of the small GTPase RAS, the CR1 is released for RAF kinase activation. Furthermore, the CRD can bind two zinc ions (to form a zinc finger motif) and phospholipids for the translocation of RAF kinases to the plasma membrane upon activation by RAS (79). The flexible and serine/threonine rich domain CR2 basically represents a hinge connecting the domains CR1 and CR3 with each other. Small and highly conserved dimers, named 14-3-3 proteins, interact with one specific site in the CR2 (Ser259 in C-RAF) and one site located in the end of the C-terminus of RAF (Ser621 in C-RAF) in order to regulate the abrogation of the phosphorylation-dependent blockade of RAF kinase activity (80). In principle, the N-terminus of the protein has a regulatory function, whereas the C-terminal half, mainly consisting of the CR3 domain, encodes for the catalytic function of RAF kinases. As in all protein kinases, the general, but highly conserved structure of kinase domains comprises a smaller N-lobe for ATP binding and a larger C-lobe for substrate binding, which was firstly described in protein kinase A (PKA) (13, 81). The CR3 is autoinhibited by the interaction with the CR1 domain, thus, mainly regulating RAF kinase activity by multiple phosphorylation and dephosphorylation steps coupled to internal conformational changes.
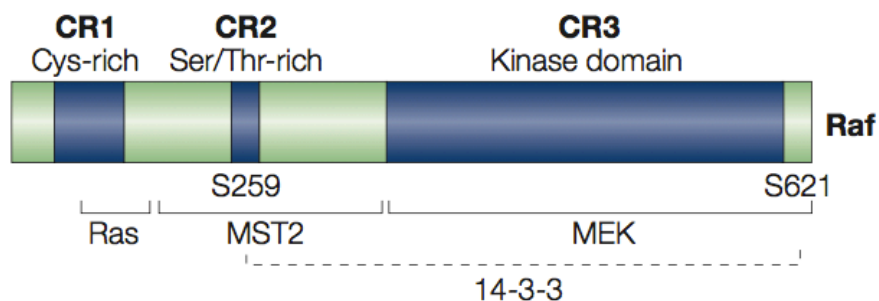
FIGURE 5: Schematic view of the structure of RAF kinases (82)**.** Three highly conserved regions (CR1 to CR3) form the RAF protein structure: the CR1 domain is partially cysteine-rich and mediates RAS binding; the serine/threonine-rich CR2 domain functions as a hinge for the dynamic interaction of CR1 and CR3; and the C-terminal half of RAF protein comprises the CR3 domain, which has catalytic function. 14-3-3 binding to Ser259 and Ser621 (in C-RAF) mediates the phosphorylation-dependent blockade of RAF kinase activity.

Despite 30 years of RAF protein research, only the isolated B-RAF kinase domain has been crystallized in 2004 (83), which was enabled due to the complex formation of RAF with BAY43-9006 (see Fig. 6). This small molecular inhibitor, also named Sorafenib, was approved for the treatment of primary kidney cancer and advanced primary liver cancer (84). Interestingly, the three-dimensional structure of the kinase domain showed a basically inactive conformation of the B-RAF kinase caused by the atypical interaction of the activation segment with the glycine-rich P-loop (also named ATP-phosphate-binding loop) (83), which is the most flexible segment of the N-lobe and responsible for the positioning of the γ-phosphate of the ATP molecule. So far, the crystallization of full-length RAF failed, possibly due to numerous phosphorylation on regulatory sites resulting in heterogeneity of the purified proteins (85).

Despite their diverged expression levels, all RAF isoforms are ubiquitously expressed in mammals (86). A-, B-, and C-RAF further possess different functions based on the emplacement of CR1, CR2, and CR3 in variable regions. An amino acid comparison of A- and C-RAF revealed high homology. Both become weakly activated by oncogenic RAS, but reach full activation levels after phosphorylation by the tyrosine kinase Src (a member of the Src family kinase (SFK) group) (87). In contrast, B-RAF, which shows in general a much higher basal activity than A- or C-RAF and becomes strongly activated by oncogenic RAS, plays a specified role in the regulation of MAPK signaling.
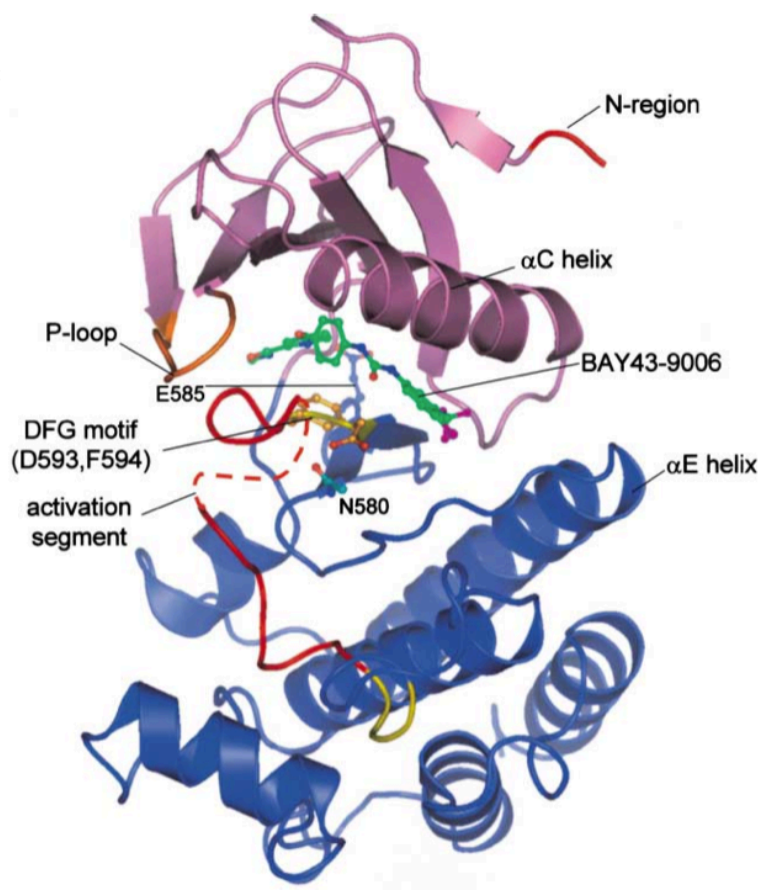
FIGURE 6: Structural illustration of the B-RAF kinase domain in complex with the inhibitor BAY43-9006 (Sorafenib) (83)**.** This three-dimensional protein structure shows in magenta the N-lobe and in marine the C-lobe of the RAF kinase domain. BAY43-9006 occupies the catalytic cleft between both lobes. The shown conformation of RAF is basically inactive due to the atypical interaction of the P-loop (orange) with the activation segment (red) that impairs the positioning of the γ-phosphate of the ATP molecule for catalysis. Consequently, this mechanism further regulates the phosphotransfer onto the RAF substrate MEK. The residues 600 to 611 of the activation segment are disordered and shown in dashed lines.

The activation of RAF by a multistep mechanism further allows dimerization, which is essential in order to reach full kinase activity. RAF proteins are able to form homo- or heterodimers (9, 88, 89). Rushworth *et al.* (90) described a higher catalytic activity for B-RAF/C-RAF heterodimers than for C-RAF homodimers. Dependency of B-RAF/C-RAF heterodimerization on the activation by RAS as well as on the phosphorylation level of Ser621 in C-RAF (a 14-3-3 binding site) was reported by Weber *et al.* (88). Furthermore, they revealed a constitutive association of the C-terminus of C-RAF with B-RAF. However, in which phase of the RAF activation process the dimerization occurs, is not completely understood.

Due to a complex activation mechanism and their key role in the mitogenic RAF/MEK/ERK signaling pathway resulting in the regulation of various cellular processes, RAF family members are critical for cancer development. Presumptive B-RAF mutations were identified in 59% of melanomas, 18% of colorectal cancers, 14% of liver cancers, 11% of gliomas, 9% of sarcomas, 4% of ovarian carcinomas, 3% of lung cancers, and 2% of breast cancers (91). In human cancers, the most commonly found mutation is B-RAF-V600E. The substitution of valine at the position

600, located within the catalytic domain of B-RAF, by glutamic acid results in RAS-independent, but significantly elevated basal RAF kinase activity, sustained MAPK signaling, and uncontrolled cellular responses, such as transformation (up to 138 times more efficient than B-RAF wild type). V600E in B-RAF probably mimic phosphorylation in the catalytic domain, since the insertion of a negatively charged residue occurs in the vicinity of a regulatory phosphorylation site (Ser599) (91).

3.3.2.2   MAP2Ks – MEK protein kinases

A further key component of the RAF/MEK/ERK pathway is the dual-specificity protein kinase MEK (abbreviation of 'mitogen-activated protein/ERK kinase'). MEK proteins are phosphorylated and activated by RAF family kinases and catalyze downstreamly ERK enzyme activity. In mammals, the active isoforms MEK1 and MEK2, which are evolutionarily conserved and ubiquitously expressed, show an overall identity of 85% and are more than 90% identical in their catalytic cores. Unique inserts in their C-terminal domains cause diverse regulation; the activity of MEK2 is seven times higher than that of MEK1 (92, 93). It was further observed that MEK1, but not MEK2, interacts with C-RAF (94). Embryonic death of MEK1-deficient mice revealed a unique role in angiogenesis during embryogenesis, whereas MEK2-deficient mice show normal embryonic development and T cell lineages suggesting that loss of MEK2 can be compensated by MEK1 (95, 96).

The MEK kinase domain forms the typical structure (similar to RAF kinases) consisting of a smaller N-lobe and a larger C-lobe for ATP and substrate binding, which comprises two-thirds of the entire protein structure (Fig. 7). Further, N-terminal sites are an ERK binding domain supporting the interaction of ERK with the active site and a region, which encodes either for a nuclear export signal or act as an inhibitory segment.
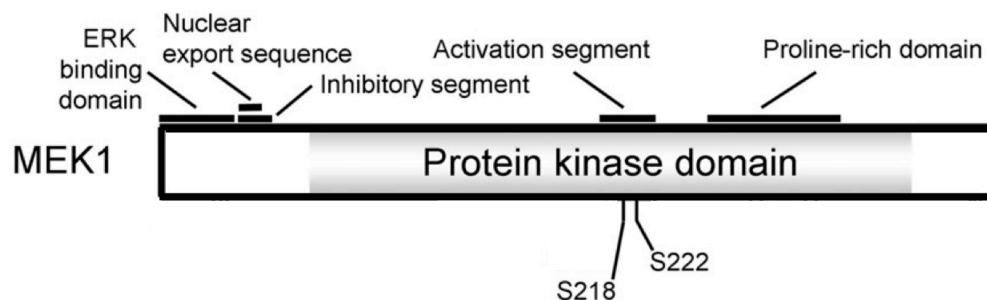
FIGURE 7: Schematic view of the structure of MEK kinases (modified from (97)**).** The structure of MEK is mainly composed of the typically formed protein kinase domain. An ERK binding domain as well as the overlapped nuclear export sequence and inhibitory segment are N-terminal located. In MEK1, Ser218 and Ser222 become phosphorylated by RAF kinases inducing conformational changes resulting in full catalytic activity of the protein kinase.

The catalytic function of MEK family proteins is regulated by the conformation of the activation segment, which exhibits either active or inactive orientation. When the aspartate side chain of the conserved DFG motif (Asp208 in MEK1) faces away from the active site, MEK undergoes inactive conformation. The active state is reached when the aspartate side chain faces into the ATP-binding pocket thereby coordinating the magnesium ion (97). Ser218 and Ser222, which are key regulators in the catalytic function of MEK1, are located within the activation segment of MEK1 closely to the DFG motif. These two residues become phosphorylated by RAF kinases that causes overall activation of the protein (98, 99). The substitution of either Ser218 or Ser222 by alanine showed abrogated EGF-stimulated MEK1 activation suggesting that the phosphorylation of both sites is required to reach kinase function. In contrast, the phosphorylation of the kinase domain-located sites Ser212 (activation segment) as well as Thr286 and Thr292 (proline-rich segment; phosphorylated by Cdk5 and ERK, respectively) or the phosphorylation of Thr386 (C-terminal; phosphorylated by Cdk5 and ERK) result in MEK1 kinase inhibition (100–104).

Beside the characteristic function as a serine/threonine kinase, MEK further catalyzes tyrosine phosphorylation in a specific TEY motif, located within the kinase domain of ERK proteins, their only known physiological substrates. It was reported that active MEK1 phosphorylates ERK1 predominantly on tyrosine *in vitro*, when ERK1 is catalytically inactive (105). Complete ERK activation is reached only in the case of serine/threonine and tyrosine phosphorylation (106).

Catalanotti *et al.* (107) reported MEK1/MEK2 heterodimerization upon the phosphorylation of Thr292 in MEK1. This negative feedback regulation facilitates the dephosphorylation of phospho-Ser218/222 within the activation loop of MEK1, mainly mediated by the protein phosphatase 2A (PP2A), leading to impaired kinase activity (107, 108). In MEK2, a Thr292-equivalent residue is absent. Strikingly, when MEK1 interaction with MEK2 is inhibited, ERK phosphorylation of MEK1 does not occur resulting in prolonged MEK2 and ERK activation. Moreover, phosphorylation of Thr292 as well as Ser298 within the proline-rich domain of MEK1 is involved in ERK2 nuclear translocation and cell proliferation (109). In principle, ERK-mediated Thr292 phosphorylation in MEK1 leads to the release of active ERK2 from MEK1. In contrast, the phosphorylation of Ser298 by PAK1 occurs in order to enhance MEK1/ERK2 interaction. These sites are phosphorylated in MEK1, but not in MEK2. Remarkably, MEK2-activated ERK2 remains in the cytoplasm allowing cell survival (109).

Although MEK mutations in human cancers are poorly explored, present MEK inhibitors are capable to impair tumor progression *in vivo*. For instance, trametinib (GSK1120212) allosterically inhibits MEK1 and MEK2 leading to impaired growth factor-mediated MAPK signaling and cell proliferation in various cancers. Additionally, this inhibitor evidenced clinical efficacy against melanoma and survival benefits and was recently approved for the treatment of melanoma (110, 111).

3.3.2.3   *MAPKs – ERK protein kinases*

The final key component of the canonical core module of three tiers of protein kinases within the RAF/MEK/ERK signaling cascade is ERK (abbreviation of 'extracellular signal-regulated protein kinase'). ERK proteins are likewise serine/threonine kinases, which become phosphorylated by MEK on serine/threonine as well as on tyrosine residues. The phosphorylation of the TEY motif, located within the activation loop of the ERK protein kinase domain, by MEK is required for complete ERK activation. In mammals, two active isoforms of these evolutionary conserved kinases are ubiquitously expressed: ERK1 and ERK2, which have similar function under most circumstances due to their high homology (84% of amino acid identity) (112–114). Lefloch *et al.* (113) reported a minimal effect on total ERK activation upon abrogated ERK1 expression due to the compensating activation of ERK2. They further

demonstrated that ERK1 and ERK2 activation occurs in parallel by all known cellular stimuli of the RAF/MEK/ERK signaling cascade (115). However, invalidation of ERK2 leads to early embryonic death due to placental defects (116–118), whereas ERK1-deficient mice show normal development (119, 120). Based on their unique N- and C-terminal extensions, ERK1 and ERK2 exhibit signaling specificity.

The catalytic domain of ERK proteins contains a highly conserved N- and C-lobe for ATP and substrate binding (as described for RAF, MEK, and other kinases) that comprises three-fourths of the entire protein structure in the case of ERK (Fig. 8). A 31-amino-acid-residue insertion (kinase insert domain) provides additional functional specificity for ERK1 and ERK2 (121). This characteristic of ERK proteins is distinctive compared to RAF and MEK kinase, which show isoform-specific properties as a consequence of variable regions outlying of the kinase domain.
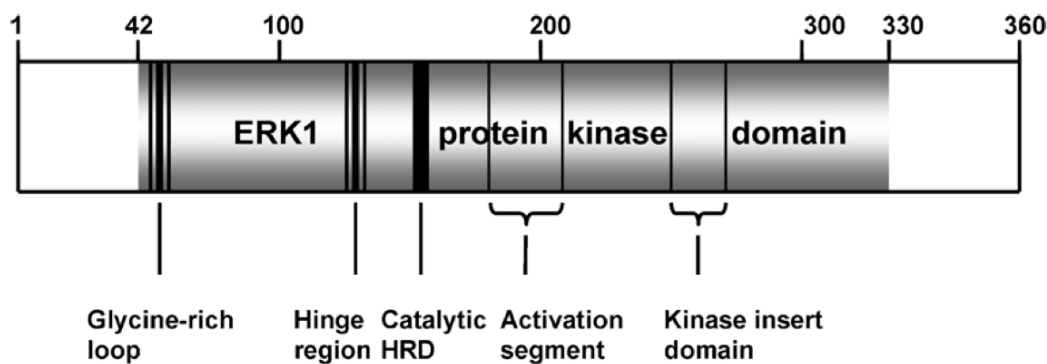
FIGURE 8: Schematic view of the structure of ERK kinases (modified from (121)**).** Similar to MEK kinases the structure of ERK is mainly composed of the typically formed protein kinase domain. The embedded kinase insert domain mediates additional signaling specificity for ERK1/2 kinases.

Similar to MEK kinases, the phosphorylation of ERK further enables protein dimerization. Therefore, changes in ERK conformation in order to allow a tight protein-protein interaction occur as a consequence of the phosphorylation of two residues located within the activation loop and the adjacent C-terminal extension of ERK kinases (122). Primarily, ERK1 and ERK2 homodimers are formed, because ERK1/ERK2 heterodimers are unstable (123). Casar *et al.* (124) demonstrated that ERK dimers are generally essential for the activation of its cytoplasmic substrates and, in contrast, its nuclear substrates associate to ERK monomers. Interestingly, they further reported that prevention of ERK dimerization is sufficient for attenuating cellular

proliferation, transformation, and tumor development.

ERK family kinases are so-called "Pro-directed" protein kinases based on the fact that they phosphorylate serines and threonines close to proline residues. Approximately 200 distinct ERK substrates have been identified so far including regulatory molecules and transcription factors; in contrast to RAF and MEK kinases with narrow substrate specificity (125, 126). One example for cytosolic substrates of ERK kinases is the actin-binding protein palladin. Actin-binding proteins play an essential role in the remodeling of the cytoskeleton in order to regulate mitogenic, morphological, and migratory cell behavior. The phosphorylation of palladin by ERK leads to an anti-migratory effect (127). Moreover, ERK phosphorylates ribosomal S6 kinase (RSK) proteins, which regulate cell growth, motility, proliferation, and survival (for review see (128)). Upon growth factor-induced activation, ERK family kinases translocate from the cytosol to the nucleus by their nuclear localization signal (NLS) (129). An example for nuclear substrates of ERK kinases is a member of the ternary complex factor subfamily of Ets(E-twenty-six)-domain transcription factors called Elk-1. Its phosphorylation results in increased transcriptional activity (130, 131). The transcription factors c-Fos and c-Jun interact with each other for the regulation of early transcriptional processes. Phosphorylation of c-Fos by ERK prevents rapid c-Fos mRNA and protein degradation. The combination of c-Fos phosphorylation catalyzed by ERK and RSK proteins stabilizes c-Fos for several hours. Additionally, ERK catalyzes the phosphorylation of c-Jun, which results in increased transcriptional activity (132–134). Interestingly, despite the various downstream substrates of ERK, this kinase is further able to phosphorylate and, hence, positively or negatively regulate upstream-acting proteins. Consequently, the generated feedback loop fine-tunes the signal transmission at several steps within the entire RAF/MEK/ERK pathway (135, 136).

3.3.3   MAPK signal transduction is bridged by KSR proteins

One of the best characterized scaffolds operating within the MAPK pathway is the kinase suppressor of RAS (KSR). It mainly helps RAF, MEK, and ERK to form a localized signaling complex in order to facilitate signal propagation. The family of KSR proteins comprises an evolutionary conserved group of molecular scaffolds that was initially identified in 1995 by genetic screens in *D. melanogaster* and *C. elegans* and described as a positive regulator of RAS

signaling (137–141). KSR homologues are found in all invertebrates and mammals, but not in yeast (142). In *C. elegans* as well as in mammals, two isoforms (named ksr-1 and ksr-2 or, respectively, KSR1 and KSR2) are existent, while in *Drosophila* only one isoform (ksr) is present (140, 141, 143–145).

3.3.3.1 *KSR proteins – a structural insight*

KSR protein family members share a common structure with all or some of five distinct domains, named conserved area (CA) 1 to 5 (see Fig. 9) (141). The N-terminal half of KSR proteins comprises CA1 to CA4, while the CA5 expands over the C-terminal half. CA1 is a KSR1-unique domain of about 40 amino acids, which mediates RAF interaction and activation. Remarkably, the sequence of this domain is incomplete in both isoforms of humans and absent in both isoforms existing in *C. elegans* suggesting a different mechanism for RAF activation (140, 143). The CA2 is a proline-rich domain consisting of 13 amino acids. Its role in KSR function is rather unknown. Similar to RAF kinases and the ζ isoform of protein kinase C (ζPKC) (kinases with atypical C1 domain), KSR proteins possess a cysteine-rich domain (CRD). This region, termed CA3, is mainly involved in protein-protein interactions and the recruitment of KSR to signaling platforms at the plasma membrane depending on the ceramide content of lipid rafts (141, 146–148). The CA3 consists of 50 amino acids that interact with diverse proteins, such as 14-3-3 proteins, the βγ subunit of heterotrimeric G-proteins, and the Cdc25C-associated kinase 1 (C-TAK1) in order to modulate RAS signaling (149–154). A serine/threonine-rich domain of variable length is named CA4, which is present in all members of the KSR protein family except KSR2 in *C. elegans* (141, 143). This region contains an FxFP motif that serves as a docking site for ERK kinases – therefore also termed as DEF motif (abbreviation for 'docking site for ERK, FxFP'). ERK binds to phosphorylate KSR on proline-directed serine and threonine residues (155). The CA5 of KSR proteins represents a putative kinase (or kinase-like) domain that mediates further RAF and MEK interaction with KSR. Despite the facts that this region includes the eleven highly conserved subdomains generally described for kinases and that a high degree of sequence similarity to RAF kinases does exist, enzymatic function of the molecular scaffolds is controversially discussed (142, 156–158).
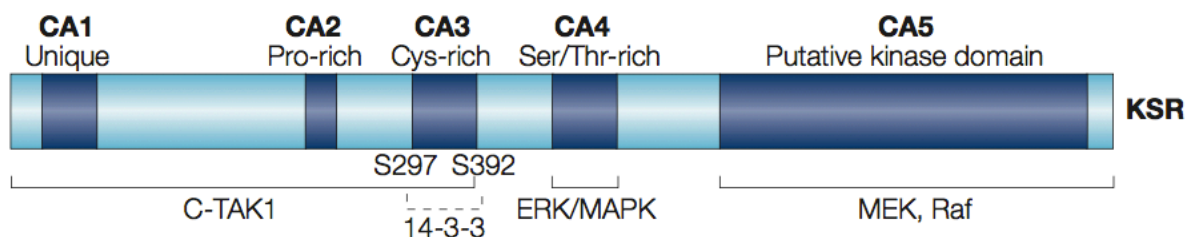
FIGURE 9: Architecture of KSR proteins (82)**.** Five highly conserved regions (CA1 to CA5) of the KSR structure: the CA1 (KSR1-unique) is involved in RAF interaction and activation; the function of the proline-rich CA2 domain is rather unknown; the cysteine-rich CA3 mediates protein-protein interactions and recruitment of KSR to the plasma membrane; the serine/threonine-rich CA4 serves as a docking site for ERK kinases; the CA5 represents a putative kinase (or kinase-like) domain, where MEK and RAF interaction take place. C-TAK1 and 14-3-3 binding to KSR modulates RAS signaling.

3.3.3.2 *Does the scaffold protein KSR have additional kinase function?*

It is well known that KSR is mainly responsible to bring components of the MAPK pathway in close proximity for facilitating signal transduction. Based on the lack of an invariant catalytic lysine in subdomain II of the kinase domain of KSR isoforms existing in *C. elegans* and mammals, KSR proteins are supposed to be enzymatically inactive kinases. In most protein kinases the referred residue is highly conserved and involved in the positioning of the ATP molecule as well as in the phosphotransfer reaction. Variously reported, this is the main argument to classify these molecular scaffolds in the subgroup of so-called pseudokinases that represent approximately 10% of all encoded protein kinases (10, 141, 143, 144). Moreover, the fact that no direct substrate was known for KSR kinases confirmed its classification at that time.

Pseudokinases differ significantly from proteins with kinase activity (10). The considered key residues being necessary for catalysis are located in four kinase active-site motifs: *i)* the flexible and glycine-rich G-loop (aa 570-575 in mKSR1) stabilizes the α- and β-phosphates of the bound ATP molecule through backbone amide interactions; *ii)* the VAIK motif (aa 586-589 in mKSR1) contains a crucial lysine (substituted in mKSR1 by an arginine) that interacts with a conserved glutamate located within helix αC; *iii)* the aspartate of the DFG motif (aa 703-705 in mKSR1; Asp702 is substituted by a leucine) chelates an active-site magnesium ion, and *iv)* another aspartate located within the HRD motif (aa 681-683 in mKSR1; Arg682 is substituted by a lysine) functions as catalytic base in enzymatically active kinases (159, 160). Consequently,

abolition of the catalytic function by substitutions at any of these motifs would be expected. Therefore, pseudokinases are meant to have no to very low kinase activity. Even more remarkable is then the fact that research done by the groups of Kolesnick, Polk, Shaw, and Barford strongly proved KSR kinase activity. They found phosphorylation of Ser218/222 in MEK1 and Thr269 in C-RAF proteins by KSR, clearly characterizing KSR as serine/threonine kinase (161–165). Indeed, KSR family proteins are structurally similar to the serine/threonine kinase family of RAF. Nevertheless, KSR in *C. elegans* and *D. melanogaster* exhibits additional tyrosine-like kinase group properties (10, 140, 141, 143, 144).

In order to activate its kinase function, an allosteric mechanism, induced by side-to-side dimerization between KSR and RAF kinases, provokes conformational changes in the KSR protein structure (Fig. 10) (160). In this case, low catalytic activity of KSR as a MEK kinase retains as a consequence of KSR/MEK heterotetramers, whereas KSR/MEK/RAF ternary complexes initiate high KSR kinase activity. Thereby, RAF binding to KSR induces indirectly the release of the buried and protected residues Ser218 and Ser222 in MEK1 by conformational changes in KSR.
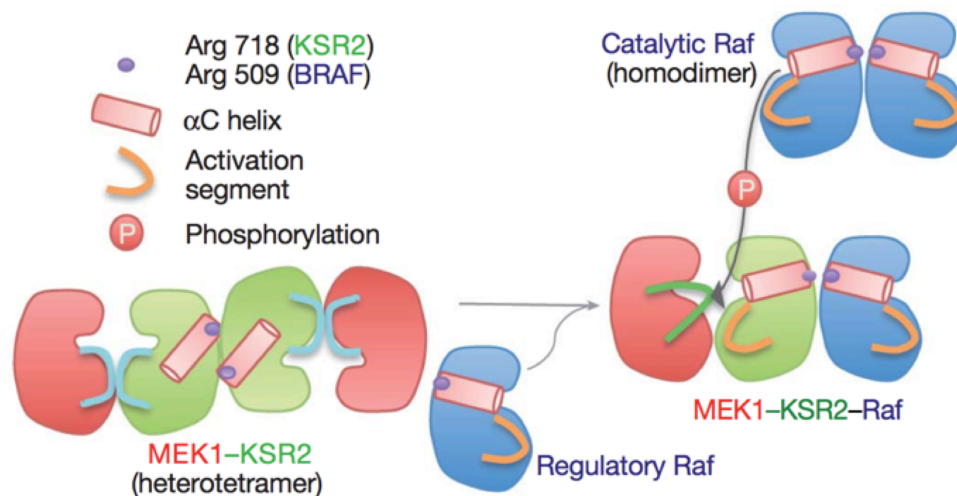
FIGURE 10: RAF-induced allosteric mechanism in KSR proteins (165)**.** Side-to-side dimerization between KSR and RAF kinases initiates changes in the protein structure of KSR consequently regulating the activation level of KSR in a conformation-dependent manner. KSR heterotetramers with MEK exhibit low kinase activity, whereas the additional interaction with a regulatory RAF molecule induces high catalytic activity. Thereby, the activation segment of KSR-bound MEK becomes released and accessible for phosphorylation by either a catalytic RAF homodimer or KSR itself.

3.3.3.3 *Regulation of KSR proteins*

It is know that KSR proteins associate with all three components of the RAF/MEK/ERK signaling core of the MAPK pathway linking MEK and, in turn, ERK to its activator (121, 166). The interaction of the CA5 domain of KSR with MEK is constitutive, while RAF and ERK binding with KSR occurs only in response to an extracellular stimulus followed by RAS activation (149, 150, 167, 168). Due to their fine-tune effect on the MAPK signaling pathway, KSR proteins need to be highly regulated. As for many other scaffold proteins, optimal expression levels of KSR are required to function bona fide and to regulate carefully the intensity of MAPK signaling (149, 169, 170).

Another possibility to control KSR function, which is a way more dynamic, occurs by the interaction with various proteins, especially kinases and phosphatases. Using mass spectrometry analysis, Morrison and co-workers (145) and Liu *et al.* (171) discovered in total more than 100 different proteins associating with recombinant KSR. Furthermore, they identified common and isoform-specific partners binding directly or indirectly to KSR within multiprotein complexes. Beside RAF, MEK, and ERK heat-shock proteins (e.g. HSP90, HSP70, and HSP68) interact with KSR proteins. In this case, the stabilization of KSR itself or of the signalosome is controlled. However, the interaction relevance is not well understood (158).

Critical for the function of the molecular scaffolds is the association with 14-3-3 proteins (Fig. 11). In quiescent cells, KSR is phosphorylated on two sites (Ser297 and Ser392 in KSR1) that flank the CA3 domain and mediate 14-3-3 interaction for sustained inactive conformation of KSR remained in the cytosol (149, 150). The highly conserved family of 14-3-3 proteins, which are ubiquitously expressed, comprise seven isoforms in mammalian cells that form homo- or heterodimers (for review see (172)). While the kinase phosphorylating Ser297 is unknown, the major 14-3-3 binding site Ser392 in KSR1 is phosphorylated by the constitutively associated serine/threonine kinase C-TAK1 (151). In response to growth factor stimulation followed by RAS activation the regulatory subunit B of the serine/threonine phosphatase PP2A is recruited to the multiprotein complex to fuse with its catalytic core (subunits A and C) constitutively bound to KSR. Active PP2A dephosphorylates the regulatory Ser392 resulting in partial dissociation of KSR from 14-3-3, exposure of the CA3 domain, and translocation of the scaffold to the plasma membrane (173, 174).

CK2 (casein kinase 2) binds constitutively to the CA3 domain of KSR thereby mediating the phosphorylation of Ser518 in KSR1 (175, 176). The interaction is needed for the scaffolding activity of KSR proteins to further facilitate the activation of bound MEK and, in turn, ERK. KSR-associated CK2 phosphorylates RAF proteins upon KSR/RAF interaction at the plasma membrane as a result of CK2 cotranslocation by the scaffold KSR.

A further interacting partner is IMP (abbreviation of 'impedes mitogenic signal propagation') (see Fig. 11). This ubiquitin E3 ligase associates with KSR in order to induce hyperphosphorylation on Ser392 that leads to the limiting of RAF/MEK complex formation and the inhibition of ERK activation (177). These changes occur due to the possibility that IMP maintains KSR in an inactivated state as a consequence of disrupted KSR homodimerization without affecting its ability to associate with MEK or RAF. However, a detailed mechanism is unknown (178). GTP-loaded RAS induces IMP recruitment by disrupting the KSR/IMP complex, which promotes IMP autopolyubiquitination and subsequent degradation close to the plasma membrane (177).

Intriguingly, ERK kinases are prominent feedback regulators of KSR proteins. In mitogen-stimulated cells, Thr260, Thr274, Ser320, and Ser443 in KSR1 are phosphorylated by ERK. This mechanism promotes *i*) the dissociation of the KSR/RAF interaction upon B-RAF phosphorylation as well, *ii*) the release of KSR1 from the plasma membrane, and, subsequently, *iii*) the attenuation of ERK signaling (149, 179, 180). Remarkably, the absence of KSR phosphorylation by ERK kinases and the additional release of 14-3-3 mediate translocation of KSR proteins into the nucleus. However, the molecular mechanism awaits clarification (181).
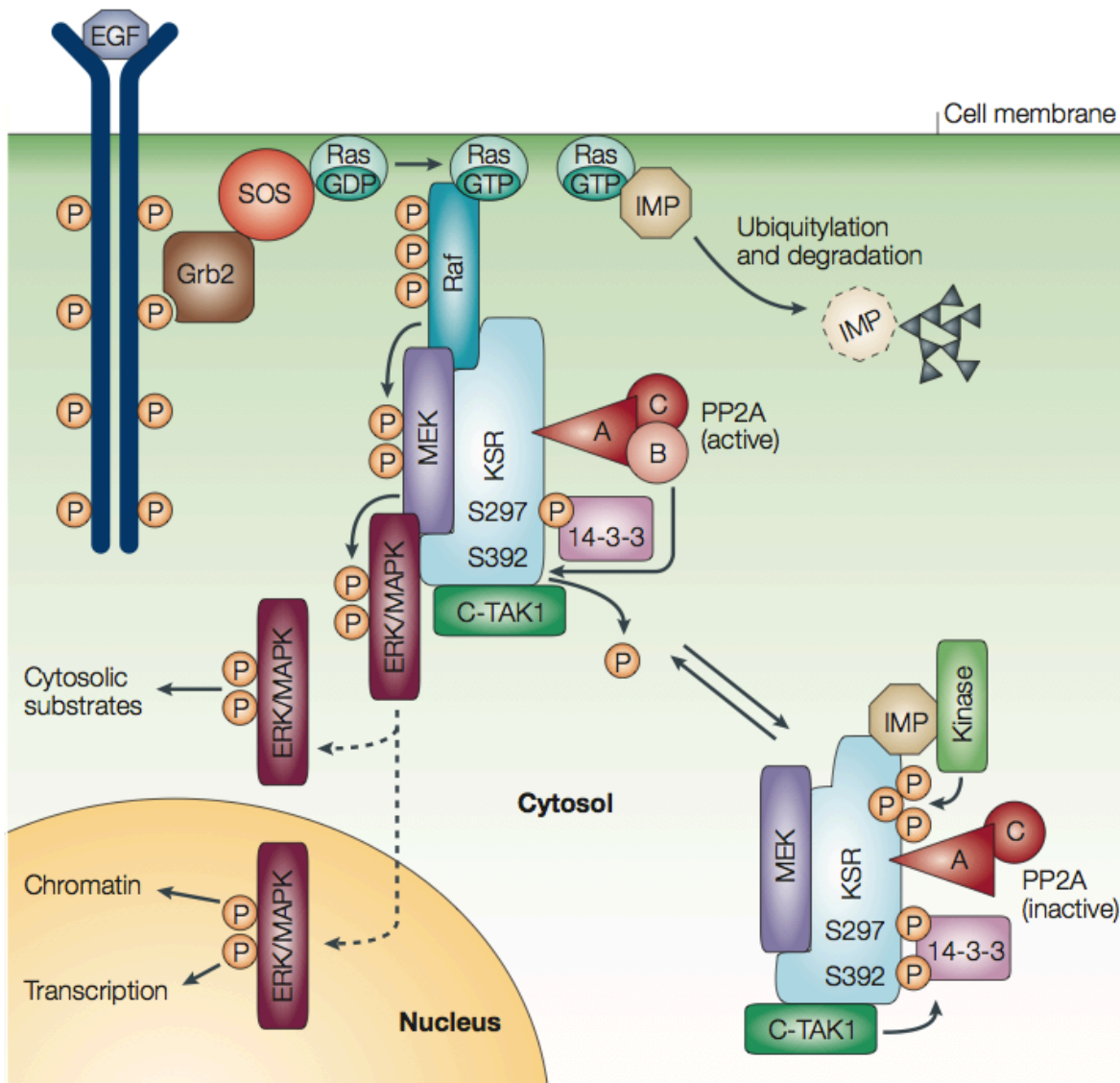
FIGURE 11: KSR function is dynamically regulated by several proteins (165)**.** The functioning of KSR proteins to work as a scaffold that facilitates MAPK signal propagation by the formation of signalosomes is highly controlled. In quiescent cells, IMP induces hyperphosphorylation on Ser392 in cytosolic KSR1. Furthermore, 14-3-3 proteins interact with phosphorylated Ser297 and Ser392 in KSR1 resulting in the inactivation of KSR. Upon stimulation, RAS-induced dephosphorylation of KSR1 on Ser392 by PP2A occurs. PP2A subunits A and C are constitutively bound to KSR, which becomes activated as a consequence of subunit B binding to the PP2A core. Subsequently, 14-3-3 is released from Ser392, which leads to the translocation of KSR to the plasma membrane in order to facilitate canonical phosphorylation between RAF, MEK, and ERK kinases. RAS-induced IMP autoubiquitylation and subsequent degradation occur close to the plasma membrane. In reverse, KSR is inactivated by 14-3-3 binding to phosphorylated Ser392 (induced by C-TAK1) combined with the reassociation with IMP (not shown).

3.3.3.4 *KSR, its role in cellular disorders and as therapeutic target*

As shown by *in vitro* studies, KSR1 may be an essential regulator for tumor necrosis factor(TNF)-stimulated survival pathways, which plays a critical role in inflammatory bowel diseases (IBDs) induced by impaired cytokine production and enhanced intestinal epithelial cell apoptosis. Cellular loss of KSR1 or disruption of KSR1 expression increase the sensitivity to chronic colitis and TNF-induced apoptosis due to the inactivation of anti-apoptotic signals (182). KSR1-deficient mice develop generally normal, but exhibit both defects in antigen-triggered T cell proliferation and resistance to antibody-induced arthritis (169, 183). Moreover, ERK activation by TNF-α and interleukin-1 is defective in embryonic fibroblasts from these mice. The described effects possibly occur due to the exclusion of MEK and ERK from high molecular weight signaling complexes that consequently reduces proliferation (184). Same experiments exhibited no cell transformation of KSR1-knockout MEFs (mouse embryonic fibroblasts) upon RAS oncogene expression reflecting high importance for KSR1 in RAS-mediated tumor formation. The research group of Kolesnick further reduced KSR1 levels by 60% in epidermoid carcinoma cells by stably transfection of an antisense KSR1 construct (185). Remarkably, these cells were not able to form tumors compared to control cells that were highly tumorigenic, when subcutaneously implanted in nude mice. Comparable with these results, the growth of RAS-dependent human pancreatic and non-small-cell lung carcinoma xenografts could be prevented due to KSR1 gene inhibition by the continuous treatment with phosphorothioate antisense oligonucleotides (AS-ODNs) in nude mice (185). Moreover in this study, regression of established pancreatic tumors and blocking of lung metastases was effected without apparent toxicity. Kolesnick and co-workers further quantified the KSR1 AS-ODN drug uptake in plasma and tumor tissues and demonstrated a high correlation of KSR1 repression in pancreatic cancer xenografts with an AS-ODN drug uptake into tumor tissues. To conclude, several proofs represent KSR proteins in the treatment of RAS-dependent tumors as a bona fide therapeutic target.

4 AIM OF THE PROJECT

KSR proteins are mainly regulated by phosphorylation and dephosphorylation events. Although several serine and threonine residues are well established as regulatory phosphorylation sites, almost nothing is known about the regulation of KSR1 by tyrosine phosphorylation. However, phosphorylated tyrosines may have fine-tuning effects on the regulation of various proteins acting at several steps during intracellular signaling similar to phosphorylated serine or threonine residues. Murine KSR1 is the most studied member of the KSR family and, hence, serves as general model for understanding the function of KSR proteins. In order to gain more knowledge with respect to regulation of KSR1 function in MAPK signaling, the main focus of this study was to identify regulatory tyrosine phosphorylation site(s) of KSR1 and to characterize its/their role in the functionality of this protein. Consequently, the following questions were raised and answered in this study: which residue(s) in KSR1 is/are targeted by the Src family kinase LCK? Does this phosphorylation have an impact on the regulation of the protein structure of KSR1, and if yes, how does conformational rearrangement occur? What are the further consequences for both the interaction of B-RAF and MEK with KSR1 and the activation of KSR1-bound MEK? And, consequently, is there an impact on cellular processes?

There is a growing body of evidence that KSR1 has a capacity to function as a true kinase. Since structural changes, induced by phosphorylation(s) may interfere with the induction of potential catalytic activity in KSR1, this work further aims at better understanding of the regulation of the KSR1 kinase activity by phosphorylation events occurring within the core of the kinase domain.

5 EXPERIMENTAL PROCEDURES

The chapter describes materials and methods utilized for this study. Experimental procedures comply with current standard techniques in scientific research.

5.1 Materials

5.1.1 Instruments

Hardware (model)	*Manufacturer*
Autoclave (VX-150)	Systec
Biological safety cabinets	
Bacteria	NuAire
Cell culture (Safe 2020)	Thermo Scientific
Cell counting chamber	Bürker
Cell sorter (BD FACS Aria III)	BD Biosciences
Centrifuges	
Avanti Centrifuge J-25 I	Beckman Coulter
Megafuge 1.0R	Heraeus Instruments
Microcentrifuge 5415R and 5417R	Eppendorf
Optima L-80 XP ultracentrifuge	Beckman Coulter
Chemiluminescence imager	INTAS Science Imaging Instruments
Electronic balance	Kern & Sohn
Electrophoresis power supply (EV202)	Peqlab
Electrophoresis unit for agarose gels (Sub-cell GT)	Bio-Rad
Electroporator (MicroPulser)	Bio-Rad
Gel scanner (ImageScanner III)	GE Healthcare
Incubators	
Cell culture incubator (Heracell 150i)	Thermo Scientific
Heating/drying oven	Memmert

Magnetic stirrer	Marienfeld-Superior, Bibby Scientific
Mass spectrometers	
LTQ-Orbitrap Velos	Thermo Scientific
LTQ-Orbitrap XL	Thermo Scientific
Microscopes (phase contrast and fluorescence)	Leica
Microwave	Privileg
PCR machines	
Primus 96 advanced	Peqlab
T3 thermocycler	Biometra
pH electrode (SenTix 21)	WTW
pH meter (inoLab pH 720)	WTW
Photometers	
Spectrophotometer (NanoDrop ND-1000)	Peqlab
UV/Vis photometer (BioPhotometer)	Eppendorf
Pipette controller and pipettes	
Accu-jet pro	Brand
PIPETMAN classic P1000, P200, P50, and P20	Gilson
Research P10 and P2.5	Eppendorf
Semi-dry electro blotter (PerfectBlue)	Peqlab
Shakers	
Bacterial shaker	Infors
See-saw rocker SSL4	Stuart
Titramax 101	Heidolph
Thermoblocks	
Fixed	Liebisch
Mixing block (MB-102)	Bioer
Transilluminator (Dark Hood DH-40/50)	Biostep
Vertical gel electrophoresis system (PerfectBlue)	Peqlab
Vortex (Vortex Genie 2)	Scientific Industries
Water bath	Memmert

5.1.2 Consumable material

Plastics	*Manufacturer*
Cell culture flasks (T25, T75, and T175)	Corning
Cryotubes	Sarstedt
FACS tubes (round bottom)	BD Biosciences
Falcon tubes (15ml and 50ml)	Corning
Filter	
0.22μm and 0.45μm	Sarstedt
Fluted filter	Schleicher & Schuell
Micro tubes (1.5ml and 2ml)	Sarstedt
MicroPulser electroporation cuvettes (0.1cm gap)	Bio-Rad
Pasteur pipettes	Brand
PCR tubes and lids	Brand
Petri dishes	
For bacterial culture (10cm)	Sarstedt
For tissue culture (10cm and 15cm)	Sarstedt
Photometer cuvettes	Sarstedt
Pipette tips	Sarstedt
Pipettes (1ml, 5ml, 10ml, 25ml, and 50ml)	Sarstedt
Scalpel	Megro
Tubes (thinwall, polyallomer, 25×89mm)	Beckman Coulter

5.1.3 Chemical reagents and general materials

Reagent / material	*Manufacturer*
1kb DNA ladder	Thermo Scientific
Acetic acid, p.a.	Carl Roth
Acrylamide(30%)/bisacrylamide(0.8%)	Carl Roth
Agarose, ultra pure	Carl Roth

Ammonium peroxydisulfate (APS)	Carl Roth
Ampicillin	Carl Roth
β-Glycerophosphate	Carl Roth
β-Mercaptoethanol	Carl Roth
Bacto-tryptone	Thermo Scientific
Blotting paper Whatman 3MM Chr	A. Hartenstein
Bovine serum albumin (BSA)	Carl Roth
Bradford protein assay solution	Bio-Rad
Brilliant Blue G 250	Carl Roth
Bromophenol Blue	Carl Roth
Buffer O	Thermo Scientific
Buffer Tango	Thermo Scientific
Calcium chloride ($CaCl_2$)	Sigma-Aldrich
Coumaric acid	Sigma-Aldrich
Dimethyl sulfoxide (DMSO), p.a.	Sigma-Aldrich
Disodium phosphate (Na_2HPO_4)	Merck
DNA polymerase reaction buffers	
Taq (BioTherm)	Genecraft
PfuUltra	Agilent Technologies
dNTP mix (10mM each)	Thermo Scientific
Dulbecco's modified eagle medium (DMEM)	Sigma-Aldrich
Dulbecco's phosphate-buffered saline (DPBS)	Gibco
ECL solutions	Millipore, Thermo Scientific
Ethanol, p.a.	Carl Roth, Sigma-Aldrich
Ethidium bromide	Carl Roth
FastAP buffer	Thermo Scientific
Fetal bovine serum (FBS)	PAA Laboratories
Glass chromatography columns (Econo-Column)	Bio-Rad
Glutathione	Sigma-Aldrich
Glutathione-sepharose 4B	GE Healthcare
Glycerol, p.a.	Carl Roth

Glycine	Carl Roth
HEPES	SERVA Electrophoresis
Hydrochloride (HCl), p.a.	Carl Roth
Hydrogen peroxide (35%)	Sigma-Aldrich
Isopropanol, p.a.	Carl Roth
Laemmli sample buffer (Roti-Load1)	Carl Roth
Lambda DNA/Eco91I Marker, 15	Thermo Scientific
LB agar powder	AppliChem
LB medium powder	AppliChem
LCK Inhibitor III	EMD Millipore
Luminol	Biomol
Methanol, p.a.	Carl Roth
Milk powder, nonfat dried	AppliChem
Minimum essential medium (MEM with NEAA)	Gibco
Nitrocellulose transfer membrane (PROTRAN)	Whatman
Nonidet P-40 (NP-40)	Sigma-Aldrich
Penicillin/streptomycin	Gibco
Polybrene	Sigma-Aldrich
Polyethylenimine (PEI) transfection reagent	Polysciences, Polyplus transfection
Polyvinylidene fluoride (PVDF) transfer membrane	GE Healthcare, Carl Roth
Ponceau-S solution	Sigma-Aldrich
Prestained protein ladder (PageRuler)	Thermo Scientific
Protease inhibitor cocktail (complete)	Roche
SDS-PAGE running buffer	Carl Roth
Sodium chloride (NaCl)	Carl Roth
Sodium dodecyl sulfate (SDS), ultra pure	Carl Roth
Sodium fluoride (NaF)	Sigma-Aldrich
Sodium hydroxide (NaOH)	Carl Roth
Sodium orthovanadate (Na_3VO_4)	Sigma-Aldrich
Sodium pyrophosphate ($Na_4P_2O_7$)	Carl Roth
T4 DNA ligase buffer	Thermo Scientific

TEMED (N,N,N',N'-Tetramethylethylenediamine)	Carl Roth
Tris (Trizma base, Trometamol)	Sigma-Aldrich
Tris-borate-EDTA (TBE) buffer	AppliChem
Tris-buffered saline (TBS)	KPL
Tween 20	Carl Roth
Water (Molecular biology reagent)	Sigma-Aldrich
Xylene cyanol	Sigma-Aldrich
Yeast extract	BD Biosciences

5.1.4   Solutions and buffers

DNA polymerase reaction buffer (Taq (BioTherm))

10× buffer was purchased together with Taq DNA polymerase from Genecraft and contains:

   670mM Tris-HCl (pH 8.8)

   160mM $(NH_4)_2SO_4$

   15mM $MgCl_2$

   0.1% Tween 20

in ddH_2O.

DNA polymerase reaction buffer (PfuUltra)

10× buffer was obtained together with PfuUltra DNA polymerase from Agilent Technologies. It contains:

   200mM Tris-HCl (pH 8.8)

   20mM $MgSO_4$

   100mM KCl

   100mM $(NH_4)_2SO_4$

   1% Triton X-100

   1mg/ml nuclease-free BSA

in ddH_2O.

Buffer Tango

10× buffer was purchased together with SpeI restriction endonuclease from Thermo Scientific. It contains:

330mM Tris-acetate (pH 7.9)

100mM Mg-acetate

660mM K-acetate

1mg/ml BSA

in ddH$_2$O.

Buffer O

10× buffer was obtained together with NotI restriction endonuclease from Thermo Scientific and contains:

0.5M Tris-HCl (pH 7.5)

0.1M MgCl$_2$

1M NaCl

1mg/ml BSA

in ddH$_2$O.

FastAP buffer

10× buffer was purchased together with the alkaline phosphatase enzyme FastAP from Thermo Scientific. It contains:

100mM Tris-HCl (pH 8.0)

50mM MgCl$_2$

1M KCl

0.2% Triton X-100

1mg/ml BSA

in ddH$_2$O.

TBE buffer

10× buffer was obtained from AppliChem and contains:

890mM Tris

890mM Boric acid

20mM EDTA-Na$_2$ × 2H$_2$O (pH 8.3)

in ddH$_2$O.

DNA gel loading dye

6× DNA gel loading dye contains:

30% (v/v) Glycerol

0.3% (w/v) Bromophenol Blue

0.3% (w/v) Xylene cyanol

in ddH$_2$O.

T4 DNA ligase buffer

10× buffer was purchased together with T4 DNA ligase enzyme from Thermo Scientific. It contains:

500mM Tris-HCl (pH 7.5)

100mM MgCl$_2$

100mM DTT

10mM ATP

250 µg/ml BSA

in ddH$_2$O.

Standard LB (Luria-Bertani) medium

Powder for LB medium was obtained from AppliChem and contains:

    10g/l Bacto-tryptone

    5g/l Yeast extract

    10g/l NaCl

with a pH range of 7.0-7.5. 20g powder were dissolved in 1l ddH_2O and sterilized by autoclaving for 20min at 121°C. If required, solution was subsequently cooled down to 50-60°C by stirring before adding appropriate antibiotics.

Salt-free LB (Luria-Bertani) medium

    10g/l Bacto-tryptone

    5g/l Yeast extract

(with a pH range of 7.0-7.5) were dissolved in ddH_2O and sterilized by autoclaving for 20min at 121°C.

LB (Luria-Bertani) agar

Powder for LB agar was purchased from AppliChem. It contains:

    10g/l Bacto-tryptone

    5g/l Yeast extract

    10g/l NaCl

    15g/l Bacto-agar

with a pH range of 7.0-7.5. 40g powder were dissolved in 1l ddH_2O. Further handling was analogous to standard LB medium. Petri dishes were filled with 20-25ml LB agar and air-dried for solidifying prior to inoculation.

2× HBS buffer

    50mM HEPES (pH 7.05 ± 0.05)

    140mM NaCl

    1.5mM Na_2HPO_4

were dissolved in 250ml ddH_2O and sterilized by filtering through the 0.22μm filter.

PBS buffer

10× DPBS buffer was obtained from Gibco and contains:

2g/l KCl

2g/l KH_2PO_4

80g/l NaCl

21.6g/l $Na_2HPO_4 \times 7H_2O$ (pH 6.7-7.0).

(Co-)precipitation buffer

10mM Tris-HCl (pH 8.0)

50mM NaCl

30mM $Na_4P_2O_7$

1mM Na_3VO_4

For cell lysis and protein binding, 1% (v/v) NP-40 and one tablet of protease inhibitor cocktail were freshly added to 25ml buffer. For sample washing during (co-)precipitation, 0.1% (v/v) NP-40 and one tablet of the protease inhibitor cocktail were freshly added to 33ml buffer.

Lysis buffer for protein purification

25mM Tris (pH 7.6)

150mM NaCl

25mM β-Glycerophosphate

25mM NaF

10mM $Na_4P_2O_7$

10% (v/v) Glycerol

0.75% (v/v) NP-40

Before use, 10mM β-mercaptoethanol, 1mM Na_3VO_4, and one tablet of protease inhibitor cocktail were freshly added to 25ml buffer.

Washing buffer for protein purification

25mM Tris (pH 7.6)

300mM NaCl

25mM β-Glycerophosphate

25mM NaF

10mM $Na_4P_2O_7$

10% (v/v) Glycerol

0.2% (v/v) NP-40

Before use, 10mM β-mercaptoethanol, 1mM Na_3VO_4, and one tablet of protease inhibitor cocktail were freshly added to 33ml buffer.

GST elution buffer

50mM Tris (pH 8.0)

20mM Glutathione

Before use, 1mM Na_3VO_4 and one tablet of protease inhibitor cocktail were freshly added to 33ml buffer. Upon elution, 10% (v/v) glycerol were added.

Bradford protein assay solution

Protein assay dye reagent concentrate was obtained from Bio-Rad. The 450ml solution contains dye, phosphoric acid, and methanol.

Laemmli sample buffer (Roti-Load1)

4× buffer was purchased from Carl Roth. It contains:

40% (v/v) Glycerol

20% (v/v) β-Mercaptoethanol

8% (w/v) SDS

0.015% (w/v) Bromophenol Blue,

which are phosphate-buffered with a pH range of 6.7-7.2.

SDS-PAGE stacking gel buffer

stock	4%
250mM Tris (pH 6.8), 0.2% SDS	7.5ml
ddH$_2$O	5.4ml
Acrylamide(30%)/bisacrylamide(0.8%)	1.95ml
TEMED	12µl
APS	112.5µl

SDS-PAGE separating gel buffer

stock	9%	10%	12%	15%
750mM Tris (pH 8.8), 0.2% SDS	15ml	15ml	15ml	22.5ml
ddH$_2$O	6ml	5.1ml	3.15ml	–
Acrylamide(30%)/bisacrylamide(0.8%)	9ml	9.95ml	12ml	22.5ml
TEMED	9µl	9µl	9µl	13.5µl
APS	300µl	300µl	300µl	450µl

SDS-PAGE running buffer

10× buffer was obtained from Carl Roth and contains:

0.25M Tris (pH 8.8)

1.92M Glycine

1% (w/v) SDS

in ddH$_2$O.

Coomassie staining buffer

1g Brilliant Blue G 250

100ml Acetic acid

450ml Methanol

were dissolved in 450ml ddH$_2$O.

Coomassie destaining buffer

140ml Acetic acid

500ml Methanol

were dissolved in 1,360ml ddH$_2$O.

Blotting buffer I – Anode buffer II

25mM Tris (pH 10.4)

10% (v/v) Methanol

were dissolved in 1l ddH$_2$O.

Blotting buffer II – Anode buffer I

300mM Tris (pH 10.4)

10% (v/v) Methanol

were dissolved in 1l ddH$_2$O.

Blotting buffer III – Cathode buffer

25mM Tris (pH 9.4)

40mM Glycine

10% (v/v) Methanol

were dissolved in 1l ddH$_2$O.

TBST buffer

10× TBS buffer was purchased from KPL. It contains:

0.5M Tris (pH 7.6)

1.5M NaCl.

Buffer was diluted in ddH$_2$O for 1× final concentration. For washing of nitrocellulose or PVDF membrane, 0.1% Tween 20 were added.

ECL solution I

    10ml Tris-HCl (stock 1M) (pH 8.5)

    1ml Luminol (stock 250mM, dissolved in DMSO)

    0.44ml Coumaric acid (stock 90mM, dissolved in DMSO)

were dissolved in 100ml ddH$_2$O.

ECL solution II

    10ml Tris-HCl (stock 1M) (pH 8.5)

    54.9µl Hydrogen peroxide

were dissolved in 100ml ddH$_2$O.

Stripping buffer

    62.5mM Tris-HCl (pH 6.7)

    2% (w/v) SDS

were dissolved in ddH$_2$O. Before use, 345µl β-mercaptoethanol were freshly added to 50ml buffer.

5.1.5 Plasmids

Plasmid/Vector	*Manufacturer*
Basic vectors	
pcDNA3	MSZ
pcDNA3.1/cMyc-his B	Invitrogen
pEBG-GST	MSZ
pUC19	Department of Microbiology
Expression plasmids	
pEF-cSrc-Y527F	Richard Marais
KRSPA-mLCK-hY505F	MSZ
KRSPA-mLCK-hK273E/hY505F	Claudia Sibilski
pcDNA3-hH-RAS-12V	MSZ

pcDNA3-mKSR1 wild type-his	MSZ
pcDNA3.1B-cMyc-hB-RAF wild type-his	Angela Baljuls
pcDNA3-hMEK1 wild type	MSZ
pcDNA3-hMEK1-K97M	MSZ
pEBG-GST-mKSR1 wild type-his	Claudia Sibilski
pEBG-GST-mKSR1-R649A-his	Claudia Sibilski
pEBG-GST-mKSR1-R649E-his	Claudia Sibilski
pEBG-GST-mKSR1-Y673F-his	Claudia Sibilski
pEBG-GST-mKSR1-Y673F/Y728F-his	Claudia Sibilski
pEBG-GST-mKSR1-S722A-his	Claudia Sibilski
pEBG-GST-mKSR1-S722D-his	Claudia Sibilski
pEBG-GST-mKSR1-Y728A-his	Claudia Sibilski
pEBG-GST-mKSR1-Y728E-his	Claudia Sibilski
pEBG-GST-mKSR1-Y728F-his	Claudia Sibilski
pEBG-GST-mKSR1-Y728H-his	Claudia Sibilski
Basic retroviral vectors	
MSCV-IRES-GFP	Robert Lewis
ψ-ecotropic packaging vector	Robert Lewis
Retroviral plasmids	
MSCV-mKSR1 wild type-FLAG-IRES-GFP	Robert Lewis
MSCV-mKSR1-Y728F-FLAG-IRES-GFP	Claudia Sibilski

5.1.6 Oligonucleotides

Primer name	Sequence (5'→3')
For cloning	
mKSR1_SpeI_for	GGACTAGTATGGATAGAGCGGCGTTGCG
mKSR1_NotI_rev	ATTTGCGGCCGCCTAATGGTGATGGTGATGGTG
For site-directed mutagenesis	
mKSR1_R649A_for	GCATTCATTCGTGGCGGACCCCAAGACGTCTCTGG

mKSR1_R649A_rev	CCAGAGACGTCTTGGGGTCCGCCACGAATGAATGC
mKSR1_R649E_for	GCATTCATTCGTGGAGGACCCCAAGACG
mKSR1_R649E_rev	CGTCTTGGGGTCCTCCACGAATGAATGC
mKSR1_Y673F_for	GGAGATCATCAAGGGCATGGGTTTTCTTCATGCAAAAGG
mKSR1_Y673F_rev	CCTTTTGCATGAAGAAAACCCATGCCCTTGATGATCTCC
mKSR1_S722A_for	GAGAACCAACTGAAACTGGCACATGACTGGCTGTG
mKSR1_S722A_rev	CACAGCCAGTCATGTGCCAGTTTCAGTTGGTTCTC
mKSR1_S722D_for	CGCGAGAACCAACTGAAACTGGACCATGACTGGCTGTGC
mKSR1_S722D_rev	GCACAGCCAGTCATGGTCCAGTTTCAGTTGGTTCTCGCG
mKSR1_Y728A_for	CTGGCTGTGCGCCCTGGCCCCCGAG
mKSR1_Y728A_rev	CTCGGGGGCCAGGGCGCACAGCCAG
mKSR1_Y728E_for	CTGGCTGTGCGAGCTGGCCCCCGAGATC
mKSR1_Y728E_rev	GATCTCGGGGGCCAGCTCGCACAGCCAG
mKSR1_Y728F_for	CTGGCTGTGCTTCCTGGCCCCCGAG
mKSR1_Y728F_rev	CTCGGGGGCCAGGAAGCACAGCCAG
mKSR1_Y728H_for	GGCTGTGCCATCTGGCCCCCGAGATCGTACG
mKSR1_Y728H_rev	CGTACGATCTCGGGGGCCAGATGGCACAGCC
mLCK_hK273E_for	GGTGGCGGTGGAGAGTCTGAAACAAGG
mLCK_hK273E_rev	CCTTGTTTCAGACTCTCCACCGCCACC
For sequencing	
mKSR1_inside11_rev	CTCGCCCATCGCTGCC
mKSR1_inside175_rev	GTCCATTTTGTGCTCCCCTCC
KSR376_for	CAAGAGCTCACACTGGATGCTC
KSR826_for	CCACCGCCAAGCCGCAAG
KSR1352_for	CTAATCCCTCCAGTGCCACC
KSR1877_for	GCATGAACCCACCTCACCTG
mLCK_H35_seqrev	GGCAGTTTTCACACACGTCAATGTTCTCC
hLCK_V178_seq	GGTGAAACATTACAAGATCC

mLCK_P211_seqrev	GGAAAAGTGATACGAGGGGAG

5.1.7 Enzymes

Enzyme	*Manufacturer*
DNA polymerases	
Taq (BioTherm)	Genecraft
PfuUltra	Agilent Technologies
FastAP (alkaline phosphatase)	Thermo Scientific
Restriction endonucleases	Thermo Scientific
DpnI	
NotI	
SpeI	
T4 DNA ligase	Thermo Scientific
Trypsin (TrypLE Express)	Gibco

5.1.8 Kits

Kit	*Manufacturer*
Plasmid DNA purification kits (Mini, Midi, Maxi)	Corning, Qiagen, Macherey-Nagel
QIAquick gel extraction kit	Qiagen
QIAquick PCR purification kit	Qiagen
Subcellular proteome extraction kit (ProteoExtract)	EMD Millipore

5.1.9 Antibodies

Antibody	*Manufacturer*
Primary antibody	
α-Actin (I-19), goat polyclonal	Santa Cruz Biotechnology
α-B-RAF (C-19), rabbit polyclonal	Santa Cruz Biotechnology
α-C-RAF (C-12), rabbit polyclonal	Santa Cruz Biotechnology
α-c-Src (32G6), rabbit monoclonal	Cell Signaling Technology
α-cMyc (9E10), mouse monoclonal	Santa Cruz Biotechnology
α-GFP (B-2), mouse monoclonal	Santa Cruz Biotechnology
α-GST (2946), rabbit polyclonal	Invitrogen
α-KDEL (10C3), mouse monoclonal	Santa Cruz Biotechnology
α-KSR1 (15), mouse monoclonal	BD Biosciences
α-KSR1 (H-70), rabbit polyclonal	Santa Cruz Biotechnology
α-LCK (3A5), mouse monoclonal	Santa Cruz Biotechnology
α-M2PK (DF4), mouse monoclonal	ScheBo Biotech
α-MEK1 (C-18), rabbit polyclonal	Santa Cruz Biotechnology
α-mKSR1-pTyr728 (IG-1258), rabbit polyclonal	immunoGlobe Antikörpertechnik
α-PARP (C-2-10), mouse monoclonal	EMD Millipore
α-pMEK1/2 (Ser217/221), rabbit polyclonal	Cell Signaling Technology
α-pTyr (4G10), mouse monoclonal	MSZ
α-RAS (18), mouse monoclonal	BD Biosciences
α-Vimentin (V9), mouse monoclonal	Santa Cruz Biotechnology
Secondary antibody (peroxidase-conjugated)	
α-goat IgG, donkey polyclonal	Dianova
α-mouse IgG, goat polyclonal	Dianova
α-rabbit IgG, goat polyclonal	Dianova

5.1.10 Bacterial strains and cell lines

Name	Source
Bacterial strains	
Escherichia coli DH10B (electrocompetent)	Department of Microbiology
Mammalian cell lines	
COS7 (fibroblast-like, monkey kidney tissue)	MSZ
HEK 293T (human embryonic kidney)	Department of Microbiology
KSR1$^{-/-}$ MEF (mouse embryonic fibroblast)	Robert Lewis

5.2 Methods

5.2.1 Microbiological methods

Generally, bacteria were grown overnight at 37°C in LB medium by shaking at 180rpm or on LB agar. Plasmid transformed bacteria were selected on LB agar containing appropriate antibiotics. Subsequently, single colonies were picked and inoculated in LB medium with selective antibiotics for further cultivation.

5.2.1.1 Preparation of electrocompetent bacteria

30ml salt-free LB medium were inoculated with *Escherichia coli* DH10B for overnight cultivation. Then, two times 14ml were diluted in 500ml salt-free LB medium for further bacterial growth until OD$_{600}$ reached a value of 0.6. Suspensions were centrifuged at 6,000×g for 15min at 4°C and supernatants were discarded. Bacteria were resuspended in 400ml ice-cold, sterile, deionized water and pelleted again. Cell pellets were washed again in 50ml ice-cold, sterile, deionized water and transferred into 50ml falcon tubes for an additional centrifugation step. Finally, bacterial pellets were dissolved in 2.5ml of 10% ice-cold and sterile glycerol and suspension was aliquoted in 50μl or 100μl samples. Aliquots were shock-frozen in liquid nitrogen and stored at -80°C.

5.2.1.2   Transformation of electrocompetent bacteria by electroporation

Frozen stocks of *Escherichia coli* DH10B were thawed on ice. 1-5μg DNA (a maximum ratio of DNA and bacterial suspension volume should not exceed 1:10) were added to a 50μl aliquot of electrocompetent cells and suspension was gently mixed by flicking. After incubation on ice for 1min, the mixture was transferred into an ice-cold electroporation cuvette and cells were porated at 1.8kV, 25μF, and 200W (program: bacteria, MicroPulser). Immediately, bacteria were gently diluted in 950μl salt-free LB medium, transferred into a sterile 1.5ml micro tube and stored on ice again, if several samples were electroporated. Bacterial suspension was shaken (1,000rpm) for 30-60min at 37°C. Then, cells were pelleted by centrifugation at 10,000rpm for 1min at room temperature. 800-900μl supernatant were discarded and cell pellet was resuspended in residual liquid. Finally, bacteria were plated on LB agar containing selective antibiotics. DNA was then extracted from resulting colonies (see chapter 5.2.2.5), and analyzed by outsourced DNA sequencing. For this, DNA concentration and quality were determined by using a spectrophotometer.

5.2.1.3   Verification of competence of prepared bacteria

Electrocompetence of prepared *Escherichia coli* DH10B was verified by transformation of the bacteria with a commercial control plasmid. 100μl bacterial suspension were gently mixed with 2μl pUC19 (stock 50pg/μl), electroporated, and mixed with 1ml salt-free LB medium. After shaking at 1,000rpm and 37°C for 2h, different dilutions of the bacteria were plated on LB agar (50μl of suspension, 50μl of a 1:100 dilution, and 50μl of a 1:1000 dilution). The next day, single colonies were counted and bacterial competence was calculated as follows: (colony number × suspension volume during shaking incubation) / (plated volume × dilution factor × DNA amount in μg). Electrocompetence was confirmed, if the number of bacteria/μg plasmid was between 10^7 and 10^9.

5.2.2   Molecular biological methods

5.2.2.1   *Primer design and DNA amplification by polymerase chain reaction (PCR)*

DNA fragments or entire plasmids can be amplified by polymerase chain reaction (PCR). Thereby, a thermostable DNA polymerase elongates DNA on a single strand by using oligonucleotides as priming sites. Oligonucleotides, so-called primers, are applied as (non-)complementary pairs (forward and reverse) in order to bind specifically to DNA for its amplification. Temperature for primer annealing during PCR is dependent on the length and the GC nucleotide content of oligonucleotides and needs to be set for each primer pair. Primer sequences can be also designed in order to integrate cleavage site(s) for restriction endonucleases or to replace nucleotide(s) for purposely achieving amino acid exchange(s) during translation for the expression of altered proteins.

For choosing the sequence of oligonucleotides, the following applies to consider. Primers are generally 20-30bp long with a melting temperature (T_m) of about 10°C above elongation temperature during PCR and bind to one strand upstream and (non-)complementary to the opposite strand downstream. T_m of flanking primers should not differ by more than 5°C. Mutagenic primers should be 25-45bp long, anneal to the same sequence on opposite DNA strands, and contain desired mutation in the middle of the primer with 10-15 bases of correct sequence on both sides. Generally, the following formula is recommended for estimating the oligonucleotide melting temperature in order to design oligonucleotides: T_m = 81.5 + 0.41(%GC) − 675/N − %mismatch (%GC represents GC content of the primer, N is the primer length in bases). Value of %mismatch is needed in the case of designing mutagenic primers. For others, same formula can be used without the value of %mismatch. Furthermore, it is recommended that oligonucleotides terminate in one or more C or G bases and are purified by either fast polynucleotide liquid chromatography (FPLC) or polyacrylamide gel electrophoresis (PAGE). Primer dimerization (annealing of oligonucleotide pair with each other) could be avoided by evading complementary structures for more than 2bp.

PCR master mix was assembled for several samples in a 1.5ml micro tube on ice. Reaction mix for one sample was composed of the following ingredients (30μl total volume):

Template DNA (20ng dilution)	1μl
Primer forward (10pmol/μl)	1μl
Primer reverse (10pmol/μl)	1μl
dNTP mix (10mM each)	1μl
DNA polymerase (preferentially *PfuUltra*)	1μl
10× DNA polymerase reaction buffer	3μl
DMSO	3μl
ddH₂O	19μl

PCR master mix for bacteria clone screening upon ligation of insert and vector (see chapter 5.2.2.4) was similarly assembled for several samples on ice. Reaction composition for one sample was as follows (20μl total volume):

DNA/bacterial colony	–
Primer forward (100pmol/μl)	0.2μl
Primer reverse (100pmol/μl)	0.2μl
dNTP mix (10mM each)	0.4μl
DNA polymerase (preferentially *Taq*)	0.1μl
10× DNA polymerase reaction buffer	2μl
DMSO	2μl
ddH₂O	15.1μl

Generally, the PCR is organized in three repeating main steps: *i)* DNA denaturation for obtaining single stranded DNA, *ii)* primer annealing, and *iii)* DNA elongation for completing the new DNA strands. The elongation time is dependent on both the properties of the used DNA polymerase (extension times are generally 1,000bp/min) and the length of the template DNA. As an example, for amplifying the mKSR1-his insert (2,600bp), PCR was performed with PfuUltra DNA polymerase and the fragment was elongated over a period of 3.5min inclusive 1min extra

for completing elongation. DNA is exponentially amplified by PCR due to DNA doubling in every running cycle.

For amplifying the mKSR1-his insert, PCR was performed as follows:

	Temperature	*Time*	
Start denaturation	95°C	3min	
Denaturation	95°C	30sec	
Annealing	50-60°C	30sec	× 35
Elongation	68/72°C	3.5min	
Final elongation	68/72°C	10min	
End	4°C	∞	

5.2.2.2 Enzymatic digestion of DNA

Double-stranded DNA is specifically cleaved by respective restriction endonucleases. Blunt or overhanging, complementary, so-called sticky ends can be created. In order to prevent DNA refusion during ligation of mKSR1-his insert with pEBG empty vector, two different restriction endonucleases were used (SpeI and NotI). Reaction composition for one sample was prepared in a 1.5ml micro tube on ice as follows (40µl total volume):

Insert or vector DNA (1µg dilution)	1µl
Restriction endonucleases	1-2µl
10× buffer for restriction endonucleases	8µl
(buffer Tango or buffer O)	
Nuclease-free ddH$_2$O	29-30µl

The mixture was incubated for 2h at 37°C. Restriction endonucleases were inactivated by incubation for 20min at 65°C. In order to prevent religation, vector DNA was treated with thermosensitive FastAP (alkaline phosphatase) for dephosphorylating the linearized vector.

Digestion sample containing vector DNA	40μl
FastAP	1μl
10× FastAP buffer	4.5μl

The mixture was incubated for 30min at 37°C and alkaline phosphatase was inactivated by incubation for 20min at 85°C. For removing the enzymes and buffers, samples were either loaded on a gel separating the DNA by agarose gel electrophoresis (see chapter 5.2.2.3), therefor, DNA gel loading dye was added to the reaction samples of insert and vector DNA, or samples were purified by use of the QIAquick PCR purification kit according to manufacturer's protocols.

5.2.2.3 *Agarose gel electrophoresis of DNA*

According to their charge and size (0.5-10kb), double-stranded DNA fragments and plasmids become separated by agarose gel electrophoresis. For gel preparation, agarose was dissolved in 1× TBE buffer with a final concentration of 0.8-2% agarose. The mixture was boiled until the agarose was dissolved in buffer. By gently shaking, the solution was cooled down to 50-60°C before pouring it into the electrophoresis chamber; a casting tray with a sample comb (different sizes are available). Subsequently, ethidium bromide (up to a concentration of 0.5μg/ml) was added and gently mixed. After gel solidification at room temperature, the comb was removed from the gel and DNA samples supplemented with DNA gel loading dye were poured into formed wells. Agarose gel electrophoresis was performed in 1× TBE buffer at 120-140V for 30-60min until required separation of DNA fragments occurred. Based on the incorporation of ethidium bromide into the DNA double strand, DNA molecules were visualized by ultraviolet light. If required, agarose gel pieces containing DNA of interest were then removed with a sterile scalpel for purifying DNA from the agarose gel by use of the QIAquick gel extraction kit according to manufacturer's protocols.

5.2.2.4 Ligation of DNA fragments

For enzymatic ligation of purified, linearized, double-stranded DNA an insert:vector DNA ratio of 6:1 was utilized, thereby, the size of insert and vector were considered: about 165ng insert DNA (mKSR1-his: 2,600bp) and 50ng vector DNA (pEBG: 6,000bp) were used. Ideally, DNA fragments should have sticky ends.

Reaction for one sample was prepared in a 1.5ml micro tube on ice and was composed of the following components (20μl total volume):

Insert DNA/water control	1μl
Vector DNA	1μl
T4 DNA ligase	1μl
10× T4 DNA ligase buffer	2μl
Nuclease-free ddH$_2$O	15μl

The mixture was incubated for 2-3h at room temperature or overnight at 16°C. Subsequently, T4 DNA ligase was inactivated for 10min at 65°C. 2μl ligation sample were transformed into 100μl electrocompetent *Escherichia coli* DH10B. DNA extracted from resulting colonies was analyzed by PCR (see chapters 5.2.2.1 and 5.2.2.5) and then by outsourced DNA sequencing.

5.2.2.5 Plasmid DNA preparation from competent bacteria

Plasmid DNA was amplified by cultivating transformed bacteria overnight in LB medium containing appropriate antibiotics: 3ml for Mini, 50ml for Midi, and 200ml for Maxi high copy plasmid DNA purification (for low copy plasmids equivalently more medium was utilized). Plasmid DNA purification was performed according to manufacturer's protocols and, subsequently, DNA concentration and quality were determined by using a spectrophotometer.

5.2.2.6 *Site-directed mutagenesis*

To obtain amino acid exchanges, deletions or insertions, single or multiple DNA nucleotides were substituted by site-directed mutagenesis according to manufacturer's instructions (QuikChange site-directed mutagenesis by Stratagene). Double-stranded plasmid DNA (vector with insert) was thoroughly amplified by PfuUltra DNA polymerase during PCR. Mutagenic primers were specifically designed (see chapter 5.2.2.1).

Reaction for one sample was prepared in a 1.5ml micro tube on ice and composed of the following ingredients (50μl total volume):

Template DNA (50ng dilution)	1μl
Primer forward (10pmol/μl)	1μl
Primer reverse (10pmol/μl)	1μl
dNTP mix (10mM each)	1μl
PfuUltra DNA polymerase	1μl
10× DNA polymerase reaction buffer	5μl
DMSO	5μl
ddH₂O	35μl

PCR for site-directed mutagenesis of pEBG-GST-mKSR1 wild type-his was performed as follows:

	Temperature	*Time*	
Start denaturation	95°C	3min	
Denaturation	95°C	30sec	
Annealing	55-60°C	1min	× 25
Elongation	68/72°C	9.5min	
Final elongation	68/72°C	10min	
End	4°C	∞	

In order to select for pure, linearized DNA carrying desired mutation(s), the (hemi-)methylated, parental, non-mutated template DNA was digested by adding 1μl DpnI (restriction endonuclease) to the mutagenesis sample and incubating the sample for 2h at 37°C. DpnI was inactivated by incubation for 20min at 80°C. Subsequently, 100μl electrocompetent *Escherichia coli* DH10B were transformed with 10μl mutagenesis sample and plated on LB agar containing appropriate antibiotics. DNA extracted from resulting colonies (see chapter 5.2.2.5) was tested for mutation(s) by outsourced DNA sequencing.

5.2.3   Biochemical methods

5.2.3.1   *Preparation of cell lysates*

For preparation of cell lysates, 10cm-dishes with 100%-confluent eukaryotic cells were washed twice with 5ml ice-cold PBS buffer before being scraped off in 1ml ice-cold (co-)precipitation buffer complemented with 1% (v/v) NP-40 and protease inhibitors. Samples were then transferred into a pre-chilled 1.5ml micro tube and cell lysis was completed by rotating the samples for 1h at 4°C. Cell lysates were clarified by centrifugation at 16,100×g for 15min at 4°C. Supernatants were transferred into clean 1.5ml micro tubes and pellets were discarded. Lysates were used for (co-)precipitation assay or directly analyzed by SDS-PAGE.

5.2.3.2   *Subcellular fractionation*

Distribution of proteins within the different cell compartments was analyzed by fractionation using the subcellular proteome extraction kit according to manufacturer's protocol for suspension-grown tissue culture cells. For fractionation, 10cm-dishes with 100%-confluent COS7 cells were utilized. Cells were harvested as described in chapter 5.2.3.4. A stepwise extraction of the subcellular proteomes by taking advantage of the different solubilities of certain compartments delivers four protein fractions from one sample: cytosolic, membrane/organelle, nucleic, and cytoskeletal fraction. The selectivity of subcellular fractionation was confirmed by SDS-PAGE and Western Blot analysis using specific marker proteins: M2PK (for cytosolic fraction), KDEL (for membrane/organelle fraction), PARP (for nucleic fraction), and Vimentin (for cytoskeletal fraction).

5.2.3.3 (Co-)Precipitation of proteins by GST pull-down assay

In order to isolate and enrich exogenously expressed GST-tagged proteins of interest by precipitation, glutathione-sepharose beads were used due to their high affinity for GST. In addition, protein-protein interactions were investigated by analyzing quality and quantity of coprecipitated proteins. For GST pull-down, glutathione-sepharose was washed two times with ddH$_2$O and one time with fully complemented buffer used for cell lysis. After each step, beads were collected by centrifugation at 800×g for 1min at 4°C. After the third wash, 160μl beads (50% slurry in (co-)precipitation buffer) were added to the prior prepared cell lysates (see chapter 5.2.3.1). Beads were incubated with lysates for 2-5h at 4°C under gentle rotation. Subsequently, protein-loaded beads were collected by centrifugation at 800×g for 3min at 4°C and washed thrice in (co-)precipitation buffer supplemented with 0.1% (v/v) NP-40 and protease inhibitors. Finally, beads were dried by removing all the liquid and resuspended in 80μl Laemmli sample buffer. Samples were boiled for 5min at 100°C and analyzed by SDS-PAGE and immunoblotting.

5.2.3.4 Purification of GST-tagged proteins

GST-fused proteins can be purified from bacteria, insect cells or mammalian cells upon exogenous expression. Similar to the protocol of the GST pull-down assay, GST-tagged proteins of interest were isolated and enriched by binding to glutathione-sepharose beads. By adding free glutathione to the mixture, proteins were released from the beads.

For purification of GST-KSR1 from mammalian cells, twenty-five 10cm-dishes of 80-90%-confluent COS7 cells were transfected with 6μg mKSR1 and either 2μg kinase-active LCK-Y505F or active RAS-12V per dish (method of transient transfection see chapter 5.2.4.3). 24h post-transfection, each plate was washed with 5ml pre-warmed PBS buffer and cells detached by adding 1ml trypsin. After 10min of incubation at 37°C, trypsinization was stopped by adding 5ml complete medium. Cells were then pooled in two 50ml falcon tubes and pelleted at 200×g for 8-10min at room temperature. Supernatants were carefully removed and cells were washed with 10ml room temperatured PBS buffer. Subsequently, cells were collected again by centrifugation, quick-frozen in liquid nitrogen, and stored at -80°C.

For lysis, cells were thawed on ice and resuspended in 12ml lysis buffer for protein purification (in total, per sample) supplemented with β-mercaptoethanol, sodium orthovanadate, and protease inhibitors. Cells were then transferred into a pre-chilled 15ml falcon tube and incubated with gentle rotation for 1h at 4°C. Cell lysates were clarified by centrifugation at 16,100×g for 15min at 4°C. Supernatants containing GST-tagged KSR1 protein were transferred into a clean 15ml falcon tube and pellets were discarded. 150µl cell lysate were taken for protein expression control by SDS-PAGE (see chapter 5.2.3.6). In order to purify GST-tagged mKSR1 proteins, clarified cell lysates were incubated with 2ml glutathione-sepharose beads (50% slurry), which were prepared before as described in chapter 5.2.3.3. After 2h of incubation on rotator at 4°C, 150µl suspension were taken for binding control. Subsequently, beads were washed three times with 10ml washing buffer for protein purification complemented with β-mercaptoethanol, sodium orthovanadate, and protease inhibitors by rotating for 10min at 4°C. Upon each washing step, beads were collected by centrifugation at 800×g for 3min at 4°C. After the third washing steps, beads were resuspended and poured into a glass chromatography column. The 15ml falcon tube was washed once with fully complemented washing buffer for protein purification and suspension was loaded onto the column. For resuspending the beads and washing the falcon tube, 10ml buffer were used in total. Beads were then sedimented by running the solution through the valve by gravity flow. Sepharose-bound GST-mKSR1 proteins were eluted three times with 1ml GST elution buffer. Drops were collected in several fractions (300µl aliquots) and 40µl glycerol were added to each fraction. The purity of recombinant mKSR1 was documented by SDS-PAGE followed by Western Blot analysis and staining with coomassie blue (see chapters 5.2.3.6 and 5.2.3.7). For protein staining, SDS-PAGE gel was incubated in coomassie staining buffer for 30-60min at room temperature with gentle shaking. Finally, gel was destained in coomassie destaining buffer overnight and results were documented with a gel scanner the next day.

5.2.3.5 *Bradford protein assay*

To measure protein concentrations of purified samples a colorimetric reagent (Bradford protein assay solution) was utilized. Dependent on the protein concentration of the sample the absorbance maximum for the acidic dye shifts from 465nm (reddish/brown) to 595nm (blue),

when protein binding occurs. This assay was performed in 1.5ml micro tubes. A known concentration of bovine serum albumin (BSA) was used as standard. For measuring the protein concentration, 1ml Bradford reagent was mixed with 10-30μl sample and incubated for 5min at room temperature in the dark. Colorimetric shift was measured with an UV/Vis photometer at 595nm wavelength. Final protein concentration was calculated by correlating obtained values to BSA standard curve. Alternatively, the protein concentration was estimated by loading a known concentration of BSA next to the protein sample(s) on an SDS-PAGE gel for coomassie staining (details see 5.2.3.4 and 5.2.3.6).

5.2.3.6   *Sodium dodecyl sulfate polyacrylamide gel electrophoresis (SDS-PAGE)*

For SDS-PAGE, which is used to separate proteins according to their molecular weight under denaturing conditions, protein samples were mixed with Laemmli sample buffer (1-2× final concentration) and boiled for 5min at 100°C. For protein denaturation, Laemmli sample buffer mainly contains both β-mercaptoethanol, which reduces disulfide bonds, and SDS, an anionic detergent that disrupts non-covalent interactions of native proteins and provides them with a highly negative charge. Vertical gels were set in between two glass plates with a spacer of 1.5mm thickness. The upper part of the gel, the stacking gel (4% acrylamide), ensures a simultaneous protein entry into the lower part, the separating gel (9-15% acrylamide), which segregates proteins by their negative charge representing their appropriate molecular weight. Thereby, the protein size affects the speed of migration through the gel. At first, ingredients for the separating gel (see chapter 5.1.4) were mixed and loaded. The top was covered by isopropanol to prevent drying of the surface, which was removed upon polymerization. Then, ingredients for the stacking gel (see chapter 5.1.4) were mixed and loaded. During polymerization, the stacking gel contained a sample comb (different sizes were used) for generating sample wells. The sample comb was removed shortly before loading the protein samples onto the gel. SDS-PAGE was performed in SDS-PAGE running buffer at 80-180V for 1.5-3h until adequate separation of proteins occurred.

5.2.3.7 *Immunoblotting*

Following protein separation by SDS-PAGE, immunoblotting (alternatively called Western Blot) is used in order to detect specifically proteins of interest in a given sample. Here, proteins were transferred to a nitrocellulose or PVDF membrane (latter needs to be activated in 100% methanol for a short while) by semi-dry electroblotting at about 30V for 2h. Blotting sandwich was composed of two layers of whatman paper soaked with blotting buffer II, one layer of whatman paper soaked with blotting buffer I, the transfer membrane, the gel (glass plates were removed and stacking gel trimmed away), and three layers of whatman paper soaked with blotting buffer III. Each layer was incubated in the relevant solution for a short while before assembling; the equilibration of the transfer membrane occurred in blotting buffer I and of the gel in blotting buffer III. By carefully rolling a glass tube over the surface of the layers air bubbles were removed for ensuring a constant protein transfer. During electroblotting, negatively charged proteins were transferred from the gel onto the membrane due to their movement to the anode. To prove blotting quality, the transfer membrane was stained with Ponceau-S for 5min. Excessive staining was removed by washing the membrane in ddH$_2$O. The membrane was blocked in TBST buffer containing 10% nonfat milk for 1h at room temperature. Before incubating with the primary antibody solution (relevant antibodies were diluted 1:200-1:10,000 in TBST buffer) overnight at 4°C, the membrane was washed three times (10min each) with TBST buffer. Primary antibodies specifically bind to antigens/proteins coupled to the transfer membrane. On the next day, before and after the incubation with the secondary antibody solution (respective antibodies were diluted 1:10,000 in TBST buffer complemented with 10% nonfat milk) for 1h at room temperature, the membrane was washed three times (10min each) with TBST buffer. Peroxidase-coupled secondary antibodies specifically interact with primary antibodies. Finally, standard enhanced chemiluminescence (ECL) reaction was performed by mixing self-made or bought ECL solution I with II (1:1) and covering the transfer membrane for 1-5min. Based on the peroxidase-catalyzed oxidation of luminol (part of ECL solution I) the emission of light was detected by x-ray films or a chemiluminescence imager representing targeted detection of proteins of interest. Coupled proteins can be redetected upon removal of bound antibodies by stripping the transfer membrane (see chapter 5.2.3.8).

5.2.3.8 Stripping of immunoblots

Proteins of interest coupled to transfer membranes can be redetected. For this, prior primary antibodies, which are directly bound to antigens/proteins on the surface of the membrane, have to be removed in order to detect the same proteins with alternative antibodies (e.g. from a different company or clone or another type of antibodies like antibodies against (non-)phosphorylated proteins). This procedure is named stripping. Upon ECL reaction, the transfer membrane was washed for at least 10min in TBST buffer and incubated with stripping buffer containing SDS and β-mercaptoethanol for 30min at 60°C in order to abolish antigen-antibody interactions (the dish containing membrane and stripping buffer was gently shaken every 10min). Subsequently, membrane was washed three times (10min each) with TBST buffer. After stripping, the transfer membrane was blocked again with TBST buffer containing 10% nonfat milk for 1h at room temperature. If a PVDF membrane was used and dried meanwhile, the membrane was reactivated in 100% methanol awhile and washed again before blocking. Finally, proteins of interest were redetected according to chapter 5.2.3.7.

5.2.3.9 Mass spectrometry analysis

Mass spectrometry (MS) is an analytical technique that determines elemental or isotopic characteristics of samples and masses of particles or molecules (such as peptides and other chemical compounds) in order to provide information about their chemical structure by classifying identified masses into known masses or a characteristic fragmentation pattern.

MS analysis of purified GST-mKSR1 wild type (coexpressed with LCK-Y505F or RAS-12V in COS7 cells, see chapter 5.2.3.4) was performed by Laxmikanth Kollipara and Dr. René P. Zahedi (Leibniz-Institut für Analytische Wissenschaften – ISAS – e.V., Dortmund, Germany) as previously described (186). In short, for detecting and characterizing novel phosphorylation sites in murine KSR1, samples of purified protein were digested in gel or in solution and phosphopeptides were enriched for the final LC-MS/MS analysis followed by MS data processing and interpretation.

5.2.4   Cell biological methods

5.2.4.1   Cultivation and seeding of eukaryotic cells

Adherent cells were cultivated in flasks at 5% CO_2, 37°C, and 95% humidity (cell culture incubator). COS7 cells and HEK 293T grew in DMEM supplemented with 10% FBS and 2% penicillin/streptomycin. Immortalized KSR1$^{-/-}$ MEFs were cultured in DMEM containing 10% FBS, 1% penicillin/streptomycin, and 0.1mM minimum essential medium with non-essential amino acids (MEM with NEAA). Cell culture work was performed under sterile conditions within a biological safety cabinet. Most used solutions (medium, supplements, PBS buffer, trypsin etc.) were pre-warmed at 37°C.

For passaging, medium was removed and mammalian cells were washed once with sterile PBS buffer. In order to detach cells, trypsin was added until surface was covered. After the cells were incubated for 5-10min in the cell culture incubator, suspension of detached cells was mixed with fresh DMEM containing supplements, which inactivated trypsin. Cells were splitted by the desired ratio and cultivated again as described above.

In order to seed a certain number of cells, cell counts in solution were calculated. Using Bürker's cell counting chamber (glass slide that have a grid pattern etched upon it and a removable cover slip on top) under the microscope, five squares were counted and mean value was calculated. Here, each square with a surface area of 1mm^2 represents a depth of 0.1mm giving a total volume of one square of 0.1mm^3 (= 10^{-4}cm^3 = 10^{-4}ml). By use of the following formula, cell count/ml was calculated: total number of counted cells / (five squares × 10^{-4}ml). Subsequently, the total number of cells could be extrapolated. Desired cell count was seeded in appropriate medium and cells were cultivated as described in this chapter.

5.2.4.2   Freezing and thawing of cell lines

Detached cells in suspension were counted before centrifugation at 200×g for 10min at room temperature (for details see chapter 5.2.4.1). Cell pellet was gently suspended in medium containing 70% complete medium, 20% FBS, and 10% DMSO. A concentration of 10^6-10^7 cells/ml is recommended. Then, 1ml suspension was transferred into a cryotube and stored for at least 24h at -80°C. Here, a polystyrene box was used for a slow cooling process in

order to avoid ice crystal formation within cells. For long-term storage, cryotubes were then transferred to liquid nitrogen.

For fast-thawing, frozen cells were defrosted by incubating the cryotube in a water bath with 37°C. Subsequently, cell suspension was mixed with 1ml pre-warmed FBS and transferred into a prepared 15ml falcon tube containing 10ml pre-warmed complete medium. Suspension was then centrifuged at 200×g for 10min at room temperature. Upon gentle removal of the supernatant, cell pellet was carefully resuspended in appropriate complete medium and cultivated as described in chapter 5.2.4.1.

5.2.4.3   *Transient transfection of eukaryotic cells*

In order to introduce plasmid DNA into adherent mammalian cells, the method of transient transfection was used according to Polyplus transfection's protocol. Here, polyethylenimine (PEI), a linear polymeric and polycationic reagent, transforms DNA into positively charged particles. As a result, DNA can bind to the surface and enter the cell, where it is released upon endosome osmotic swelling and rupture, and DNA is then free to diffuse to the nucleus.

24h prior to transfection, cells were seeded to obtain a confluence of 80-90% the next day. For transfecting cells in a 10cm-dish, 8μg desired recombinant DNA were diluted in 500μl NaCl (stock 150mM) in one 1.5ml micro tube per sample. Respectively, 16μl PEI and 500μl NaCl (stock 150mM) were mixed per sample. For the latter, a master mix was prepared. Tubes were mixed by vortexing for 10sec. Then, 500μl PEI-NaCl suspension were carefully added to the DNA-NaCl mix. Final solution was mixed again by vortexing for 10sec and incubated for 30min at room temperature. In the meantime, medium was either replaced by fresh complete medium or removed and cells were washed with 5ml pre-warmed PBS buffer before adding 10ml serum-free or serum-reduced medium (starvation condition: 0.5% FBS). Subsequently, 1ml DNA-PEI-NaCl suspension was added drop-wise to the plate with seeded cells and solution was homogenized by gently swirling the plate. 24h post-transfection, cells were treated as described above (see chapters 5.2.3.1 to 5.2.3.4).

5.2.4.4 *Viral infection and FACS sorting for generation of stable cell lines*

For generating stable cell lines, plasmid DNA was introduced into eukaryotic cells using retroviruses. MSCV-mKSR1-Y728F-FLAG-IRES-GFP was obtained by substitution of tyrosine at the position 728 in murine KSR1 wild type by phenylalanine using site-directed mutagenesis (for details see chapter 5.2.2.6). Three different cell lines were generated by viral infection: KSR1$^{-/-}$ MEFs stably expressing empty vector and exogenous mKSR1 wild type as well as mKSR1-Y728F.

For retrovirus production, $10\text{-}12\times10^6$ HEK 293T were seeded in 20ml DMEM supplemented with 10% FBS and 1% penicillin/streptomycin on two 15cm-dishes, 24h prior to transfection. 22.5μl expression plasmid and 22.5μl ψ-ecotropic packaging vector (stock 1μg/μl each) were mixed in a tube. 400μl CaCl$_2$ (stock 2.5M) and 1.6ml ddH$_2$O were added by gently pipetting. 2ml 2× HBS buffer were added drop-wise to the DNA mixture while bubbling with a Pasteur pipette. When finished, bubbling was continued for 30sec. Before adding drop-wise the transfection mixture all over the plate with seeded cells, suspension was left for 15min at room temperature. Finally, plate was gently swirled for homogenization and incubated at 37°C. At the earliest 6h post-transfection, medium was replaced by 20ml pre-warmed complete medium. 48 and 72h post-transfection, viral supernatants were harvested by transferring into a 50ml falcon tube and centrifuging at 3,500rpm for 15min at 4°C. Supernatants were then filtered through a 0.45μm filter. Flow-throughs were pooled and stored at 4°C awhile. For long-term storage, viral supernatants were concentrated. Therefor, filtered supernatant was transferred to two tubes for ultracentrifugation. Tubes were filled up with complete medium and balanced. Using the SW 32 Ti rotor, viruses were pelleted at 30,000rpm for 120min at 4°C. Supernatants were carefully aspirated and tubes were left upside down on a tissue for 10min. Pelleted viruses were resuspended in 1-2ml sterile ice-cold PBS buffer and aliquoted in 200μl samples.

24h prior to infection, KSR1$^{-/-}$ MEFs were seeded in 10cm-dishes. Then, medium was replaced by a mixture of 6ml viral supernatant, 4ml complete medium, and 6μg/ml polybrene (stock 4μg/μl). Due to the facts that virus-infected MEFs expressed green fluorescence protein (GFP) and that the GFP expression was proportional to the KSR1 expression level, cells were cultivated until they reached a suitable amount for FACS sorting (approximately one week).

In order to sort cells of different levels of KSR1 expression by FACS, MEFs were detached by treatment with trypsin (as described in chapter 5.2.4.1) and filtered through the membrane of a FACS tube to avoid cell aggregate formation. Based on different levels of GFP expression, cells were sorted according to fluorescence signal with the BD FACS Aria III Cell Sorter. Uninfected cells were used for measuring baseline fluorescence. Upon sorting, cells were cultivated as described in chapter 5.2.4.1. Levels of protein expression were confirmed by SDS-PAGE followed by immunoblotting (see chapter 5.2.3.6 and 5.2.3.7).

5.2.4.5   *Proliferation assay of adherent cells*

The proliferation of generated MEF cells stably expressing empty vector, mKSR1 wild type, and mKSR1-Y728F was performed and analyzed as previously described (186).

5.2.5   Bioinformatic methods

5.2.5.1   *3D structure modeling and MD simulations of the kinase domain of murine KSR1*

Based on the template structure of human KSR2 in complex with rabbit MEK1 (165) the three-dimensional structure of the kinase domain of murine KSR1 was modeled by Prof. Thomas Müller (Department of Molecular Plant Physiology and Biophysics, Julius-von-Sachs Institute for Biosciences, University of Würzburg, Germany) as previously described (186). Additionally, simulations of molecular dynamics (MD) of the mKSR1 kinase domain were performed and analyzed by Prof. Thomas Müller as published.

5.2.5.2   *Statistical analysis*

Statistical analysis is based on two or three independent experiments. Data are presented as mean ± SD of the respective measured parameters. *P* values: ns (not significant), ≥ 0.05; * (significant), $P < 0.05$; ** (highly significant), $P < 0.01$; *** (extremely significant), $P < 0.001$ versus corresponding WT control.

6 RESULTS

6.1 LCK is involved in regulation of KSR1 function

In its amino acid sequence and pattern of regulation, KSR1 shows a high homology to RAF kinases, which are known to be regulated by Src family kinases (SFKs) c-Src and LCK (phosphorylation of C-RAF on Tyr340/341 and A-RAF on Tyr301/302) (72, 87, 187). Therefore, possible regulation of KSR1 by SFKs has been hypothesized.

6.1.1 KSR1 phosphorylation is induced by direct binding to LCK

In order to test whether SFKs are involved in the regulation of KSR1, the binding of LCK to KSR1 and the tyrosine phosphorylation of KSR1 were investigated by coprecipitation assays (GST pull-down). To this end, GST-fused KSR1 was coexpressed with kinase-active (Y505F) or kinase-inactive (K273E/Y505F) LCK mutants in COS7 cells. Upon cell lysis, GST-KSR1 was precipitated with glutathione-sepharose beads. As shown in Fig. 12*A*, kinase-active LCK associates with KSR1 for tyrosine phosphorylation, whereas no tyrosine phosphorylation was found in the KSR1 sample coexpressed with kinase-inactive LCK, despite equal binding properties. Cell treatment with an allosteric LCK inhibitor (100μM of LCK inhibitor III), two hours prior to cell harvesting, confirmed obtained results. Although the LCK inhibitor stabilized the interaction of KSR1 with LCK, it completely abolished the LCK-induced tyrosine phosphorylation of KSR1 (see Fig. 12*B*).
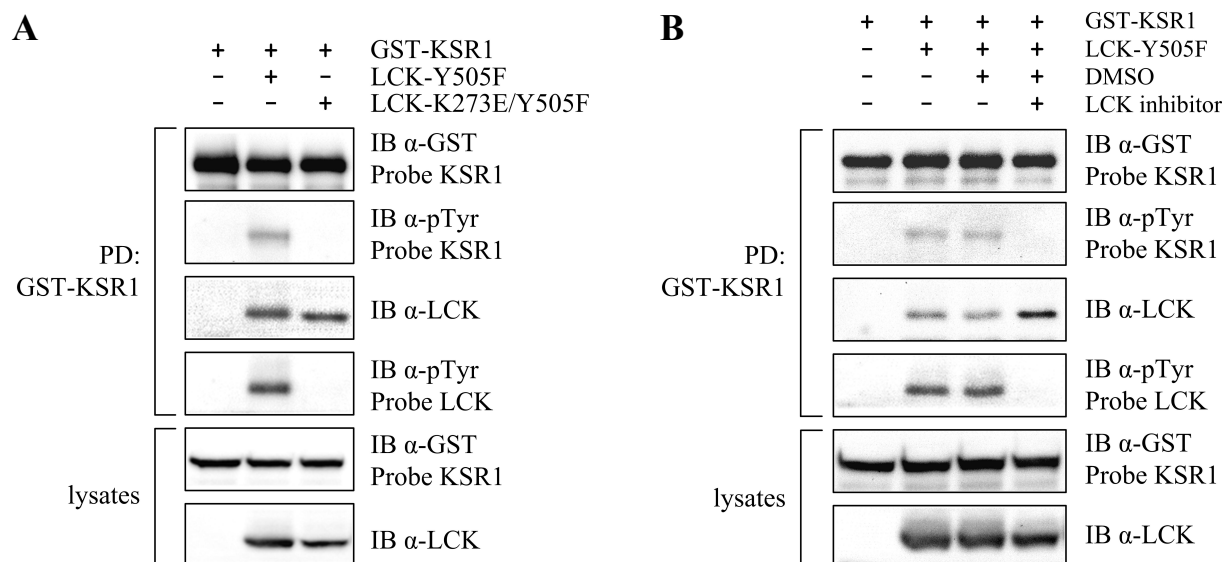
FIGURE 12: Kinase-active LCK interacts with KSR1 for its phosphorylation on tyrosine residue(s). *A*, COS7 cells were transfected with GST-KSR1 together with kinase-active (Y505F) or kinase-inactive (K273E/Y505F) LCK mutants. Upon cell lysis, GST-tagged KSR1 was precipitated with glutathione-sepharose beads and tested for binding of LCK and induced tyrosine phosphorylation. Amounts of (co)precipitated proteins were determined using appropriate antibodies. Tyrosine phosphorylation of KSR1-bound LCK (self-activation) and LCK-mediated tyrosine phosphorylation of precipitated GST-KSR1 were detected using an anti-phospho-tyrosine antibody. *B*, GST-tagged KSR1 was coexpressed with LCK-Y505F in COS7 cells. Upon treatment of the cells with LCK inhibitor (100μM) or solvent (DMSO) two hours prior to cell harvesting, KSR1 was precipitated via its GST-tag and tested for binding of LCK and for tyrosine phosphorylation of LCK and KSR1. Amounts of (co)precipitated proteins and levels of tyrosine phosphorylation were determined using appropriate antibodies. *PD*, GST pull-down; *IB*, immunoblot; *α*, anti.

6.1.2 KSR1 recruits LCK to the cytoskeleton

LCK is primarily anchored to the plasma membrane by myristoylation and palmitoylation in addition to its non-covalent association with the cytoplasmic domains of the cell surface glycoproteins CD4 and CD8 (57, 62, 188). In contrast, KSR proteins are mainly localized in the cytoplasm. A fraction of KSR is also targeted to actin filaments by several cytoskeleton-associated proteins like LSP1, FHOS, and FHL3 (189). To answer the question, in which cellular compartment the interaction between KSR1 and LCK and the phosphorylation of KSR1 by LCK may take place, subcellular fractionation was performed. Therefore, GST-fused KSR1 was expressed in COS7 cells in the presence or absence of LCK and vice versa. Upon lysis, subcellular fractions (cytosolic, membrane/organelles, nuclear, and cytoskeletal fraction) were extracted. This approach revealed that subcellular distribution of KSR1 is not significantly

altered by coexpression of LCK, while LCK localization at the cytoskeleton is strongly increased when KSR1 is coexpressed (Fig. 13) suggesting that KSR1 recruits LCK to cytoskeleton.
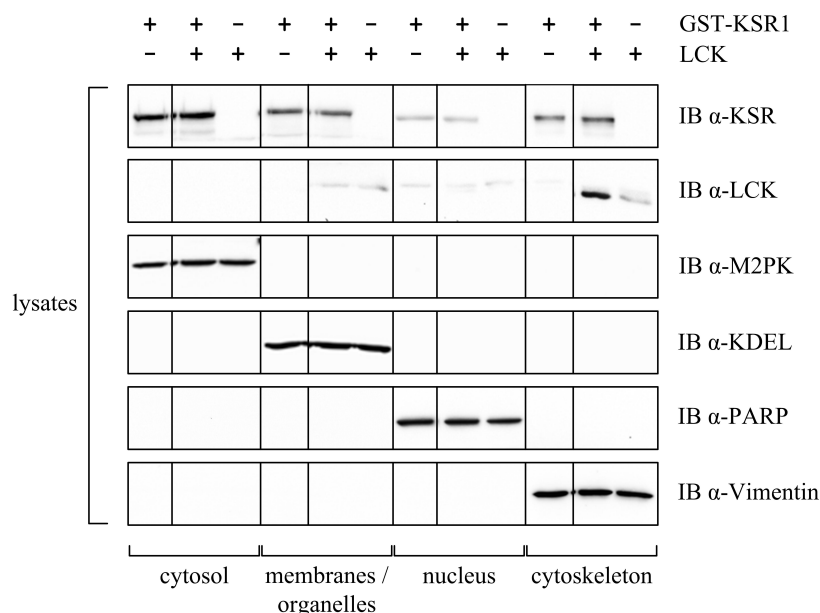

FIGURE 13: Impact of KSR1 on the subcellular distribution of LCK. COS7 cells expressing GST-fused KSR1 and LCK were lysed and subcellular fractions (cytosolic, membrane/organelles, nuclear, and cytoskeletal fraction) were extracted for analyzing the enrichment of overexpressed proteins within the different cell compartments. The amounts of exogenous proteins were determined using appropriate antibodies. Immunodetection for fractionation control: anti-M2PK for cytosolic fraction, anti-KDEL (ER marker) for membrane/organelles fraction, anti-PARP for nuclear fraction, and anti-Vimentin for cytoskeletal fraction.

6.1.3   LCK stabilizes MEK binding to KSR1

In order to determine the effect of the KSR1/LCK interaction on MEK binding and activation, KSR1 and/or LCK were coexpressed with MEK in COS7 followed by cell lysis and precipitation of GST-tagged KSR1. Despite the dogma that MEK is constitutively bound to KSR1, overexpression of LCK stabilized KSR1/MEK interaction (Fig. 14*A*). Thereby, the phosphorylation level of KSR1-bound MEK was significantly increased (shown in Fig. 14*A* and *B*). Accordingly, the cellular fraction of phosphorylated MEK was raised upon cotransfection with LCK, as illustrated in Fig. 14*A* and *C*.
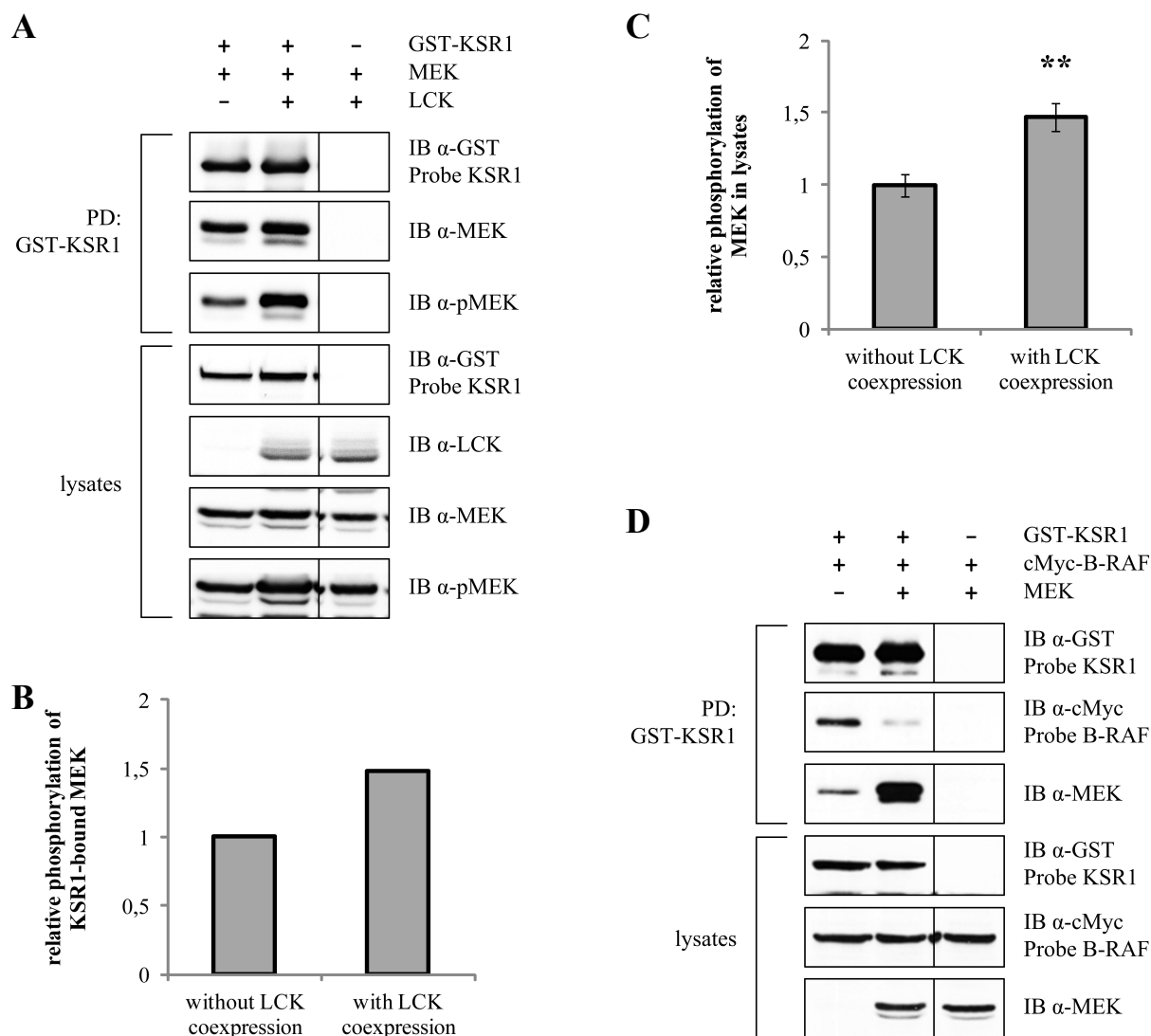
FIGURE 14: KSR1/MEK interaction and MEK activation are altered by LCK expression causing changes in KSR1/B-RAF binding. *A*, MEK activation was determined by transfecting COS7 cells with GST-KSR1 and/or LCK combined with MEK coexpression. Upon cell lysis and precipitation of GST-tagged KSR1 with glutathione-sepharose beads, both coprecipitation and phosphorylation of MEK were investigated. Amounts of (co)precipitated proteins were determined using appropriate antibodies (α-MEK antibody detects endogenous and exogenous protein). *B* and *C*, relative values of the phosphorylation of KSR1-bound MEK and cytoplasmic MEK are shown in *B* and *C*, respectively. For the diagrams, data from two (in *B*) or three (in *C*) independent experiments were quantified by optical densitometry. Bar diagrams show the relative amounts of phosphorylated MEK either bound to KSR1 (in *B*) or in the lysates (in *C*), where 1-fold represents MEK phosphorylation without LCK coexpression. Data are presented as mean (in *B* and *C*) ± SD of the respective measured parameters (in *C*). *P* values: ns (not significant), P ≥ 0.05; * (significant), P < 0.05; ** (highly significant), P < 0.01; *** (extremely significant), P < 0.001 versus corresponding control. *D*, COS7 cells were transfected with GST-KSR1, cMyc-B-RAF, and MEK. Upon cell lysis, GST-tagged KSR1 was precipitated with glutathione-sepharose beads and tested for interaction with cMyc-B-RAF and MEK. Amounts of (co)precipitated proteins were determined using appropriate antibodies.

In complex with KSR2, the activation segment of MEK1 is inaccessible for phosphorylation. Its release is induced by a conformational change of the KSR2 kinase domain as a consequence of KSR2 interaction with a regulatory RAF molecule allowing catalytic RAF to phosphorylate MEK (165). This suggests that binding of B-RAF to KSR1 weakens KSR1/MEK interaction and vice versa. Indeed, the data presented in Fig. 14*D*, support this assumption. In this experiment, overexpressed GST-tagged KSR1 was precipitated with glutathione-sepharose beads from COS7 cell lysates and tested for coprecipitated exogenous cMyc-B-RAF and MEK. As a consequence of exogenous expression, the preferential binding of MEK to KSR1 strongly suppressed the interaction between B-RAF and KSR1 reflecting the ability of MEK to trap KSR1 kinase in a conformation, which is unfavorable for its binding to regulatory B-RAF. These data suggest that the stabilization of KSR1/MEK interaction by LCK and the mediated phosphorylation of KSR1 might antagonize the binding of regulatory B-RAF to KSR1.

6.1.4 ERK-mediated feedback regulates tyrosine phosphorylation of KSR1

In the 1990s it has been reported that LCK is feedback-regulated by MAPKs: kinase-active ERK phosphorylates LCK on Ser59, which increases kinase activity and changes the electrophoretic mobility of LCK (190–192). In order to test whether the ERK-dependent feedback regulation of LCK activity has an impact on tyrosine phosphorylation of KSR1, the kinase-inactive MEK mutant (K97M) was overexpressed together with LCK and GST-tagged KSR1 in COS7 cells. Here, GST-KSR1 was enriched by binding to glutathione-sepharose. Exogenous and endogenous MEK as well as overexpressed LCK were coprecipitated. As shown in Fig. 15, MEK-K97M did not cause significant changes in LCK binding to KSR1. However, the high abundance of overexpressed kinase-inactive MEK resulted in reduced tyrosine phosphorylation and, therefore, impaired catalytic activity of LCK. Accordingly, the tyrosine phosphorylation of KSR1 by LCK was also visibly reduced upon overexpression of MEK-K97M suggesting that the ERK-dependent feedback regulation of LCK has an impact on its kinase activity towards KSR1.
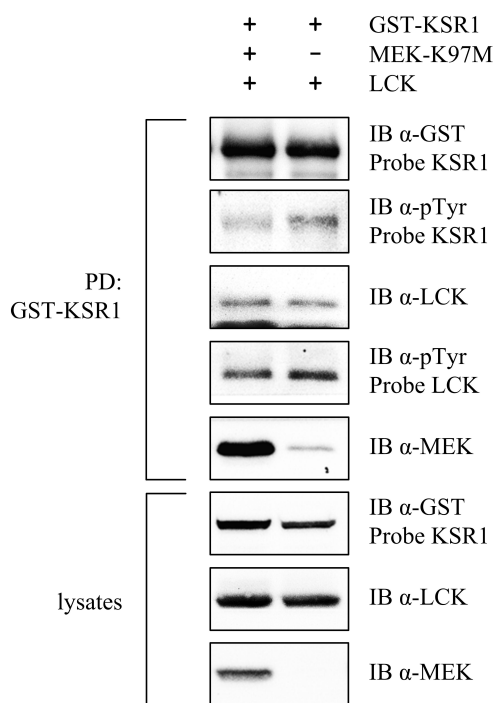
FIGURE 15: Expression of the kinase-inactive MEK mutant reduces tyrosine phosphorylation of KSR1.
GST-KSR1 was coexpressed with LCK and the kinase-inactive MEK-K97M mutant in COS7 cells. LCK and MEK were coprecipitated with GST-tagged KSR1 on glutathione-sepharose beads. Amounts of (co)precipitated proteins were determined using appropriate antibodies (α-MEK antibody detects endogenous and exogenous protein). Levels of tyrosine phosphorylation of KSR1-bound LCK and levels of LCK-induced GST-KSR1 tyrosine phosphorylation were detected using an anti-phospho-tyrosine antibody.

6.2   Mass spectrometry analysis identified Tyr728 of KSR1 as a potential target for LCK-mediated phosphorylation

The finding that LCK associates with and phosphorylates KSR1 raised the question, which residue(s) is/are targeted by LCK? Tyr673 in mouse KSR1 was considered as a prospective target for LCK, since this residue is referred on *PhosphoSitePlus* (a database of observed post-translational protein modifications (www.phosphosite.org)) as a potential phosphorylation site identified by MS analysis. To prove whether Tyr673 is a target for LCK-mediated phosphorylation and to identify further potential candidate(s), which might be phosphorylated by LCK, MS analysis of murine KSR1 was performed.

For this purpose, GST-tagged KSR1 was expressed in COS7 cells in the presence and absence of active LCK and subsequently purified and enriched by binding to glutathione-sepharose. Since it is known that RAS induces the phosphorylation of several serines and threonines, but not of tyrosine residues in RAF, and that KSR proteins entirely lack the RAS-binding domain (in

contrast to related RAF kinases), coexpression of KSR1 with active H-RAS-12V was used as an additional negative control. Up to 78% coverage of the entire protein sequence could be provided by three independent MS measurements. In Fig. 16*A* and *B*, the results obtained for KSR1 phosphorylation induced by coexpression with kinase-active LCK-Y505F (*A*) and active RAS-12V (*B*) mutants are summarized. In total, twenty-one known phosphorylation sites in KSR1 were confirmed by MS analysis in the present study (one of them was found exclusively phosphorylated in the sample transfected with KSR1 alone: Ser253). In addition, seventeen novel phosphorylation sites were identified in murine KSR1 (three of them were found in the sample transfected with KSR1 alone: Thr58, Ser183, and Ser234). Five sites (Ser450, Ser454, Ser547, Tyr728, and Thr865) were found phosphorylated exclusively in the KSR1 sample coexpressed with active LCK, thus, assumed as LCK-induced phosphorylation sites. Since LCK is a tyrosine kinase, only Tyr728 may become phosphorylated directly by LCK, while the phosphorylation of other sites seems to be induced indirectly. Of note, MS analysis in this study could not confirm the phosphorylation of Tyr673. Additionally, four sites were found only in the KSR1 sample coexpressed with active RAS (Ser63, Thr98, Ser300, and Ser838), suggesting that on these sites phosphorylation occurs in a RAS-dependent manner. As expected, no tyrosine phosphorylation sites were found in KSR1 expressed alone or coexpressed with active RAS.

A

B
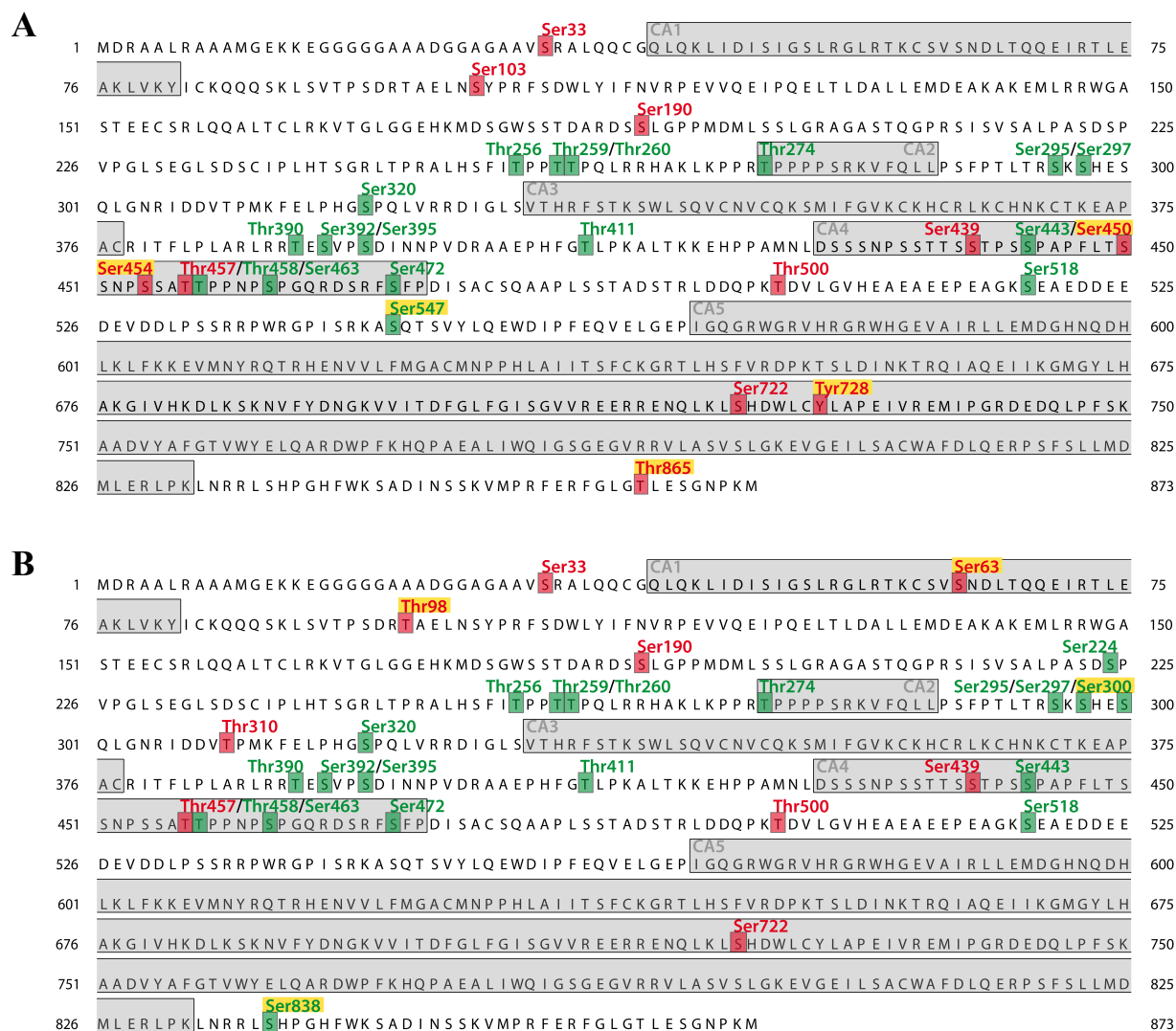
FIGURE 16: MS analysis of murine KSR1 identified numerous phosphorylation sites. Amino acid sequences of mouse KSR1 depicting phosphorylation sites in KSR1 samples coexpressed with either kinase-active LCK-Y505F (*A*) or active RAS-12V (*B*) mutants. Highlighted are known phosphorylation sites (in green), newly identified phosphorylation sites (in red), and predicted LCK- or RAS-induced phosphorylation sites (in yellow). Conserved regulatory domains in murine KSR1 are grey-shaded.

6.3 Tyr673 maintains the functional conformation of KSR1 kinase domain

For the first time, tyrosine phosphorylation in murine KSR1 was described for Tyr673 (see www.phosphosite.org). Tyr673, which is located within the kinase domain, is highly conserved between all KSR (see Fig. 17*A* and *B*) and RAF proteins, respectively. Previously, Tyr538, the Tyr673 homologue in *Drosophila* RAF (D-RAF), was likewise considered as a potential phosphorylation site, but could not be confirmed experimentally. Xia *et al.* (193) reported that

the substitution of the highly conserved Tyr538 by a phenylalanine completely blocked the catalytic activity of D-RAF, which might represent a critical role of Tyr538 in the functional structure of the kinase domain of D-RAF. In light of these data, Tyr673 might have a similar function in the structure of the kinase domain of KSR1, rather than being a regulatory phosphorylation site.

In order to address this issue, Tyr673 was substituted by phenylalanine, a non-phosphorylatable amino acid, and it was firstly tested whether this would affect KSR1 phosphorylation by LCK. Secondly, the binding of both MEK and B-RAF to KSR1 and subsequent phosphorylation of KSR1-bound MEK by RAF kinases were analyzed. To this end, COS7 cells were transfected with GST-tagged KSR1 wild type (WT) and KSR1-Y673F in the presence or absence of LCK or B-RAF, followed by cell lysis and precipitation of GST-KSR1 with glutathione-sepharose beads. As depicted in Fig. 18*A*, similar amounts of LCK were bound to KSR1-WT and KSR1-Y673F, however, tyrosine phosphorylation of KSR1-Y673F was notably increased. Along with the data from the MS analysis, these results suggest that Tyr673 of KSR1 might be either a minor target for LCK-mediated phosphorylation or not phosphorylated by LCK at all. Confirming the structural function of Tyr673 for the kinase domain of KSR1, Fig. 18*B* and *D* shows that binding and phosphorylation of endogenous KSR1-bound MEK are significantly impaired by KSR1-Y673F substitution. Additionally, the cytosolic level of MEK phosphorylation is visibly reduced. Moreover, B-RAF association with KSR1 is significantly diminished by Y673F substitution (Fig. 18*C* and *E*). Based on these results it can be concluded that Tyr673 is critical for maintaining the functional conformation of the KSR1 kinase domain, similar to Tyr538 in D-RAF (193).

FIGURE 17: KSR1 protein structure and KSR protein alignment. *A*, the upper part shows a schematic representation of the structure of KSR1 proteins, whereas the lower part depicts a multiple sequence alignment of a part of the kinase domain of KSR1 proteins from different species. Graduated conservation of amino acids (weak to high) is represented by light to dark purple shading. *B*, pairwise alignment of a part of the kinase domains of murine KSR1 and KSR2. For *A* and *B*, amino acid sequences were obtained from NCBI (accession numbers: NP_038599, Q8IVT5, NP_001101754, NP_001186688, XP_684771, AAF52021, NP_509396, NP_001108017) and merged with Jalview software. Red-framed amino acids are in focus of this study.
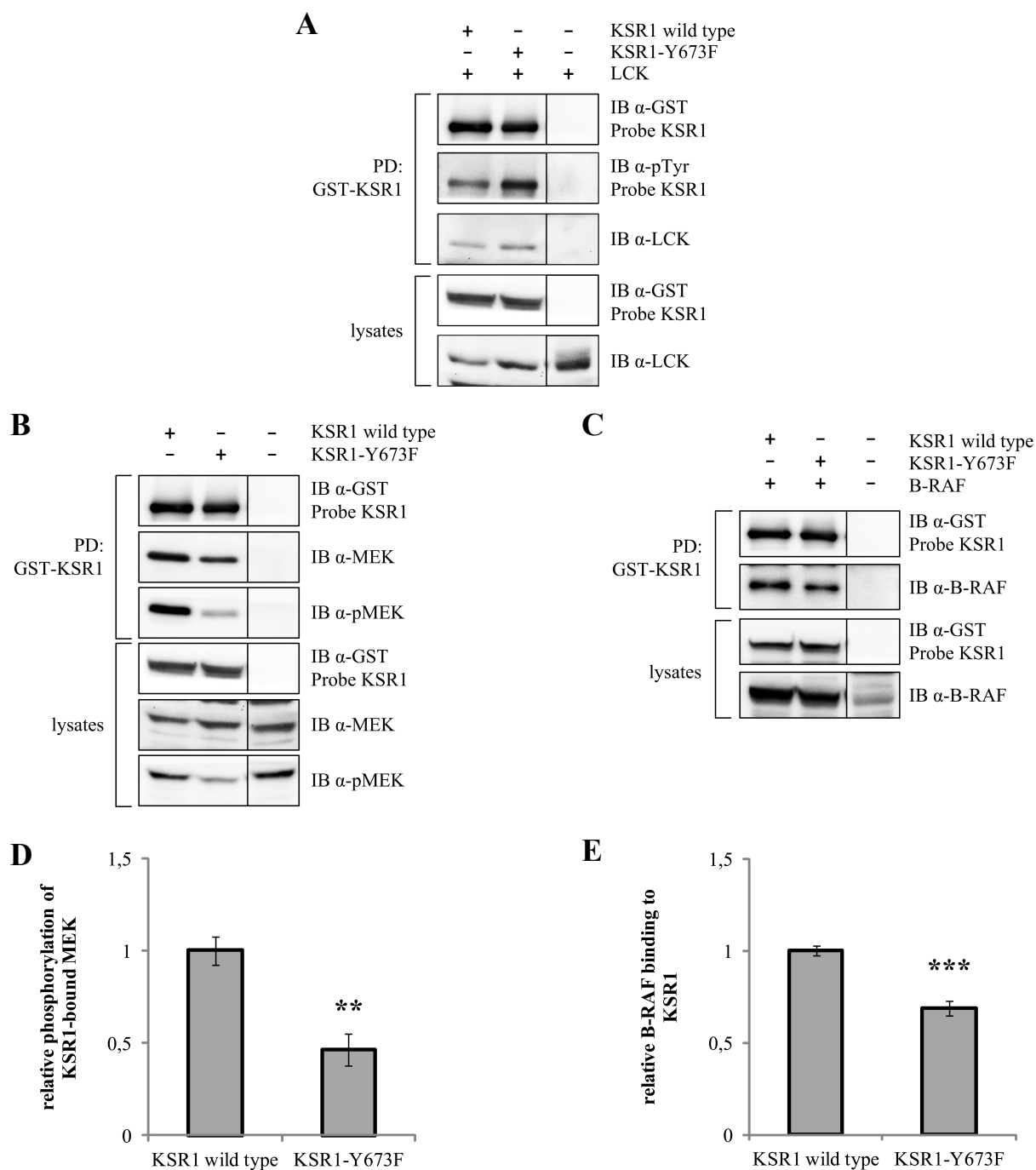
FIGURE 18: Substitution of Tyr673 in KSR1 impairs MEK phosphorylation. *A-C*, KSR1-Tyr673 (Y) was replaced by phenylalanine (F). In COS7 cells, GST-tagged KSR1 wild type (WT) and KSR1-Y673F were expressed in the presence or absence of LCK or B-RAF. Cell lysis was followed by precipitation of GST-KSR1 with glutathione-sepharose beads. Amounts of (co)precipitated proteins were determined using appropriate antibodies. Levels of LCK-induced KSR1 tyrosine phosphorylation were detected using an anti-phospho-tyrosine antibody. *D* and *E*, relative values of the phosphorylation level of endogenous KSR1-bound MEK, where 1-fold represents the phosphorylation of MEK associated with KSR1-WT (*D*, adapted from *B*)**,** and relative values of B-RAF binding to KSR1, where 1-fold represents B-RAF binding to KSR1-WT (*E*, on the basis of *C*). For the diagrams, data from three independent experiments were quantified by optical densitometry. Data are presented as mean ± SD of the respective measured parameters. *P* values: ns (not significant), P ≥ 0.05; * (significant), P < 0.05; ** (highly significant), P < 0.01; *** (extremely significant), P < 0.001 versus corresponding control.

6.4   Phosphorylation of KSR1-Tyr728 affects MEK activation

Tyr728 is located within the KSR1 kinase domain, which has been shown to bind and prime MEK1 for activating phosphorylation by RAF kinases (165), and is conserved between KSR1 proteins of different species, but replaced by a histidine in KSR2 (compare Fig. 17*A* with *B*). These observations raised the fundamental question whether the Tyr728 has a regulatory or structural function for the KSR1 kinase domain, or both? To address this question, the effects of Tyr728 phosphorylation and substitution on function and stability of KSR1 protein were investigated by biochemical and structural assays.

The characterization of Tyr728 was conducted in the same way as it has been done for Tyr673. Tyr728 was substituted by a phenylalanine, a non-phosphorylatable amino acid, and it was tested whether this would affect KSR1 phosphorylation by LCK. Subsequent studies of KSR1 association with MEK or B-RAF and, additionally, of the activating phosphorylation of KSR1-bound MEK were performed. Therefore, GST-fused KSR1-WT and mutated KSR1-Y728F were exogenously expressed in the presence or absence of LCK or B-RAF in COS7 cells. Upon cell lysis, GST-KSR1 was precipitated with glutathione-sepharose beads. As shown in Fig. 19*A*, the levels of coprecipitated LCK are comparable for KSR1-WT and KSR1-Y728F, however, tyrosine phosphorylation of KSR1-Y728F is strongly diminished confirming results of MS analysis. In Fig. 19*B*, binding of endogenous MEK to KSR1-Y728F is strongly reduced compared to the interaction with KSR1-WT. Unlike this, the activating phosphorylation of KSR1-Y728F-bound MEK on Ser218 and Ser222 was three times higher than the phosphorylation level of MEK interacting with KSR1-WT (see Fig. 19*D*). Accordingly, binding of B-RAF to KSR1 mutant was increased compared to KSR1-WT (Fig. 19*C* and *E*). Taken together, these data clearly show that Tyr728 is a major target for LCK-mediated tyrosine phosphorylation of KSR1. Furthermore, the effects on MEK and B-RAF binding to KSR1 as well as MEK phosphorylation suggest a regulatory function of Tyr728 in the KSR1 kinase domain.
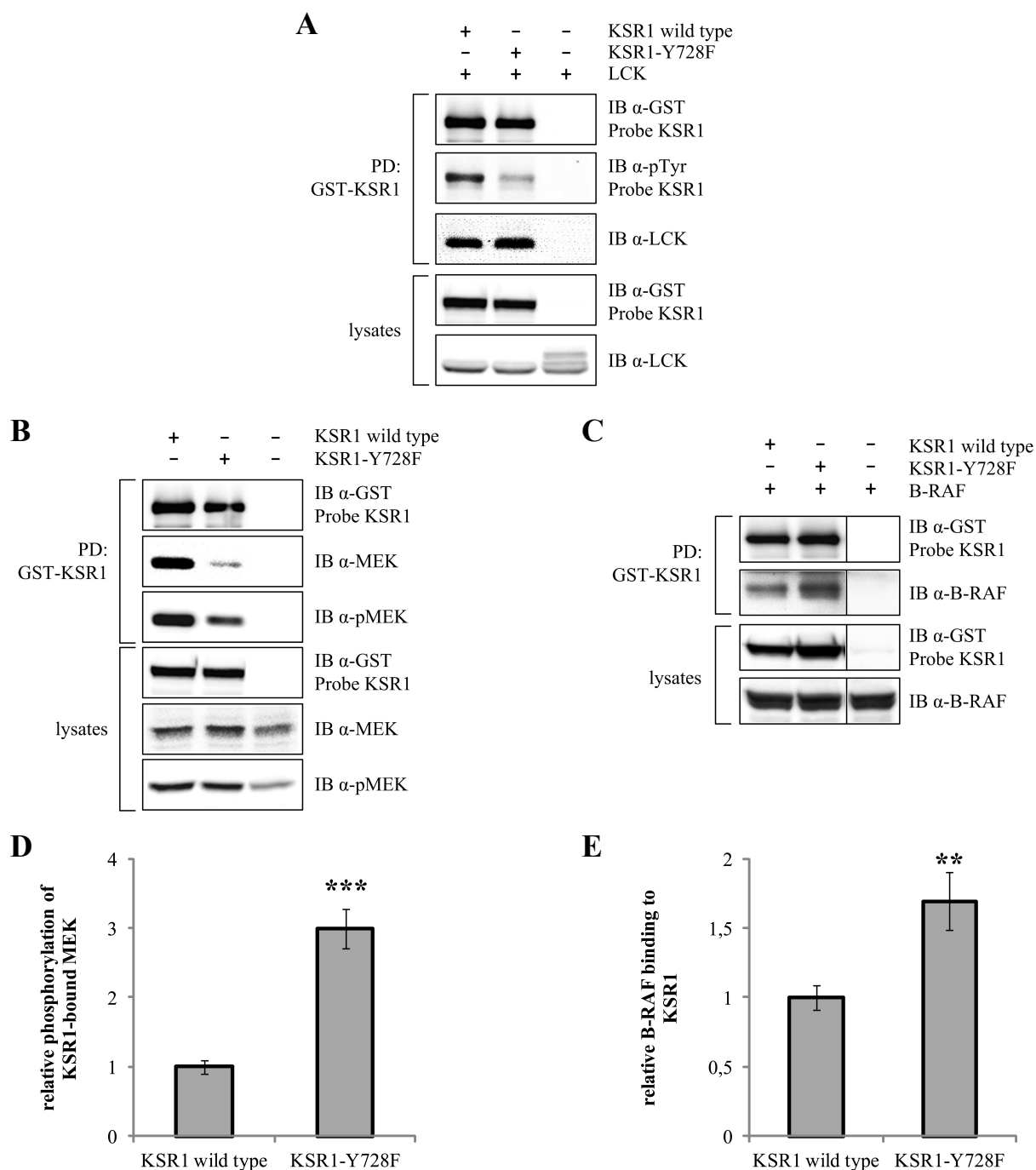
FIGURE 19: LCK-induced phosphorylation of Tyr728 in the KSR1 kinase domain plays a regulatory role in MEK binding and activation. KSR1-Tyr728 (Y) was replaced by phenylalanine (F). *A-C*, GST-fused KSR1-WT and KSR1-Y728F were expressed in the presence or absence of LCK or B-RAF in COS7 cells. GST-KSR1 was precipitated with glutathione-sepharose beads after cell lysis. Amounts of (co)precipitated proteins were determined using appropriate antibodies. Levels of LCK-induced GST-KSR1 tyrosine phosphorylation were detected using an anti-phospho-tyrosine antibody. *D*, relative values of phosphorylation of endogenous KSR1-bound MEK (adapted from *B*), where 1-fold represents phosphorylation of MEK associated with KSR1-WT. *E*, relative values of B-RAF binding to KSR1 (on the basis of *C*), where 1-fold represents B-RAF binding to KSR1-WT. For the diagrams, data from three independent experiments were quantified by optical densitometry. Data are presented as mean ± SD of the respective measured parameters. *P* values: ns (not significant), $P \geq 0.05$; * (significant), $P < 0.05$; ** (highly significant), $P < 0.01$; *** (extremely significant), $P < 0.001$ versus corresponding control.

6.5 Characterization of the structural elements in the KSR1 kinase domain affected by Tyr728 phosphorylation

To acquire more knowledge about the effects of the LCK-induced KSR1-Tyr728 phosphorylation on regulation and structure of the KSR1 protein, the structural environment of Tyr728 as well as interacting residues were investigated. Thereby, the focus of this section is on the stability of the KSR1 protein structure with respect to interaction of KSR1 with MEK or RAF kinases and the catalytic activity of KSR1, both affected by the LCK-induced phosphorylation of KSR1-Tyr728.

6.5.1 Model of the KSR1 kinase domain suggests a structural rearrangement prior to phosphorylation of Tyr728

Based on the very high homology between mouse KSR1(KD) and human KSR2(KD) (indicated by 69% sequence identity and 86% sequence homology, see also Fig. 17*B*), the protein sequence of murine KSR1(KD) was docked onto the template complex of human KSR2(KD) bound to rabbit MEK1, which was published in 2011 by Brennan *et al.* (165). No manual loop building or modeling of deletions was required to built a valid mKSR1 model for structural and functional analysis. Using the model, the entire structure of the KSR1 kinase domain including phosphorylated Tyr728 as well as its effects on the stability of the protein structure of KSR1(KD) and on the interaction interface to MEK could be characterized. This possibly discloses the mechanism by which Tyr728 phosphorylation may regulate the KSR1 function as scaffold protein.

The model in Fig. 20*A* revealed that Tyr728 in murine KSR1, equivalent to His841 in human KSR2, is located in a short helical element C-terminal of the activation loop and buried inside the core of the KSR1 kinase domain. This strongly suggests that for phosphorylation of Tyr728 a conformational rearrangement compared to the 'bound' conformation of KSR1/MEK must occur in order to open the protein structure so that LCK can gain access to this phosphorylation site in KSR1. In contrast to Tyr728, Tyr673 is partially buried inside the KSR1 kinase domain and a part of a conformationally restrained helical element (see Fig. 20*C*). Therefore, it is most likely

that Tyr673 is not accessible for phosphorylation by LCK, which is in accordance with the results obtained from biochemical studies shown in Fig. 18.

Remarkably, the phospho moiety of phosphorylated Tyr728 forms a network of direct hydrogen bonds (purple dashed lines in Fig. 20*B*) with several surrounding amino acids in the KSR1(KD) mainly placed in protein structure-stabilizing helices. One of those residues is Arg649, which is placed in the αD helix, face to face with Tyr728. Hereby, the strong hydrogen bonds, between Arg649 and phospho-Tyr728 in addition to weaker interactions of the phospho moiety with His645 (αD helix) and Glu763 (αF helix), might have stabilizing effects on internal structures of the KSR1 kinase domain upon Tyr728 phosphorylation. Consequently, Arg649 is supposed to function as the major anchor point of phospho-Tyr728. Due to the proximity of the KSR1/MEK interaction interface to Tyr728, stabilizing effects, caused by phosphorylation, may further regulate MEK association with KSR1 as it is shown by biochemical studies and described in chapter 6.4. However, as a result of the distant position to the MEK activation loop, MEK phosphorylation on Ser218 and Ser222 seems to be not directly affected by the phosphorylation of Tyr728 in KSR1.

Based on the high similarity between the protein sequence of KSR and RAF kinases, a catalytic activity of KSR1 is conceivable. However, the issue whether mammalian KSR is a pseudokinase or has a kinase function is still controversially discussed (154, 156–158, 165, 167). In kinases, the catalytic loop controls both the orientation of the ATP molecule inside the catalytic cleft and the subsequent phosphate transfer. Fig. 20*A* demonstrates that Tyr728 is closely located to the catalytic loop of the KSR1 kinase domain. Therefore, it is very likely that the phospho-Tyr728-induced conformational rearrangement of the KSR1(KD) may interfere with the functionality of KSR1 to work as a true kinase by stabilizing the γ-phosphate group of the ATP for the relevant transfer reaction.

Furthermore, the model of the KSR1(KD) in complex with MEK revealed that constitutively associated MEK interacts with KSR1 via lower lobes of both kinase domains; especially by interfacing their activation segments and αG helices with each other (see Fig. 20*C* and *D* and reference (165)). The activation segment of KSR1, which is located very close to Tyr728 within the spatial model, consists of a rather long loop with a large number of polar and/or charged residues and no stabilizing secondary structure (also shown in Fig. 20*A*). Consequently, the structure suggests that the activation segment is released in the 'unbound' conformation of

KSR1(KD) non-interacting with MEK. This would prevent that the activation segment is conformationally restrained and possibly allow Tyr728 to be positioned at the protein surface accessible for phosphorylation by LCK before MEK binding occurs. Therefore, the mechanism of LCK-induced Tyr728 phosphorylation may only occur as a result of a conformational rearrangement from the so-called 'bound' to 'unbound' conformation of KSR1. This assumption is in agreement with the results presented in chapter 6.4 and is supported by the observation from Brennan *et al.* (165), who reported that in the hKSR2/rMEK1 complex, a part of the activation segment of KSR2 exhibits no observable electron density due to disorder. The crossover of the αG helices in the lower lobes of both kinase domains represents the largest surface in the binding interface of KSR1 with MEK (Fig. 20*C* and *D*). Remarkably, all amino acids located within these structures, are conserved between KSR1 and KSR2 and show direct contact with residues of MEK, which suggests a high similarity of their kinase-kinase interaction mechanisms.
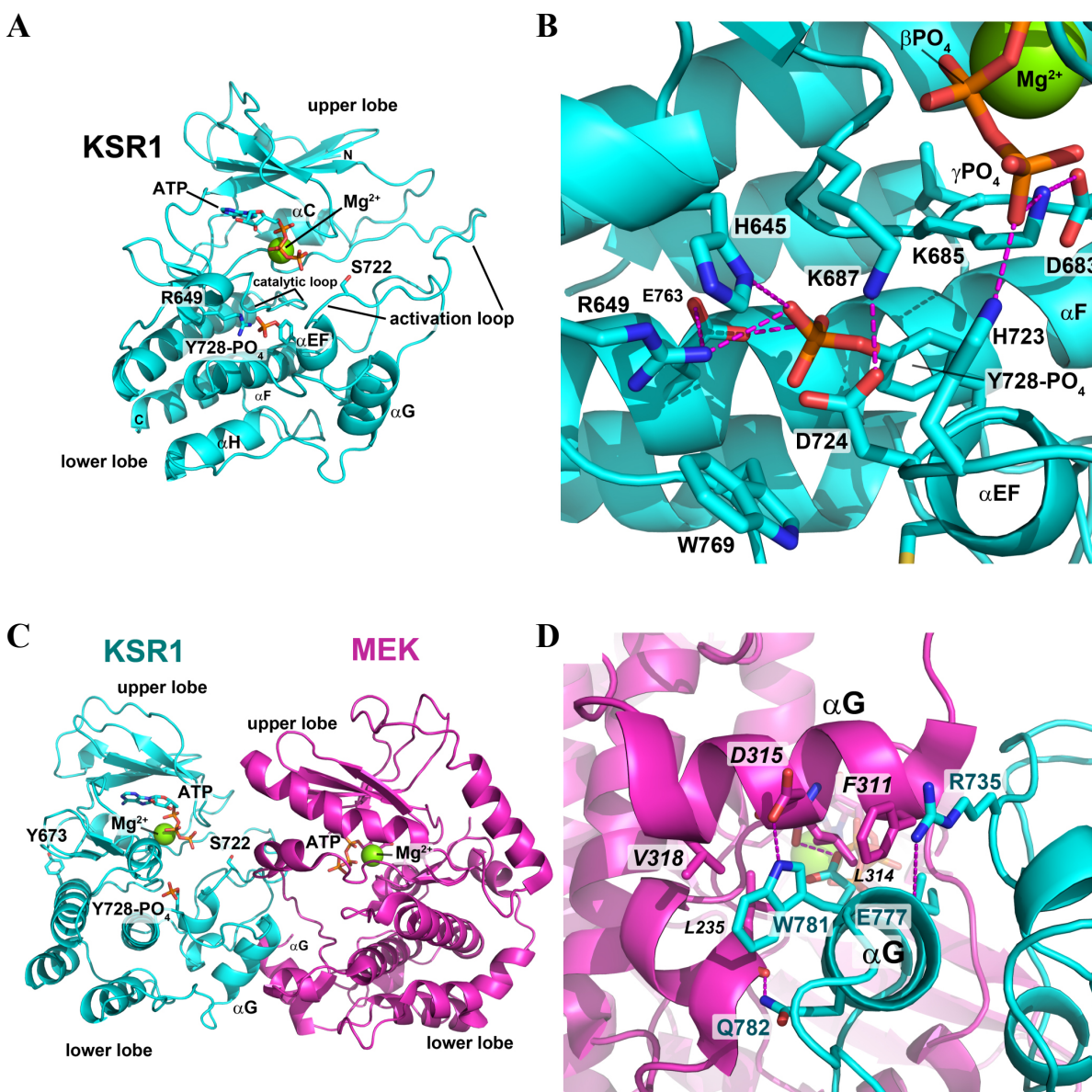
FIGURE 20: The bound conformation of the murine KSR1 kinase domain with focus on Tyr728 phosphorylation and KSR1/MEK interaction. The protein sequence of the kinase domain (KD) of murine KSR1 was docked onto the template complex hKSR2(KD)/rMEK1, which was published by Brennan *et al.* (165). Phospho-Tyr728 and ATP moieties are shown as orange sticks; magnesium ion is indicated as green sphere. *A*, overall view of the mKSR1(KD) highlighting phosphorylated Tyr728 as well as catalytic and activation loop. *B*, detailed view of direct hydrogen bonding (purple dashed lines) mainly formed between the phosphate group of phospho-Tyr728 and surrounding amino acids located in helical elements of the mKSR1(KD). Additionally, close proximity of phospho-Tyr728, buried inside the core of the KSR1 kinase domain, to the ATP molecule, located inside the catalytic cleft, is exhibited. *C*, overall view of the modeled complex of murine KSR1(KD) interacting with MEK. This association is mediated by crossed interaction of residues located, primarily, in the αG helix and, secondarily, in the activation loop of both kinases. *D*, detailed view of the interacting surface of the αG helix interface of both kinase domains. [1]

---

[1] The protein structure of the kinase domain of murine KSR1 was predicted by Prof. Thomas Müller.

6.5.2 Structural analysis of intramolecular interactions in KSR1 kinase domain affected by amino acid alteration at position 728

Intramolecular hydrogen bonding plays a role in the formation of secondary and tertiary structures of nucleic acids and proteins. In Fig. 21 it is shown that the phosphorylation of KSR1-Tyr728 by LCK leads to an increase in the number of hydrogen bonds with surrounding amino acids (compare Fig. 21*A* with *B*). As mentioned above, Arg649 in KSR1 could function as the major anchor point for the phosphate moiety of phospho-Tyr728. Indeed, hydrogen bonding occurred in the KSR1 kinase domain model containing non-phosphorylated Tyr728, but not between the tyrosine hydroxyl group and Arg649 (compare Fig. 21*A* with *B*). Unlike this fact, the substitution of KSR1-Tyr728 by both histidine and glutamic acid (Fig. 21*C* and *D*, respectively) abolished (almost) completely the hydrogen bond formation. In light of these data, the substitution of KSR1-Tyr728 by histidine in KSR2 (His841) might have a structural effect within the kinase domain of KSR proteins, which was further analyzed by biochemical studies as described in chapter 6.5.3.

Taken together, Tyr728 phosphorylation- or substitution-induced properties, revealed by modeling the three-dimensional structure of the mouse KSR1 kinase domain, confirm the experimental data obtained by biochemical studies (described in chapter 6.4). The results hint towards an enhanced stability of internal structures within the KSR1 kinase domain compared to non-phosphorylated or substituted Tyr728, which, in turn, might alter MEK and/or RAF binding to KSR1. The model-derived prediction is consistent with shown effects in the form of strongly reduced MEK binding to KSR1, but increased interaction with B-RAF (Fig. 19*B*, *C,* and *E*) resulting in elevated phosphorylation of KSR1-bound MEK upon KSR1-Y728F substitution (Fig. 19*B* and *D*). The gained knowledge uncovers a dual role for the functional properties of phospho-Tyr728 by having consequences for maintaining the 'bound' conformation of KSR1 kinase domain in complex with MEK, which may indirectly influence both the association of KSR1 with MEK as well as the RAF-induced phosphorylation of MEK associated with KSR1.
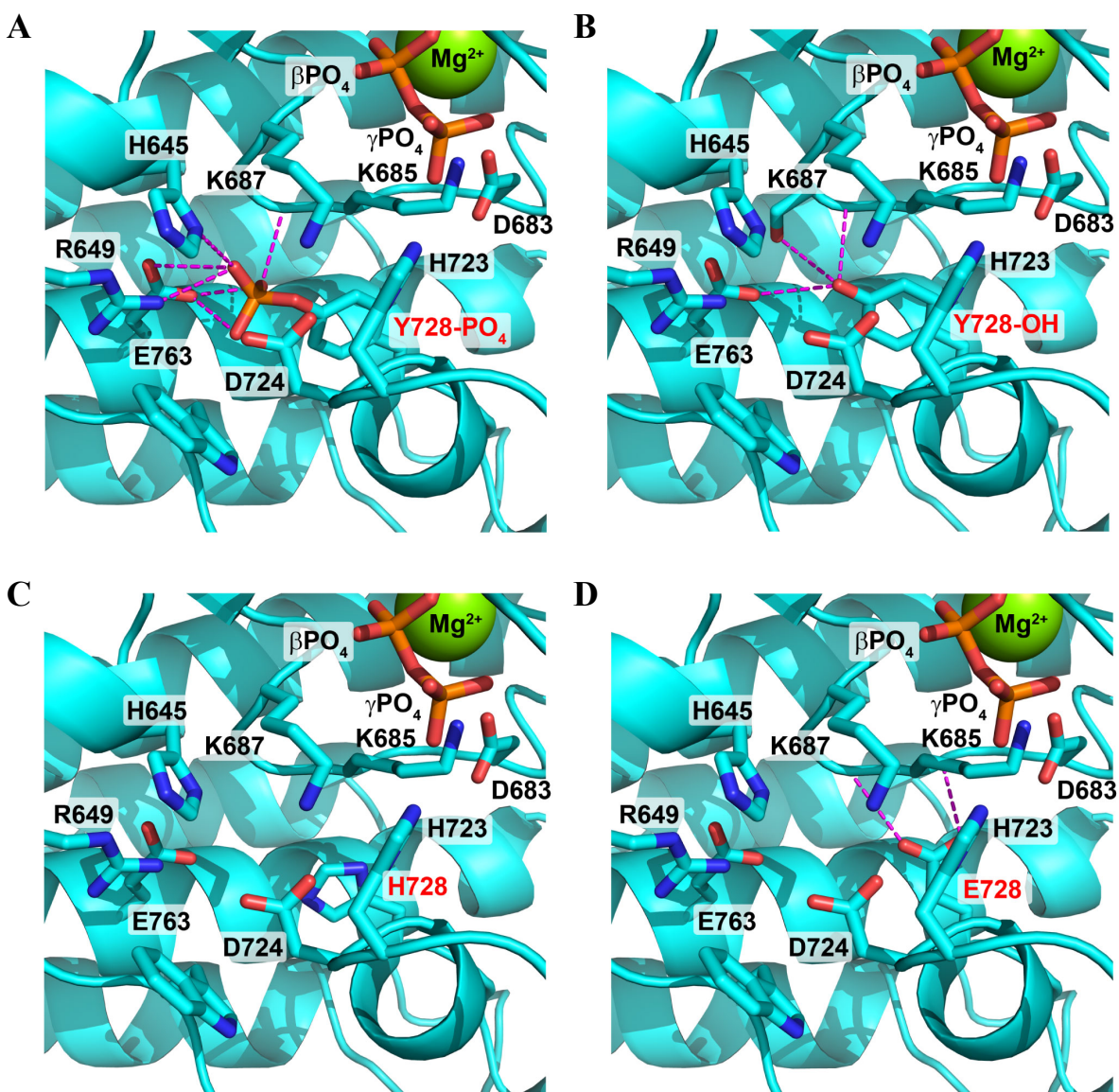
FIGURE 21: Detailed structural insights into the kinase domain of mKSR1 including phosphorylated and non-phosphorylated Tyr728 and indicated substitutions. Close-up view on the three-dimensional structure of the mouse KSR1 kinase domain modeled by use of the structure of human KSR2(KD) in complex with MEK as a template (165). Hydrogen bonds (purple dashed lines) are formed between phosphorylated (*A*) or non-phosphorylated tyrosine (*B*), histidine (*C*) or glutamic acid (*D*) at the position 728 and surrounding residues in the mKSR1(KD). The phospho moieties of phospho-Tyr728 and ATP are shown as orange sticks; the magnesium ion is indicated as green sphere. [2]

6.5.3 Chemical structure of the residue at position 728 affects functional properties of KSR1

As described by Fig. 19*B*, the ability of the KSR1 mutant Y728F to bind MEK was strongly reduced compared to KSR1-WT. In order to test whether this was specific for Tyr728 phosphorylation in KSR1, substitutions of the tyrosine by glutamic acid (negatively charged and polar), alanine (aliphatic and non-polar) or histidine (positively charged and aromatic) were tested for their binding to MEK and subsequent induction of MEK activation.

For precipitation, GST-KSR1-Tyr728 wild type and mutants were expressed in COS7 cells and enriched by binding to glutathione-sepharose upon cell lysis. Samples were analyzed for coprecipitation and phosphorylation of endogenously expressed MEK. It was expected that the substitution of Tyr728 by glutamic acid could mimic phosphorylation at this position on the one hand and accordingly stabilizes the KSR1 kinase domain structurally similar on the other hand (structural details are described in chapter 6.5.2). Opposite results might have been conceivable for the substitution of Tyr728 by a histidine, which is equivalently replaced in KSR2 (His841), assuming an effect on KSR1 functionality. As a neutral amino acid, alanine would possibly have almost no influence on the stability of the KSR1(KD) and, therefore, almost no effect on phosphorylation and binding of MEK to KSR1. Unpredictably, the binding of MEK to KSR1-Y728E was completely abolished compared to KSR1-WT (Fig. 22*A*). In contrast, the interaction of KSR1-Y728H with MEK was not altered, but the phosphorylation level of KSR1-Y728H-associated MEK was considerably weaker in comparison to wild type control (see also Fig. 22*B*). Therefore, the histidine substitution at the position 728 in KSR1 suggests a structural role for His841 in KSR2 with respect to KSR2-bound MEK phosphorylation. Results obtained by the substitution of KSR1-Tyr728 by alanine exhibited the opposite trend: KSR1-Y728A/MEK interaction was restricted, while KSR1-Y728A-bound MEK phosphorylation was significantly increased, similar to the substitution by phenylalanine (compare Fig. 19*B* and *D* with Fig. 22*A* and *B*).

Taken together, results from mutational analyses disclosed that the residue at the position 728 has dual importance (structural and regulatory) for the functional properties of KSR1 due to the facts that *i)* it is involved in maintaining the 'bound' conformation of the KSR1 kinase domain associated with MEK, therefore, *ii)* influences KSR1/MEK association, and *iii)* affects

RAF-induced phosphorylation of MEK. Obtained results further suggest that these functions are interrelated. In conclusion, not solely the phospho moiety of phospho-Tyr728 *per se* seems to play a crucial role in the regulatory function of KSR1, but also the amino acid structure with its chemical properties at this position, which favors the tight binding of MEK, reduces phosphorylation of associated MEK reflecting a structural function of KSR1. This might be important for the functionality of KSR1 proteins to interact with and to prime subsequently MEK1 for the activating phosphorylation by RAF kinases.
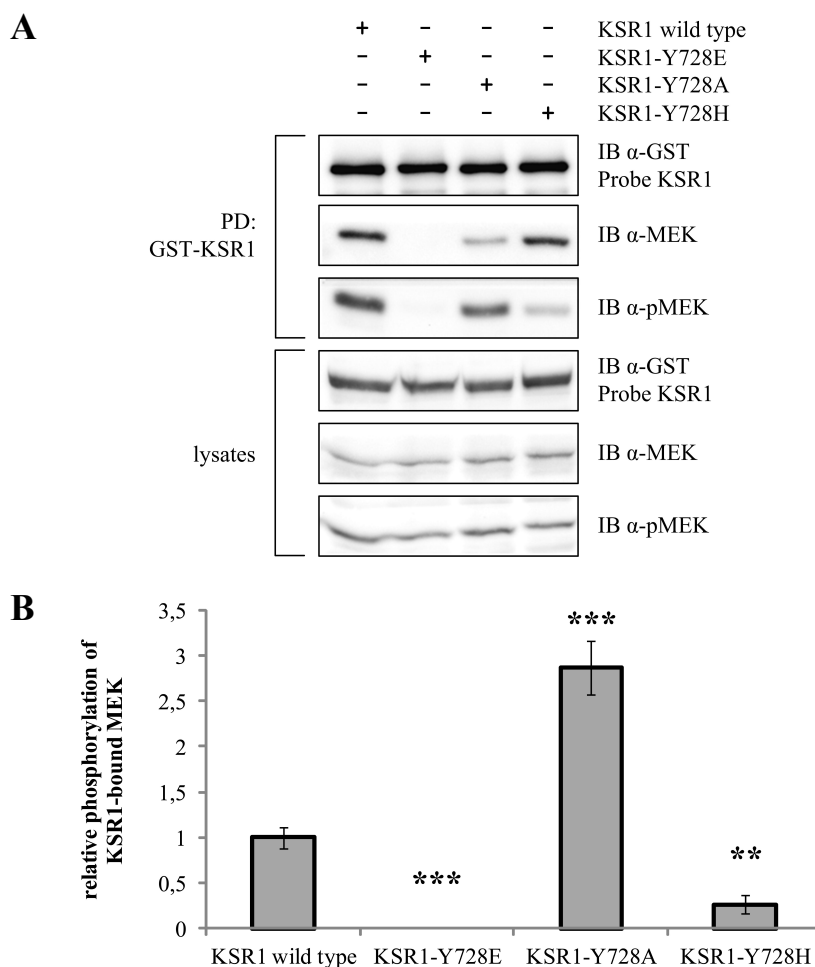

FIGURE 22: Substitution of Tyr728 alters both KSR1/MEK association and phosphorylation of KSR1-bound MEK. KSR1-Tyr728 (Y) was replaced by glutamic acid (E), alanine (A), and histidine (H) for biochemical studies. *A*, COS7 cells were transfected with GST-tagged KSR1-WT, KSR1-Y728E, KSR1-Y728A, and KSR1-Y728H. Upon cell lysis, GST-KSR1 was precipitated with glutathione-sepharose beads. Amounts of (co)precipitated proteins were determined using appropriate antibodies. *B*, relative values of the phosphorylation level of MEK associating with the different variations of KSR1 (adapted from *A*), where 1-fold represents phosphorylation of endogenous MEK interacting with KSR1-WT. For the diagram, data from three independent experiments were quantified by optical densitometry. Data are presented as mean ± SD of the respective measured parameters. *P* values: ns (not significant), $P \geq 0.05$; * (significant), $P < 0.05$; ** (highly significant), $P < 0.01$; *** (extremely significant), $P < 0.001$ versus corresponding control.

6.5.4 Arg649 stabilizes the 'bound' conformation of the kinase domain of KSR1 associated with MEK

As shown by Figs. 20 and 21, phospho-Tyr728 forms a stabilizing hydrogen bond with Arg649, which is an anchor point for the phosphate moiety of phospho-Tyr728. The model of the KSR1 kinase domain suggests that Arg649, located in the αD helix of the KSR1 kinase domain, may further stabilize internal secondary structures surrounding phospho-Tyr728. Biochemical studies of Arg649 in KSR1 should give more insights into the mechanism of how this residue might impair Tyr728 phosphorylation, kinase-kinase interaction between KSR1 and MEK, and caused effects on MEK activation as presumed by the structural modeling of the KSR1(KD) described in chapter 6.5.1. For that purpose, Arg649 in KSR1 was substituted by alanine (aliphatic and non-polar) or glutamic acid (negatively charged and polar) for disrupting hydrogen bonding with phospho-Tyr728 that might have consequences for the stability of the KSR1 kinase domain and thereby alter KSR1/MEK association.

COS7 cells were transfected either with GST-fused KSR1-WT or substitutional mutants and cotransfected with LCK and MEK. GST-KSR1 was precipitated using glutathione-sepharose beads and analyzed for tyrosine phosphorylation and coprecipitated proteins. Similar to the results obtained for KSR1-Y728F, KSR1-R649A strongly reduced and KSR1-R649E completely abolished KSR1/MEK complex formation (Fig. 23*A*). These data confirm the model-derived assumption that Arg649 might be involved in stabilizing the 'bound' conformation of the kinase domain of KSR1 associated with MEK. Additionally, the substitution of Arg649 by both alanine and glutamic acid led to an increased binding of LCK to KSR1 and resulted in a remarkably higher tyrosine phosphorylation (most probably Tyr728 phosphorylation) compared to KSR1-WT (see Fig. 23*A* and *B*). These findings suggest that due to the amino acid exchange at the position 649 in KSR1, the balance of the KSR1 folding stages might be shifted towards the stage, where Tyr728 is placed on the surface of the KSR1 protein, which makes it accessible for phosphorylation by LCK.
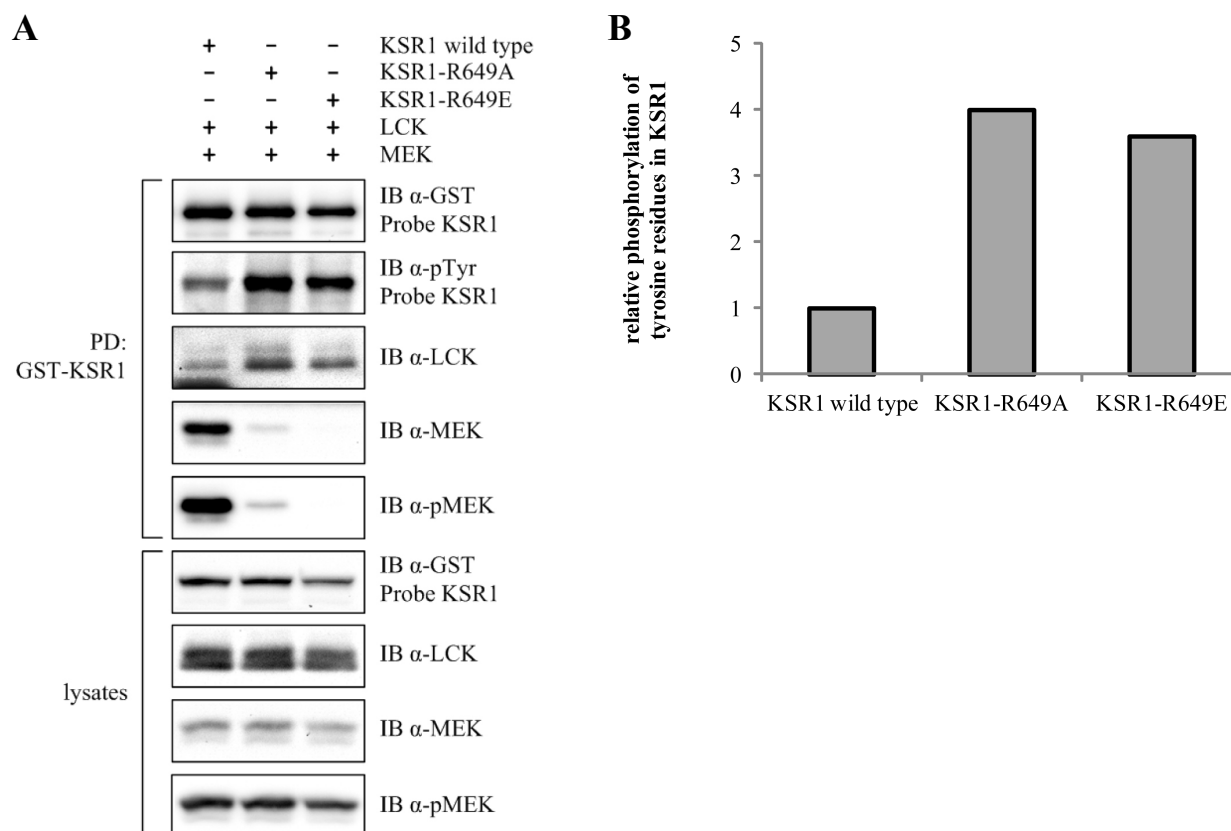
A

B

FIGURE 23: Substitution of Arg649 results in enhanced KSR1 tyrosine phosphorylation by LCK, but abolishes MEK association with KSR1. *A*, GST-fused KSR1-WT and indicated mutants were expressed in the presence of LCK and MEK in COS7 cells. Upon lysis, GST-KSR1 was precipitated by use of glutathione-sepharose beads. Amounts and phosphorylation levels of (co)precipitated proteins were determined by use of appropriate antibodies. *B*, relative values of KSR1 tyrosine phosphorylation induced by Arg649 substitution, where 1-fold represents phosphorylation of tyrosine residues in KSR1-WT. For the diagram, data from two independent experiments were quantified by optical densitometry. Data are presented as mean of the respective measured parameters.

6.5.5   Phospho-Tyr728 affects the dynamics of structural elements involved in KSR1 kinase activity and KSR1/MEK complex formation

To gain more insights into whether and how phosphorylation of Tyr728 in KSR1 might alter protein structure, potential kinase activity or the complex formation of KSR1 with MEK, molecular dynamics (MD) simulations were performed in explicit water for analysis of the physical movements of atoms in the theoretically formed KSR1 kinase domain. MD simulations allow insights into molecular motion on an atomic scale for a period of time. Thereby, the root-mean-square (abbr.: r.m.s.) deviation measures the average distance between backbone (Cα-) atoms of superimposed proteins. In order to study complex protein conformations,

structural similarities of the backbone coordinates are measured in 3D upon optimal rigid body superposition.

The computational model of the KSR1(KD) with either phosphorylated or non-phosphorylated Tyr728 was placed in a water box with ions at a concentration of 150mM for neutralizing protein charges. 5ns unrestrained trajectories were calculated after stepwise minimization. As depicted in Fig. 24, fluctuations of various secondary structure and loop elements in the kinase domain of KSR1 were observed using visual molecular dynamic (VMD) with respect to the formation of hydrogen bonds and r.m.s. deviation. Fig. 24*A* shows in stereo view the localization of determined structural elements placed within the KSR1 kinase domain and possibly affected by the phosphorylation of Tyr728. Stabilization of internal structures of the KSR1(KD) upon Tyr728 phosphorylation, predicted in this study, could be confirmed by MD simulations of hydrogen bonding between the side chain of Tyr728 and surrounding residues. Here, conformational and positional variations of the backbone atoms of phospho-Tyr728 were significantly lower compared to non-phosphorylated Tyr728 in KSR1 (r.m.s. deviation is about 2Å or between 2 and 4Å, respectively, see Fig. 24*B*). Consequently, hydrogen bonding between the side chain of Tyr728 and surrounding amino acids was stronger in the case of phosphorylated versus non-phosphorylated Tyr728 with respect to number as well as duration of hydrogen bonding. This suggests that the helical element containing phospho-Tyr728 and elements that interact with phospho-Tyr728, are possibly stabilized. Remarkably, MD simulations of other structural elements appeared similarly less flexible in the case of KSR1 with phospho-Tyr728 (see Fig. 24*C-G*).

In kinases, the activation loop controls the access of the substrate to the active site and is usually displaced by phosphorylation of serine and/or threonine residues present in this segment, which then counteract positive charged amino acid(s) in the catalytic loop. As already described, Tyr728 is located C-terminally of the activation loop within the KSR1(KD). By use of structural modeling, an interaction of the phospho moiety of phospho-Tyr728 with Lys685 could be identified; a residue, which is located within the catalytic loop and highly conserved in all protein kinases generally coordinating the transfer reaction of the γ-phosphate of the ATP molecule onto the substrate (Figs. 24 and 25). Surprisingly, the activation loop in KSR1 exhibited lower fluctuations for the Cα-atoms in the case of phosphorylated unlike non-phosphorylated Tyr728 as in contrast to the catalytic loop that appears to be not significantly

affected (Fig. 24*C* and *E*, respectively). Similarly, further elements seem to be not significantly impaired according to MD simulation: αD helix (contains Arg649), αG helix (interface to MEK), and the potential interface to RAF (see Fig. 24*D*, *F*, and *G*). Here, hydrogen bonding did not considerably differ as an effect of possibly being independent of Tyr728 phosphorylation with respect to structural stability. Consistent with the results from the biochemical studies presented in chapter 6.4, these findings may indicate that phosphorylation of Tyr728 leads to the stabilization of both the phosphorylation site *per se* and the activation loop of KSR1 proteins that, in turn, could influence KSR1 complex formation with (the potential substrate) MEK in order to release the activation loop of MEK for phosphorylation on Ser218 and Ser222 by KSR1 itself or another protein kinase.
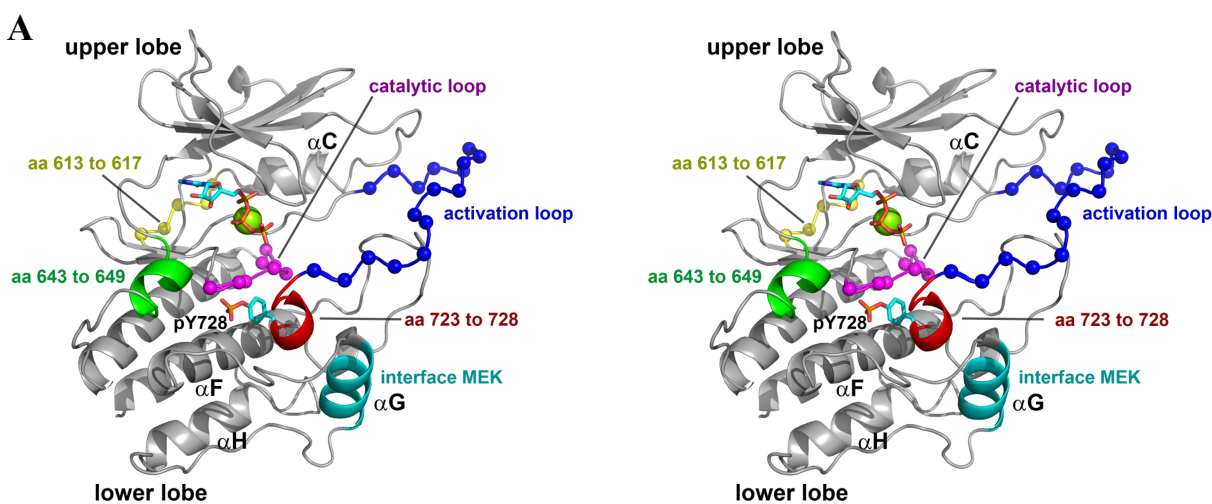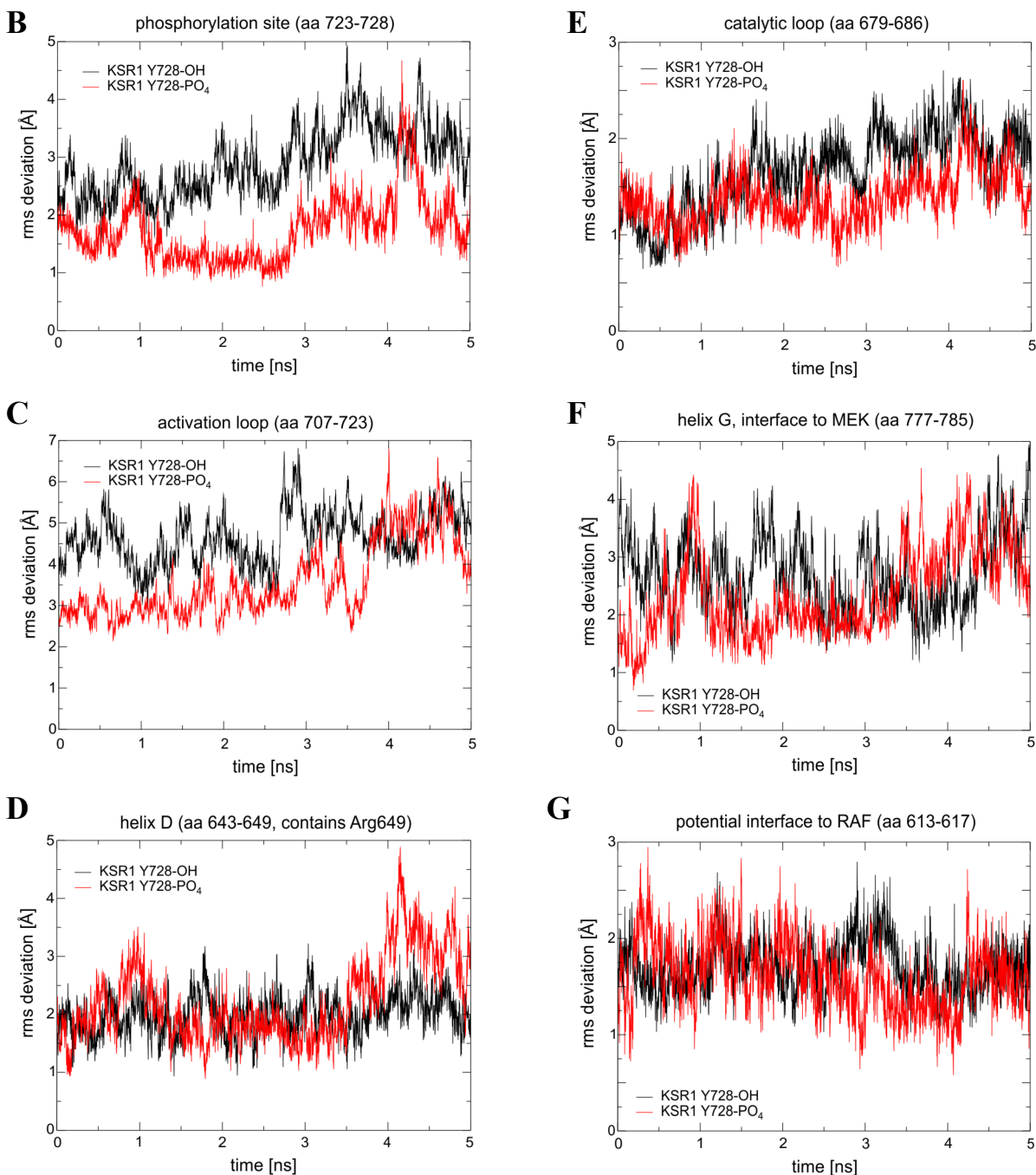
FIGURE 24: The impact of Tyr728 phosphorylation on intramolecular dynamics (MD simulations). *A*, stereo view of the kinase domain of murine KSR1 modeled by docking its protein sequence onto the template complex hKSR2(KD)/rMEK1 (165). Structural elements analyzed by r.m.s. deviation for backbone (Cα-) atoms are highlighted in different colors: red (helical element harboring Tyr728, for *B*), dark blue (activation loop, for *C*), green (short helix containing the anchor point Arg649, for *D*), magenta (catalytic loop containing Lys685, for *E*), cyan (αG helix, which is a part of the KSR1 interface to MEK, for *F*), and yellow (potential interface to RAF kinases, for *G*). Moieties of phospho-Tyr728 and ATP are shown as orange sticks. The magnesium ion is indicated as green sphere. *B-G*, 5ns trajectory MD simulations of structural elements (indicated in *A*) using the software NAMD (NAMD, Scalable Molecular Dynamics software package). Illustrated curves represent fluctuations of the backbone (Cα-) atoms of non-phosphorylated Tyr728 (shown in black) or phosphorylated Tyr728 (shown in red) within the KSR1(KD) and, therefore, reflect the stability of hydrogen bonding with Tyr728-surrounding elements. [3]

With respect to structural stabilization of the catalytic loop in the KSR1(KD) by LCK-induced phosphorylation of Tyr728, Lys685 seems to be a direct link between the phospho moiety of phospho-Tyr728 and the γ-phosphate group of the ATP molecule (as shown in the structural modeling in Fig. 25*A*). Throughout the 5ns trajectory, a highly restrained side chain conformation for KSR1 being phosphorylated on Tyr728 was predicted, whereas for KSR1 with non-phosphorylated Tyr728 the distance between the amino group of Lys685 and the γ-phosphate of the ATP molecule significantly varied representing far more flexibility of the lysine residue (Fig. 25*B*). Therefore, it appears that the groups, involved in the catalytic cycle of phosphate transfer reaction, are not properly lined up over the time emphasizing the importance of the KSR1-Tyr728 phosphorylation by LCK for regulation of KSR1 kinase activity.

To test whether the Tyr728 phosphorylation exerts a long-range effect by changing the stability of the KSR1 interface either to MEK (αG helix) or to the regulatory RAF molecule (loop element ahead of αC helix), fluctuations of the backbone atoms of phosphorylated and non-phosphorylated KSR1-Tyr728 were analyzed. As shown by Fig. 24*F* and *G*, no significant differences could be observed in the r.m.s. deviation. Since these results revealed that the LCK-induced phosphorylation of Tyr728 does not lead to a stabilization of the KSR1/MEK interface, the distance between the backbone atom of Tyr728 and Ala778 was analyzed (corresponding structural model is shown in Fig. 25*C*). Ala778 is located on the MEK facing side of the αG helix and one of the KSR1 residues being in direct contact with MEK. As illustrated in Fig. 25*D*, the Cα-Cα distance between Tyr728 and Ala778 throughout MD simulations is shorter in the case of phosphorylated compared to non-phosphorylated Tyr728. This indicates a more compact kinase-kinase interface, which may facilitate KSR1/MEK binding and interfere with the RAF-induced phosphorylation of MEK upon Tyr728 phosphorylation by LCK, because KSR1/RAF interaction is not stabilized and the activation segment of MEK might be less accessible for phosphorylation.

Taken together, phosphorylation of Tyr728 within the mKSR1(KD) may cause a conformational rearrangement most likely induced by the higher stability of the activation loop. This may lead to a tightened KSR1/MEK complex formation and reduced KSR1-bound MEK phosphorylation due to limited access of RAF kinases to the phosphorylation sites Ser218 and Ser222 within the activation loop of the MEK kinase domain. This may affect the activation of the entire MAPK signal transmission and, consequently, cellular behavior as it is shown in

Fig. 29. The restrained side chain conformation further indicates that the LCK-induced phosphorylation of Tyr728 potentially influences KSR1 kinase activity by stabilizing the catalytic loop via Lys685 and shortening the distance between this conserved amino acid in the KSR1(KD) and the ATP molecule located within the catalytic cleft. In detail, Lys685 becomes conformationally fixed between the phosphate moieties of phospho-Tyr728 and ATP, such that it can ideally facilitate the transfer of the γ-phosphate from ATP to an acceptor hydroxyl group in a substrate. In contrast, the conformational flexibility of the KSR1/RAF interface is not altered upon KSR1-Tyr728 phosphorylation. However, further structural elements seem to play a crucial role in the increase of B-RAF binding to KSR1 upon Tyr728 substitution by phenylalanine (as shown in Fig. 19*C* and *E*).
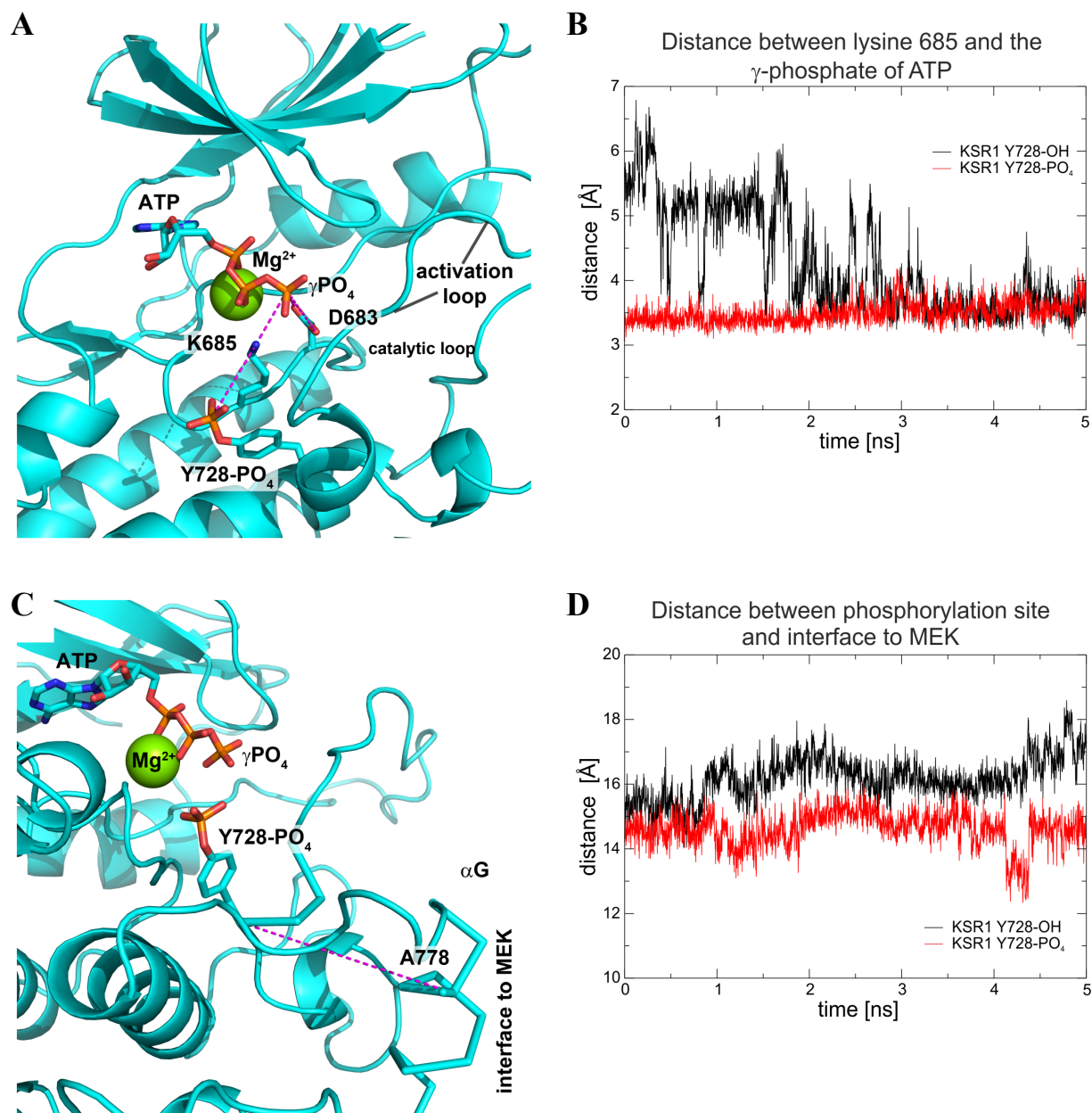
FIGURE 25: Structural modeling and MD simulations revealed conformational rearrangements that may affect KSR1 kinase activity and KSR1/MEK complex formation upon Tyr728 phosphorylation. The 3D structure of the murine KSR1 kinase domain was modeled using the complex hKSR2(KD)/rMEK1 as a template (165). *A*, close-up view of the mKSR1(KD) with the focus on hydrogen bonding formed between the phosphate groups of phospho-Tyr728 and ATP and the central amino acid Lys685, which is highly conserved and located in the catalytic loop of KSR1. Moieties of phospho-Tyr728 and ATP are shown as orange sticks, the magnesium ion is indicated as green sphere, and purple dashed lines represent hydrogen bonds (also in *C*). *B*, structural elements were analyzed for variations in distance between the amino nitrogen atom of Lys685 and the γ-phosphate atom of the ATP, located nearby phosphorylated (red curve) or non-phosphorylated Tyr728 (black curve) in the KSR1(KD), throughout the 5ns trajectory of MD simulations using the software NAMD (NAMD, Scalable Molecular Dynamics software package) (also in *D*). *C*, close-up view of the mKSR1(KD) with the focus on the potential long-range interaction between phospho-Tyr728 and the αG helix, which is the major contact surface of the KSR1 interaction with MEK. *D*, Structural elements were analyzed for variations in distance between the backbone atoms of Tyr728 and Ala778, located within the αG helix of the KSR1(KD), under Tyr728 phosphorylated or non-phosphorylated conditions (red and black curve, respectively). [4]

6.5.6 Ser722 is involved in KSR1 tyrosine phosphorylation and MEK activation

MS analysis, performed in this study, revealed the conserved Ser722 as novel phosphorylation site of murine KSR1 (see Fig. 16*A* and *B* and Fig. 17*A*). Phosphorylation of this residue was found in all replicates, suggesting that Ser722 is one of the major phosphorylation sites in KSR1. As shown in Fig. 17*A* as well as Fig. 20*A* and *C*, Ser722 is located within the activation loop of the KSR1 kinase domain, six residues ahead of Tyr728 in the linear sequence of amino acids, and in close proximity to the catalytic cleft in the model of KSR1(KD). Therefore, Ser722 might be involved in the regulation of Tyr728 phosphorylation, catalytic activity and/or substrate specificity of the KSR1 protein.

To address this issue, KSR1-Ser722 was substituted by alanine (aliphatic and non-polar) or aspartic acid (negatively charged and polar). Aspartic acid might mimic phosphorylation at this position, while alanine cannot be phosphorylated. KSR1 mutants as well as KSR1-WT were coexpressed with LCK in COS7 cells. Upon lysis, GST-tagged KSR1 was precipitated with glutathione-sepharose beads and tested for tyrosine phosphorylation and coprecipitated proteins. Surprisingly, substitution of KSR1-Ser722 had no significant effect on the KSR1/MEK complex formation although Ser722 is located within the activation loop of the KSR1(KD), which is responsible for KSR1/MEK complex formation together with the αG helix interface of both kinases. However, upon the exchange of Ser722 to either alanine or aspartic acid, the phosphorylation level of KSR1-bound MEK was significantly diminished compared to phospho-MEK associated with KSR1-WT (shown in Fig. 26*A* and *B*). Remarkably, the phosphorylation level of the cytoplasmic MEK was visibly reduced in the case of KSR1-S722D expression (see Fig. 26*A*, lysates, pMEK, *lane 3*). Furthermore, KSR1-S722A and KSR1-S722D considerably enhanced KSR1/LCK binding as well as tyrosine phosphorylation of KSR1 (probably phosphorylation of Tyr728).

These data suggest that Ser722 plays a dual role in the function of KSR1: it might regulate the access of Tyr728 for phosphorylation by LCK and additionally control the level of the activating phosphorylation on Ser218/222 in KSR1-bound MEK. Thereby, Ser722 *per se* and less its phosphorylation might be important for these processes. Moreover, the fact that Ser722 in KSR1 is replaced by a non-phosphorylatable amino acid (Gln835) in KSR2 (see Fig. 17*B*) strongly suggests that it may play an isoform-specific role.
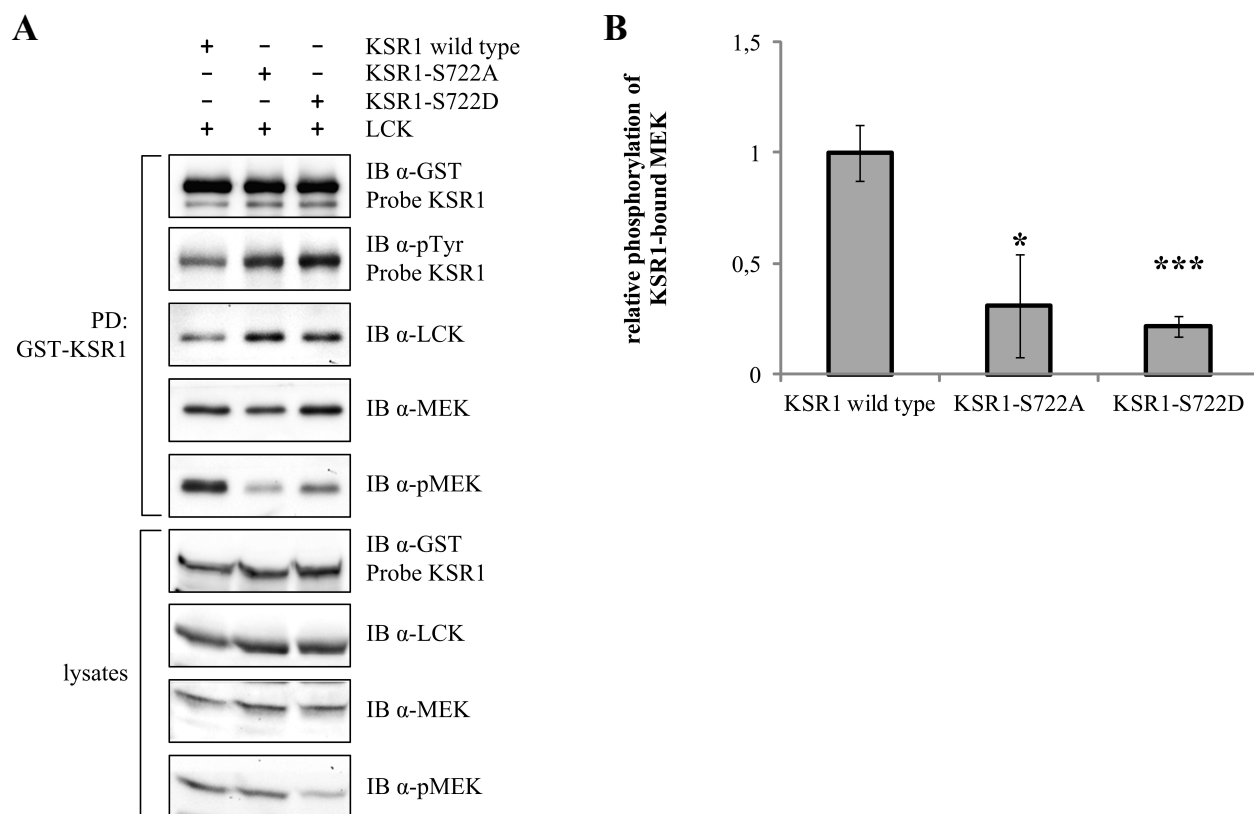
A

B

FIGURE 26: Substitution of Ser722 leads to enhanced KSR1 tyrosine phosphorylation by LCK that abolishes MEK phosphorylation. *A*, GST-fused KSR1-WT and indicated mutants were expressed in the presence of LCK in COS7 cells. Upon lysis, GST-KSR1 was precipitated by use of glutathione-sepharose beads. Amounts and phosphorylation levels of (co)precipitated proteins were determined by use of appropriate antibodies. *B*, relative values of phosphorylated MEK bound to KSR1, where 1-fold represents phosphorylation level of MEK interacting with KSR1-WT. For the diagram, data from three independent experiments were quantified by optical densitometry. Data are presented as mean ± SD of the respective measured parameters. *P* values: ns (not significant), $P \geq 0.05$; * (significant), $P < 0.05$; ** (highly significant), $P < 0.01$; *** (extremely significant), $P < 0.001$ versus corresponding control.

6.6 Generation and validation of an anti-phospho-Tyr728 antibody for murine KSR1

In order to study the conditions under which KSR1-Tyr728 becomes phosphorylated by LCK in more detail, an antibody directed against phospho-Tyr728 in murine KSR1 was generated in cooperation with immunoGlobe Antikörpertechnik. Using KSR1 constructs with substituted amino acids at positions, which were determined by previous experiments in this work to have an effect on KSR1 tyrosine phosphorylation (Arg649, Tyr673, Ser722, and Tyr728), antibody specificity was validated.

SFKs contain an SH2 domain to phosphorylate their substrates on so-called immunoreceptor tyrosine-based activation motifs (ITAMs) (45, 196). For creating a matching peptide, murine KSR1 was screened for those recognition patterns. Despite the proven phosphorylation of Tyr728, no ITAM motif was found in murine KSR1. Nevertheless, the following peptide sequence was designed, synthesized, purified, and coupled to activated Keyhole Limpet Hemocyanin (KLH) for rabbit immunization by the cooperating company: CSYLAPE. The peptide was acetylated at the N-terminus and amino-coupled at the C-terminus. Polyclonal antibodies were purified from animal serum by affinity chromatography and tested for substrate specificity by Western Blot. GST-tagged KSR1-WT and mutants (single substitutions: Y673F, Y728F/E/A/H, R649A/E, S722A/D and double substitution: Y673F/Y728F) were expressed in the presence of LCK in COS7 cells. Upon lysis, GST-KSR1 was precipitated with glutathione-sepharose beads and analyzed for Tyr728 phosphorylation using the specific antibody. Obtained results revealed that the phosphorylation signal was almost completely abolished in samples containing KSR1-Y728F mutant. In contrast, no change of the phosphorylation signal was observed in samples containing KSR1-Y673F, suggesting that the generated antibody specifically recognizes the phosphorylation of Tyr728 in KSR1 (see Fig. 27*A*). Beyond this, the generated antibody seems to be more specific for KSR1-Tyr728 phosphorylation than the general anti-phospho-tyrosine antibody used before, since the signal differences between Tyr728 substitutions and KSR1-WT were more pronounced by utilizing the anti-phospho-Tyr728 antibody than by detecting KSR1 proteins with the commercial anti-phospho-tyrosine antibody (compare phosphorylation levels of KSR1-WT and indicated mutants probed with anti-pTyr728 or anti-pTyr antibody in Fig. 27*B*).

In order to confirm the data obtained with the commercial anti-phospho-tyrosine antibody and described in chapters 6.5.4 and 6.5.6, KSR1 constructs with substituted Arg649 and Ser722 were used for detection with the generated specific anti-phospho-Tyr728 antibody. In agreement with the results described before, the predicted mechanism of LCK-induced Tyr728 phosphorylation in KSR1 affected by Arg649 could be verified; the exchange of Arg649 in KSR1 enhances Tyr728 phosphorylation (see Fig. 27*C*). Additionally, a slight gel shift of GST-tagged KSR1 was visible in the case of substituted Arg649 reflecting a different level of activation (compare anti-pTyr728 signal in *lanes 2* and *3* with others in Fig. 27*C*). Contrary to expectations, utilizing the specific anti-phospho-Tyr728 antibody revealed that the phosphorylation of KSR1-Tyr728

seems to be not significantly affected by the substitutions of Ser722 (compare *lane 1* (KSR1-WT) with *lanes 4* and *5* (Ser722 mutants) in Fig. 27*C*). Unfortunately, endogenous phosphorylation of KSR1-Tyr728 under normal conditions could not be detected by the generated antibody directed against phospho-Tyr728 in murine KSR1.
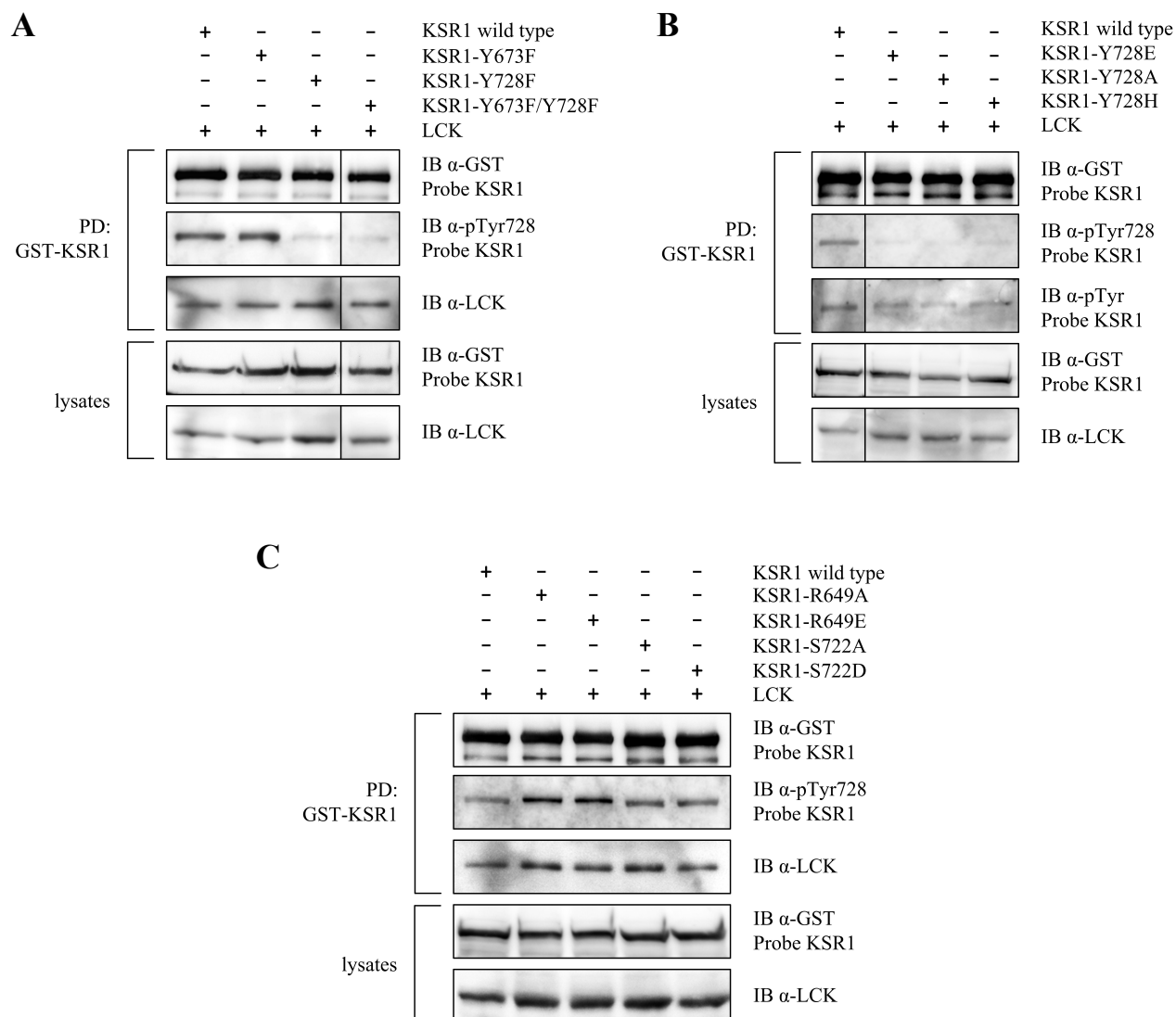
FIGURE 27: Validation of the generated polyclonal antibody directed against phospho-Tyr728 in murine KSR1. In COS7 cells, GST-KSR1-WT and indicated mutants were coexpressed with LCK. Upon cell lysis, GST-fused KSR1 was precipitated by use of glutathione-sepharose beads. Amounts of (co)precipitated proteins were determined by use of appropriate antibodies. Utilizing the anti-phospho-Tyr728 antibody and a commercial anti-phospho-tyrosine antibody, levels of LCK-induced GST-KSR1 tyrosine phosphorylation were detected.

6.7   The effects of KSR1-Tyr728 phosphorylation on cellular behavior

6.7.1   Phosphorylation of KSR1 by the SFK member c-Src

LCK is a member of SFKs specifically expressed in T cells. The phosphorylation of KSR1 by LCK would suggest a cell type-specific function of the phosphorylation site Tyr728 in KSR1. In order to test whether Tyr728 is solely phosphorylated by LCK or additionally by c-Src, which is ubiquitously expressed, COS7 cells were transfected with KSR1-WT or KSR1-Y728F in the presence of active c-Src or LCK (Fig. 28). After cell lysis, GST-tagged KSR1 was precipitated with glutathione-sepharose beads. The precipitation assay demonstrated a profound increase on the level of tyrosine phosphorylation in KSR1 as an effect of coexpression with highly active c-Src. Interestingly, B-RAF and MEK binding to KSR1 was visibly reduced by KSR1 association with c-Src in comparison to the interaction with LCK (Fig. 28*A*). These results clearly show that KSR1 is phosphorylated by active c-Src and suggest that either the binding of c-Src to KSR1 or the tyrosine phosphorylation of KSR1 impair its interaction with MEK and B-RAF.

Subsequently, the binding affinity of active c-Src to KSR1-Y728F mutant and its effects on the interaction of KSR1 with MEK or B-RAF as well as MEK and KSR1 phosphorylation were investigated (Fig. 28*B*). For this purpose, COS7 cells exogenously expressing c-Src combined with KSR1-WT or KSR1-Y728F were lysed and GST-tagged KSR1 was enriched by binding to glutathione-sepharose. Surprisingly, the tyrosine phosphorylation level in KSR1-Y728F versus KSR1-WT was not reduced, as it was shown for the phosphorylation by LCK (compare Fig. 28*B* with Fig. 19*A*). Of note, B-RAF binding to KSR1-Y728F was not altered by c-Src coprecipitation. Strikingly, the effects of Y728F substitution on the interaction of KSR1 with MEK and on the phosphorylation of KSR1-associated MEK were similar to those observed upon KSR1 coprecipitation with LCK; MEK binding to KSR1 was decreased, whereas the phosphorylation level of KSR1-bound MEK was elevated (see Figs. 19*B* and 28*B*). Taken together, these results suggest that c-Src does not phosphorylate KSR1 on Tyr728, but on other(s) not yet identified site(s). Furthermore, Tyr728 seems to be phosphorylated exclusively by LCK and, as a consequence, have a cell type-specific function in mammals.
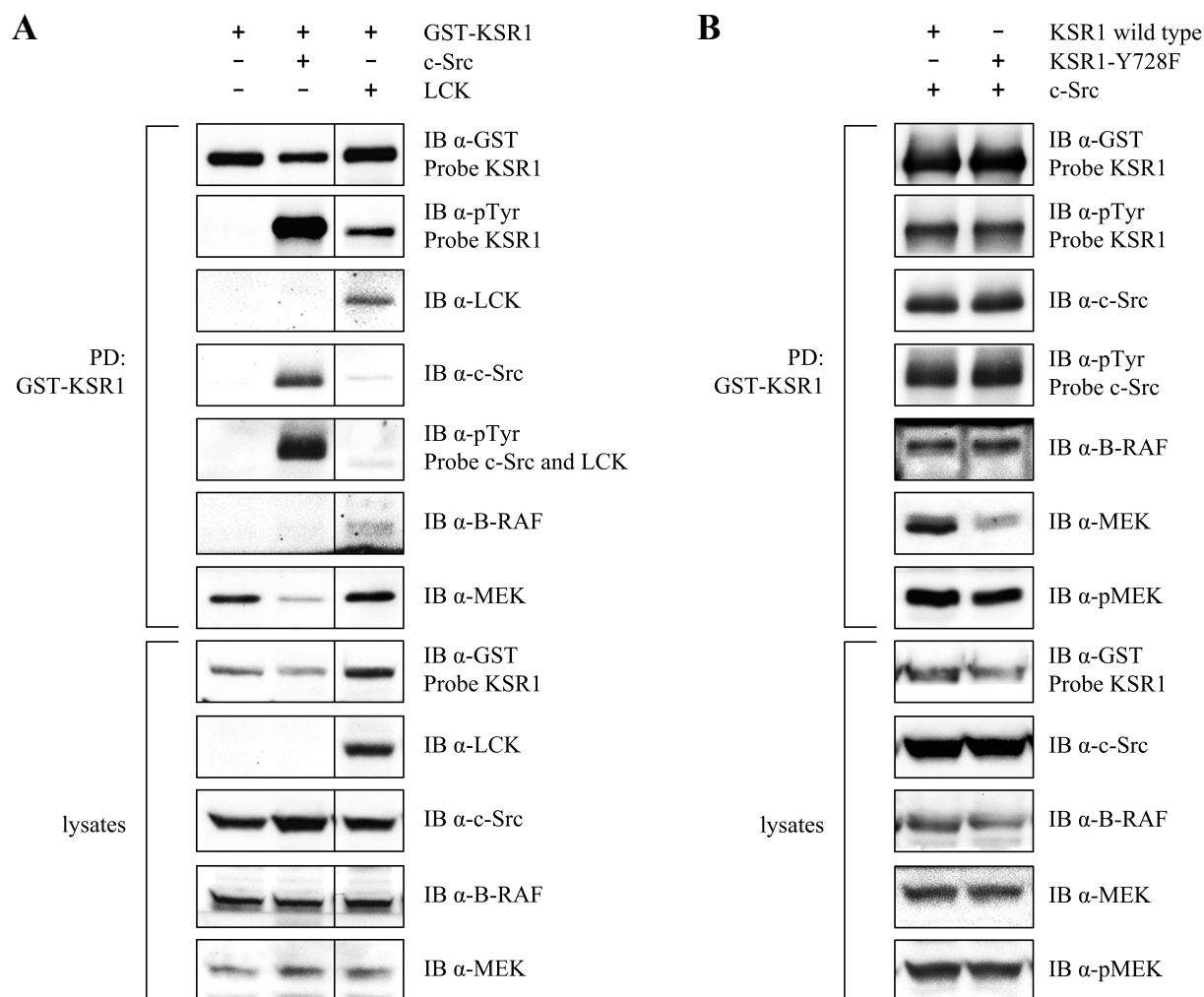
FIGURE 28: Tyrosine phosphorylation of KSR1 by c-Src impairs complex formation with MEK and B-RAF. *A*, KSR1 was expressed in the presence or absence of active c-Src or LCK in COS7 cells. Upon cell lysis, GST-fused KSR1 was precipitated with glutathione-sepharose beads. Amounts of (co)precipitated proteins were determined using appropriate antibodies. Levels of tyrosine phosphorylation in KSR1, c-Src, and LCK were detected using an anti-phospho-tyrosine antibody. *B*, COS7 cells exogenously expressing KSR1-WT and KSR1-Y728F combined with c-Src were lysed and KSR1 proteins were enriched by binding to glutathione-sepharose. Amounts of (co)precipitated proteins were determined by use of appropriate antibodies. Levels of tyrosine phosphorylation in KSR1 and c-Src were detected using an anti-phospho-tyrosine antibody.

6.7.2   Phospho-Tyr728 plays a critical role in cell morphology and proliferation

The family of KSR proteins is known as positive mediator of MAPK signaling. ERK stimulation in the absence of KSR was diminished in a variety of systems, including tumor growth and T cell activation (169). Experimental data, obtained in the present study, suggest that the phosphorylation of KSR1 on Tyr728 negatively regulates MEK activation and may result in the inhibition of cellular processes depending on MAPK signal transduction. To gain insights

into the physiological role of Tyr728 phosphorylation in KSR1, the effects of Tyr728 substitution on cell morphology and proliferation were investigated. For this purpose, mouse embryonic fibroblasts (MEFs) derived from KSR1-deficient mice (KSR1$^{-/-}$ MEFs) (169, 194) were infected with retroviruses for stably expressing KSR1-WT or KSR1-Y728F and sorted in four groups depending on their GFP coexpression level (1-4, where 4 represents the group with the highest protein expression) (Fig. 29*A*). For the following experiments, cells from fraction 4 were utilized.

In general, the structural framework for animal tissues is formed by fibroblasts; an attached-growing cell type, which is elongated with a bipolar or multipolar spindle-shaped morphology. As depicted in Fig. 29*B* (see white arrows), MEFs stably expressing exogenous KSR1-WT formed notably longer protrusions than control cells with empty vector. The protrusion length of the cells stably expressing exogenous KSR1-Y728F seems to be marginally shorter than those of control vector cells, and, therefore, considerably shorter than those of KSR1-WT MEFs. These results suggest that the phosphorylation of Tyr728 in KSR1 may play a critical role in the regulation of cell morphology by inducing the formation of cell protrusions.

Moreover, investigated MEFs considerably vary in terms of their population doubling times. During the time frame of the performed proliferation assay, cells were kept in the exponential growth phase by trypsinizing and seeding every third day. The proliferation rate of infected MEFs was investigated by counting living cells on day 3, 6, 9, and 12 after synchronizing their cell-division cycle. Population doubling time (PDT) and proliferation curves were calculated as described by Cabeza-Arvelaiz *et al.* (195). As illustrated in Fig. 29*C*, MEFs expressing KSR1-Y728F need significantly less time to go through the cell-division cycle than KSR1-WT cells. Interestingly, MEFs expressing KSR1-WT show a similar PDT to control cells over the experimental time span. Comparable effects of the proliferation rate linked to the level of exogenous KSR1-WT expression have been previously described by Kortum and Lewis (194). Fig. 29*D* represents the total amount of cell counts during the time frame of the assay and proves that KSR1-Y728F MEFs proliferate faster than those infected with KSR1-WT, which grew at a similar rate as cells expressing empty vector. These results are consistent with the biochemical analysis showing that substitution of KSR1-Tyr728 by phenylalanine increases the activating phosphorylation of KSR1-bound MEK by B-RAF (see Fig. 19). This supports the assumption

that phosphorylation of KSR1-Tyr728 interferes with the B-RAF-mediated activation of MAPK signaling and consequently alters cell morphology and delays proliferation.
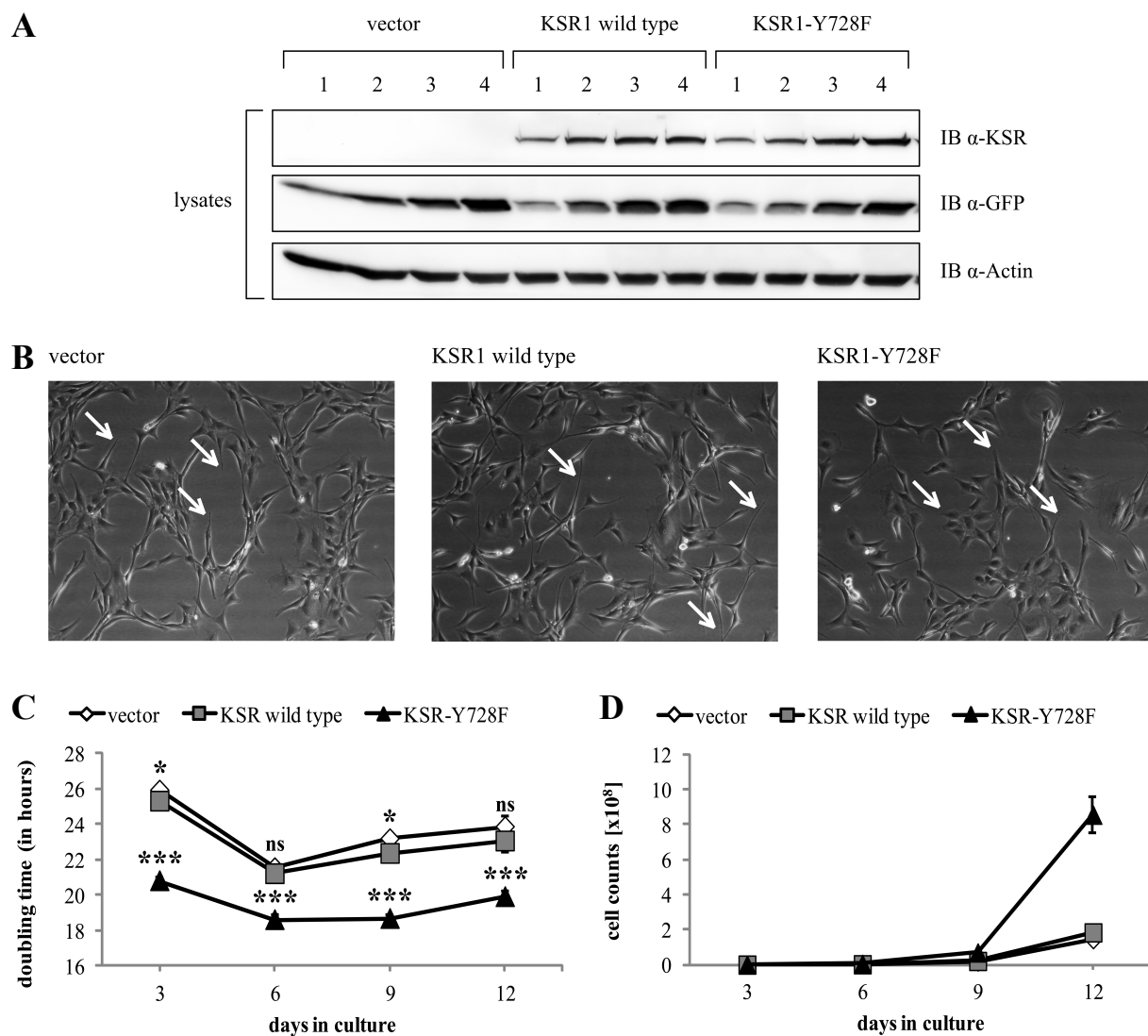

FIGURE 29: Cell morphology and proliferation are affected by the substitution of Tyr728 in KSR1. For stable expression of exogenous KSR1 (WT or Y728F) in mammalian cells, MEFs derived from KSR1 deficient mice (KSR1$^{-/-}$ MEFs) (169, 194) were infected with loaded retroviruses. Empty vector was used for control cells. Subsequent cell sorting according to their GFP signal differences yielded four groups with diverse KSR1 expression level. *A*, Western Blot analysis of MEFs. From fraction 1 to 4, GFP as well as KSR1 (WT or Y728F) expression levels were increased. For subsequent experiments, cells from fraction 4 (with the highest protein expression levels) were used. *B*, illustration of morphological changes on MEFs stably expressing vector (empty control), KSR1-WT, and KSR1-Y728F with the focus on the formation of cell protrusions (see white arrows). *C* and *D*, MEFs were kept in their exponential growth phase by trypsinizing and seeding every third day. Living cells were then counted on day 3, 6, 9, and 12 after synchronization of the cell cycle in order to determine their population doubling time (PDT, see *C*) and total amount of cell counts (see *D*). PDTs and proliferation curves were calculated as described by Cabeza-Arvelaiz *et al.* (195). *Points*, mean of three independent experiments; *bars*, SD. *P* values: ns (not significant), $P \geq 0.05$; * (significant), $P < 0.05$; ** (highly significant), $P < 0.01$; *** (extremely significant), $P < 0.001$ versus corresponding empty vector control.

7   DISCUSSION

The main characteristic of KSR1 refers to its scaffold function in order to facilitate the intracellular MAPK signal transduction from RAF via MEK to ERK. Despite its structural similarity to RAF kinases, KSR1 catalytic activity is still controversially discussed (142, 156–158). While much attention has been devoted to the scaffold function of KSR1 proteins with the focus on KSR1/RAF dimerization and/or constitutive binding of MEK to KSR1, with a few exceptions, little is known about the role of phosphorylation in the KSR1 activation process needed for its scaffold and/or catalytic activity. Especially, tyrosine phosphorylation in KSR1 is poorly understood. The present study, in which the aspects of KSR1 phosphorylation and activation have been examined, provides more insight into the phosphorylation-dependent regulation of KSR1 proteins to work as scaffolds as well as true kinases in order to direct intracellular MAPK signaling for biological responses.

7.1   Interaction with and phosphorylation by LCK affect the scaffolding function of KSR1, in turn, feedback-regulating LCK kinase activity

As has been reported by several research groups, the Src kinase family member LCK induces MAPK signal transduction by phosphorylating and activating RAF kinases on tyrosine residues in order to regulate cellular behavior (42, 43, 70–72). Based on the structural similarity of KSR1 family proteins to RAF kinases, it was assumed that KSR1 might be a target for LCK-induced tyrosine phosphorylation. Indeed, results from the present study revealed that kinase-active LCK binds to KSR1 and phosphorylates it on one or multiple tyrosine residues (Fig. 12). Binding of LCK to the scaffold protein KSR1 leads to changes in the protein dynamics of the MAPK signalosome. It was experimentally proven that presence of LCK stabilizes KSR1/MEK complex formation and significantly facilitates MEK phosphorylation (Fig. 14). On the other hand, strong association between MEK and KSR1 reduces the presence of B-RAF in the signaling complex (Fig. 14*D*). A possible steric hindrance between RAF and MEK binding to KSR1 is excluded due to the fact that RAF is predicted to bind to residues 613-617, whereas MEK associates with

amino acids 777-785 in the KSR1 kinase domain. Additionally, the three-dimensional structure of the mouse KSR1 kinase domain modeled by use of the structure of human KSR2(KD) in complex with rabbit MEK1 as a template revealed that MEK and B-RAF do not directly compete with each other regarding KSR1 interaction due to missing spatial proximity of their binding sites (see Fig. 24*A*). Consequently, based on the key-lock principle, the access for RAF to associate with KSR1 might be diminished due to conformational changes upon LCK-induced KSR1/MEK interaction and vice versa. These aspects raise the question how the overexpression of LCK increases then the activating phosphorylation of KSR1-bound MEK on Ser218 and Ser222 located in the activation segment of MEK? Two possibilities can be taken into consideration. Overexpression of LCK may lead to increased activation of a separate catalytic C-RAF molecule due to phosphorylation of this RAF isoform on Tyr340/341 by LCK. Increased activation of C-RAF would result in elevated phosphorylation of KSR1-associated MEK. It is also possible that LCK-mediated phosphorylation of KSR1 may revive the latent kinase activity of KSR1 towards MEK. In this case, KSR1 would be engaged in MAPK signaling not only as a scaffold, but also as a MEK-phosphorylating kinase.

Whereas MEK interaction with the kinase domain of KSR1 is constitutive, binding of RAF and ERK kinases to the KSR1(KD) is inducible (149, 150, 167, 168). Interestingly, KSR1 scaffolding with RAF, MEK, and ERK and signal transmission from one kinase to the other has consequences for the catalytic activity of LCK (190, 197–199). Kinase-active ERK is described to phosphorylate LCK on Ser59 leading to a modified SH2 domain in LCK that reduces the accessibility to or affinity for phosphoproteins. The SH2 domain usually interacts with the regulatory Tyr505 in LCK, which impairs catalytic activity of the tyrosine kinase. Additionally, LCK is further inactivated by active SHP-1, which dephosphorylates LCK on Tyr394 (200). The feedback phosphorylation of LCK by ERK prevents SHP-1 recruitment and allows long-lasting signaling that is necessary for gene regulation involved in T cell activation and signal transmission. Results of the experiment, in which KSR1 and LCK were expressed together with kinase-inactive MEK mutant (K97M) (see Fig. 15), are in agreement with the previously reported findings. When KSR1-bound MEK is catalytically inactive, kinase activity of ERK is reduced. Hence, upon diminished Ser59 phosphorylation, LCK association with KSR1 is slightly increased, possibly, due to SH2 domain interaction with phosphorylated Tyr505 in LCK

resulting in a weakened catalytic activity of the LCK kinase towards bound KSR1 interfering with KSR1 function.

7.2   Tyr673 and Tyr728 play a crucial role in maintaining KSR1 structure and function

Until recently, the invariant Tyr673 was the only known putative phosphorylation site in murine KSR1, which was identified in 2006 by MS analysis of human KSR1 (Tyr721) (published on the website of *PhosphoSitePlus*; a database of observed post-translational protein modifications, see www.phosphosite.org), but has not been experimentally confirmed so far. In 2013, an additional tyrosine residue, Tyr552, was identified as a site for post-translational modification by phosphorylation in murine KSR1 (201). Tyr552 is located within the conserved region, seventeen residues ahead of the kinase domain of KSR proteins in the linear sequence of amino acids (143). Strikingly, Tyr552 is equivalent to Tyr340 in C-RAF that, beside Tyr341, becomes phosphorylated by Src and LCK in order to achieve full kinase activity of RAF (70–72, 165). Due to the fact that it is replaced by phenylalanine in KSR2 (Phe665), phosphorylation of Tyr552 may play an isoform(KSR1)-specific role.

In the present study, a systematic analysis of regulatory phosphorylation sites of murine KSR1 was performed by mass spectrometry. Numerous serines and threonines could be confirmed as phosphorylation sites (see Fig. 16). In addition, phosphorylation of the highly conserved Tyr728, located in close proximity to the activation and catalytic loop within the structure of the KSR1 kinase domain (Fig. 20*A*), was identified as a novel site for LCK-induced tyrosine phosphorylation. Interestingly, Tyr728 is replaced by a histidine in KSR2 (His841) (see Fig. 17*B*) suggesting that the phosphorylation of Tyr728 plays a KSR1-specific role, possibly with respect to its structural and functional regulation, in order to work as a scaffold and/or a kinase. Interestingly, neither Tyr673 nor Tyr552 in KSR1 could be confirmed as phosphorylation sites by MS analysis in the present study suggesting that the phosphorylation on these sites may be mediated by other tyrosine kinase(s) or may occur only under specific conditions or in specific cell types.

7.2.1 Rearrangements of the secondary structure of KSR1 are regulated by Tyr673 and Tyr728

Proteins are structurally flexible and, consequently, not strictly static objects, which is essential for their biological role. Transitions between the different states occur on a variety of length and time scales (202). Protein dynamics of entire domains control the allosteric formation of protein complexes that play an important role in cell signaling and regulation (203).

The phosphate transfer reaction is one of the possibilities to induce rearrangements of the secondary structure of proteins. Usually, phosphorylation sites are located on the protein surface (12). In contrast, Tyr673 and Tyr728 are partially or completely buried inside the KSR1 kinase domain and are not classical easily accessible for phosphorylation (Fig. 20*C*). However, phosphorylation of buried residues is not unique to KSR1. Actually, 15% of the phosphorylation sites are packed into the domain core of proteins and are not exposed to the solvent. Jiménez *et al.* (204) further reported that the modification of buried residues could have three major structural/functional effects: *i)* regulation of function by affecting functional sites, *ii)* spatial rearrangements (presumably by rigid body movements) of domains within a protein, and *iii)* opening of the structure, leading to local flexibility. Moreover, buried phosphorylation sites are frequently located at or in the vicinity of active sites and binding pockets of proteins thereby affecting the integrity of the functional sites. According to the structural model of the KSR1(KD) shown in Fig. 20*C*, Tyr673 is a part of a rigid helical element, whereas the structures surrounding Tyr728 seem to be more flexible. Additionally, Tyr728 is located close to both the activation and catalytic loop. Considering all these facts, Tyr673 and Tyr728 are thought to play a crucial role in the arrangement of the KSR1 protein structure possibly adjusting its function.

7.2.2 Tyr673 and Tyr728 in KSR1 interfere with KSR1/RAF/MEK complex formation and MEK activation

Although Tyr673 is not the major target for LCK-mediated phosphorylation of KSR1, this residue is crucial for maintaining the structural function of the KSR1 kinase domain. As shown in Fig. 20*C*, Tyr673 is located within a rigid helical structure facing the KSR1/RAF interaction interface. The association of KSR with regulatory RAF is described to occur via side-to-side dimerization, with contacts mainly made between the N-terminal lobes of the kinase domains

inducing an allosteric activation of the binding partners providing that KSR adopts a kinase-activated conformation (165, 205). In contrast, catalytic activity of KSR1 is independent of bound MEK (206). Eventual phosphorylation of Tyr673 might enhance KSR1/RAF dimer formation as a result of induced intramolecular alterations within the kinase domain of KSR1 and, therefore, induce catalytic activity of KSR1. Since KSR-bound RAF is sterically unable to phosphorylate MEK associated with KSR (165), MEK might be phosphorylated and activated by either separated catalytic RAF or kinase-active KSR1 induced by RAF-mediated allosteric activation. Additionally, the release of the activation segment of MEK in complex with KSR1 might be facilitated upon conformational changes in KSR1 induced by RAF binding. In line with these considerations, substitution of the highly conserved Tyr673 significantly reduces B-RAF association with KSR1 and MEK phosphorylation (Fig. 18). Similar to its conserved homologue in *Drosophila* RAF (Tyr538), KSR1-Tyr673 was previously considered as a potential phosphorylation site, but could not be experimentally confirmed. Interestingly, it was shown that the Y538F substitution completely abolished the catalytic activity of D-RAF (193). In accordance with all these facts, Tyr673 in KSR1 is proposed to play an important role in the structural function of the KSR1 kinase domain, similar to Tyr538 in D-RAF (193), rather than being a regulatory phosphorylation site.

In contrast to Tyr673, Tyr728 is a part of a flexible structural element, although it is also packed inside the core of the kinase domain in the 'bound' conformation of KSR1 and is likely not accessible for phosphorylation by LCK, as it was revealed by the structural model of KSR1(KD) (see Fig. 20). Consequently, conformational rearrangement of the KSR1 kinase domain is required for placing Tyr728 at the protein surface for enhanced accessibility in order to get phosphorylated by LCK. Contrary to Tyr673, Tyr728 in the KSR1 kinase domain is closely located to both the activation and catalytic loop. The close proximity to the activation loop suggests that Tyr728 regulates KSR1/MEK interaction, whereas the vicinity to the catalytic loop points to the possible role of Tyr728 in stimulating MEK phosphorylation on Ser218 and Ser222 by RAF or KSR1 kinases. As demonstrated in this study, the phosphorylation of KSR1-Tyr728 induces conformational rearrangement and, hence, interferes with KSR1/MEK association as well as phosphorylation of KSR1-bound MEK *in vivo*. These changes in the kinase domain of KSR1 disclose structural and regulatory roles of Tyr728 phosphorylation. Relevant details are further discussed in the following chapters.

7.3   Tyr728 phosphorylation induces conformational alterations within the KSR1(KD) required for its control of biological responses

In the present study, the effects of KSR1-Tyr728 phosphorylation on MEK activation obtained from biochemical experiments were confirmed and complemented by spatial modeling of KSR1 kinase domain using the published structure of the hKSR2/rMEK1 complex as a template (165). Molecular modeling revealed conformational rearrangement of the KSR1(KD) upon Tyr728 phosphorylation, which might stabilize internal structures of the protein. These findings point to a novel mechanism of KSR1 regulation in order to act as a scaffold and/or a protein kinase and uncover new aspects in the KSR1-dependent regulation of cellular processes.

7.3.1   Tyr728 affects surrounding structural elements within the KSR1 kinase domain

Arg649, located within the αD helix of the KSR1(KD), is conserved in KSR1 and KSR2 (see Fig. 20*A* and *B* as well as Fig. 17*A* and *B*) underlining its general importance for the structure of KSR proteins. As shown in the KSR1(KD) model, Arg649 may stabilize the 'bound' conformation of the protein, because the cationic side chain of Arg649 forms a hydrogen bond with the phosphate moiety of phospho-Tyr728. Thus, Arg649 is supposed to act as the major anchor point for phosphorylated Tyr728, which is supported by the interaction of Tyr728 with His645 and Glu763 (Fig. 20*B*). Furthermore, it is very likely that Arg649 also interacts with the aromatic Trp769. In general, the interaction between the cationic side chain of an aliphatic amino acid (here: Arg649) and the side chain of an aromatic residue (here: Trp769), named as cation-π interaction, significantly contributes to stabilization of secondary structures of proteins (207). Consequently, substitution of Arg649 was expected to relax the protein structure surrounding Tyr728 and to gain access for phosphorylation by LCK. Indeed, replacement of Arg649 in KSR1 by alanine or glutamic acid led to enhanced binding of LCK accompanied by increased phosphorylation of Tyr728 (Fig. 23 and 27*C*). Structural analyses of non-phosphorylated or substituted Tyr728 revealed abolished hydrogen bonding between Arg649 and the relevant residue at the position 728 in KSR1 confirming the positive effect on the KSR1(KD) stability induced by Tyr728 phosphorylation (Fig. 21). Surprisingly, MD simulations of the αD helix

(contains Arg649) revealed that the flexibility of the Arg649-surrounding structure seems to be not significantly affected suggesting independency of Tyr728 phosphorylation (Fig. 24*D*). Together, these findings suggest that, upon its phosphorylation, Tyr728 and adjacent elements might move towards Arg649 for stabilizing hydrogen bonding and away from the KSR1/MEK interface thereby loosen their kinase-kinase interaction.

The hydroxyl group of non-phosphorylated Tyr728 forms a network of interactions with surrounding residues, which may stabilize the conformation of the activation segment required for the binding to MEK (Fig. 21*B*). Since the network of interactions is extended by several direct hydrogen bonds between the phosphate group of phosphorylated Tyr728 and surrounding residues in the KSR1(KD), phospho-Tyr728 may stabilize the functional conformation of the activation segment even more efficiently (compare Fig. 21*A* with *B*). According to the structural model, a phosphomimetic amino acid, such as glutamic acid, at the position 728 would not substitute for (non-)phosphorylated tyrosine in terms of stabilization of the activation segment, because its predicted pattern of interactions with surrounding residues substantially differs from that of phospho-Tyr728 and non-phospho-Tyr728 (compare Fig. 21*A* and *B* with *D*). Consistently, replacement of tyrosine at the position 728 with glutamic acid completely abolished KSR1/MEK association (Fig. 22*A*).

7.3.2 Phosphorylation of Tyr728 regulates complex formation between KSR1, RAF, and MEK

The present study clearly demonstrated that LCK-mediated phosphorylation of Tyr728 in KSR1 has significant effects on the association with MEK and its activation that further affects MAPK signal propagation and cellular responses. Biochemical studies using KSR1 substitution mutant revealed a strongly decreased MEK binding to KSR1 followed by increased RAF interaction with KSR1 resulting in elevated MEK activation, if Tyr728 was replaced by phenylalanine (Fig. 19). In order to build on the results obtained by MD simulations and to focus on the formation of the KSR1/MEK complex affected by phosphorylation of Tyr728, it is assumed that the interaction of KSR1 with MEK is tightened by conformational rearrangement (Fig. 20*C* and *D*). KSR1/MEK binding is mediated by their catalytic sites facing each other via their αG helices (major part) and activation segments (minor part) (165). As mentioned before,

the structural modeling of the KSR1(KD) bound to MEK revealed that Tyr728 is located in a short helical element just C-terminally of the activation segment. Changes in the conformation of the activation segment in the kinase domain of KSR1 are supposed to interfere not only with the catalytic competence of KSR1, but also with its ability to bind MEK. In agreement with this assumption, dependent on KSR1-Tyr728 phosphorylation, the activation loop interface may regulate the kinase-kinase interaction interface with MEK as concluded from lower fluctuations upon Tyr728 phosphorylation shown in MD simulations. In contrast, the flexibility of the αG helix interface was not significantly affected by post-translational modification of Tyr728 (compare Fig. 24*C* with *F*). As presumed, this effect may arise due to the proximity of Tyr728 to the activation loop in the linear sequence of amino acids, which also seems to be closer within the spatial structure of the KSR1 kinase domain than to the αG helix (see Fig. 20*A*). Strikingly, the distance between the Cα-atom of the phosphorylation site and Ala778, located within the αG helix (interface to MEK), is shortened when Tyr728 is phosphorylated (Fig. 25*C* and *D*) confirming tightened protein-protein interaction between the kinase domains of KSR1 and MEK. Accordingly, substitution of Tyr728 by phenylalanine or alanine – the neutral residues that may not form any stabilizing interactions with surrounding residues in the structural model – resulted in significantly reduced MEK binding to KSR1 facilitating MEK activation (Fig. 19*B* and *D* as well as Fig. 22*A* and *B*). These results suggest that a less flexible and more compact activation segment interface might be formed in order to enhance MEK binding to KSR1 and, moreover, diminish MEK activation. Consequently, the binding affinity of MEK to KSR1 as well as the accessibility of the MEK activation loop, including Ser218 and Ser222, for its activating phosphorylation and sequential MAPK signaling transmission is affected by the level of Tyr728 phosphorylation in KSR1.

KSR/MEK complexes assemble either KSR/MEK heterotetramers or KSR/MEK/RAF ternary complexes via side-to-side dimerization of two KSR molecules or of one KSR and one RAF molecule, respectively. Brennan *et al.* (165) suggested that the inaccessible activation segment of MEK is released through the interaction of KSR with a regulatory RAF molecule in *cis*, allowing a separate catalytic RAF molecule in *trans* to phosphorylate KSR-bound MEK. Experimental data presented in this work are in agreement with this hypothesis. Substitution of the tyrosine at the position 728 in KSR1 by a phenylalanine, which is supposed to loosen KSR1/MEK interaction, demonstrated enhanced KSR1/B-RAF heterodimerization and increased activating

phosphorylation of MEK in complex with KSR1 (Fig. 19). However, MD simulation of the KSR1/RAF interface could not confirm the stabilization of structural elements required for the interaction with RAF upon KSR1-Tyr728 phosphorylation (Fig. 24*G*) suggesting that further structural elements are involved in the regulation of the complex formation between RAF and KSR1 proteins.

In summary, in order to phosphorylate Tyr728, buried inside the core of the KSR1 kinase domain, the 'bound' conformation of KSR1 in complex with MEK has to be rearranged by inducing an 'unbound' or loosen conformation of KSR1. Consequently, it might be conceivable that binding of a regulatory RAF molecule to the scaffold non-phosphorylated on Tyr728 may induce allosteric activation of KSR1. Conformational changes enable Tyr728 phosphorylation on the surface of the KSR1 protein by LCK followed by tightened MEK association with KSR1 and loosen KSR1/RAF interaction. Due to internal hydrogen bonding of the phospho moiety of phospho-Tyr728 with surrounding residues, internal structures of the KSR1(KD) are stabilized. Particularly Arg649 works as an anchor point for the phospho moiety of phospho-Tyr728 in the kinase domain of KSR1. Furthermore, the MEK activation segment may be inaccessible resulting in diminished MEK phosphorylation by a catalytic RAF molecule.

7.3.3   MAPK-regulated cellular behavior is affected by the phosphorylation of Tyr728 in KSR1

In order to address the issue which cellular processes are affected by stabilized internal structures of the KSR1 kinase domain upon Tyr728 phosphorylation, the cellular behavior of KSR1-deficient MEFs infected with a virus carrying KSR1 wild type or Y728F substitution mutant was analyzed in this study (Fig. 29). It is well established that EGF receptor (EGFR) activation induces cellular motility (208). Upon growth factor binding to EGFR, the MAPK cascade is activated and intracellular signal transmission from RAF via MEK to ERK is enhanced by complex formation with KSR1. Since KSR1 regulates the catalytic activity of ERK by controlling MEK phosphorylation, altered MEK binding to KSR1 as well as the degree of access of the MEK activation loop for its phosphorylation may impair ERK activation and consequently affect cell motility. As demonstrated in this study, the substitution of Tyr728 by phenylalanine induced a loosen KSR1/MEK interaction followed by enhanced MEK

phosphorylation and activation, but which consequences does this have for the control of cellular motility? Interestingly, MEFs stably expressing exogenous KSR1-Y728F form considerably shorter protrusions than KSR1-WT cells (Fig. 29*B*) suggesting the involvement of LCK-mediated Tyr728 phosphorylation in the regulation of cytoskeleton rearrangement and, consequently, in the regulation of cell motility. Since LCK is known as membrane-anchored protein, it is very likely that phosphorylation of KSR1 by LCK occurs after the recruitment of KSR1 to the plasma membrane upon extracellular stimulation. However, the finding that coexpression with KSR1 causes recruitment of LCK to the cytoskeleton (Fig. 13) suggests that LCK-mediated phosphorylation of KSR1 may also occur at this cellular compartment.

Previously published studies report a new role for KSR1 in the regulation of cell motility. Low levels of KSR1 enhance cell motility, while high levels of KSR1 expression inhibit motility and cause major changes in cellular morphology (209). Analog to these findings, MEFs stably overexpressing high levels of KSR1-WT protein form notably longer protrusions than KSR1-deficient control cells expressing empty vector, as demonstrated in Fig. 29*B* of the present study. In addition, KSR1 interacts with a protein called FHOD1, a regulator of cell motility, actin cytoskeleton, and gene transcription. Disruption of the KSR1/FHOD1 interaction inhibits the ability of KSR1 to enhance cell migration (209). More important, the F-actin binding protein Leukocyte-specific protein 1 (LSP1) has been also shown to target KSR, MEK1, and ERK2 to peripheral actin filaments supporting a model, in which MEK1 and ERK2 are organized in a cytoskeletal signaling complex together with KSR (189). In light of the reported findings, results from the present study suggest that LCK may regulate the cytoskeleton-associated function of KSR1.

In addition to its role in regulating cellular motility, KSR1 is known to play a critical role in the control of cell proliferation. As already mentioned, KSR1-Y728F substitution mediates an untightened KSR1 interaction with MEK followed by enhanced MEK phosphorylation and activation. Based on its major role in the regulation of MAPK signal propagation from RAF via MEK to ERK by particularly affecting MEK binding and phosphorylation, Tyr728 phosphorylation in KSR1 may consequently interfere with cellular growth. Indeed, the proliferation rate of MEFs infected with KSR1-Y728F mutant was significantly increased in comparison to MEFs exogenously expressing KSR1 wild type (see Fig. 29*C* and *D*) representing a pivotal role of the phosphorylation of Tyr728 in KSR1 in the downregulation of cell

proliferation. Moreover, KSR1 is essential for the proper activation of the MAPK pathway that causes biological output in primary T lymphocytes (210). In contrast to KSR1, the function of KSR2, which carries His841 homolog to Tyr728 in KSR1, cannot be regulated by the lymphocyte-specific tyrosine kinase LCK suggesting a KSR1-specific role in modulating the sensitivity of MAPK pathway activation in T cells (210). In conclusion, a hypothetic model is proposed on the basis of the results from this work, in which phospho-Tyr728 induces alterations in MEK and RAF binding to KSR1 as well as in MEK activating phosphorylation leading to changes on cellular level (see Fig. 30).

Since LCK is expressed specifically in lymphocytes, which other tyrosine kinase(s) is(are) considered for KSR1-Tyr728 phosphorylation in MEF cells? One possible candidate is c-Src. Based on the findings that Tyr340/341 in C-RAF and the homolog residues in A-RAF (Tyr301/302) can be phosphorylated by both c-Src and LCK (72, 87, 187), these two kinases may phosphorylate tyrosine residues located in similar substrates. As shown in Fig. 28*A*, c-Src phosphorylates KSR1 and, consequently, strongly reduces B-RAF and MEK binding to KSR1. However, in contrast to results obtained with LCK, the substitution of Tyr728 did not reduce tyrosine phosphorylation of KSR1 upon coexpression with c-Src suggesting that Tyr728 in KSR1 is not a major target for phosphorylation by c-Src. Interestingly, MEK binding to KSR1 was decreased and the phosphorylation level of KSR1-bound MEK was elevated caused by c-Src-induced tyrosine phosphorylation in KSR1, similar to results obtained with LCK (see Fig. 28*B*), suggesting that Tyr728 might be phosphorylated by c-Src. However, the strong phosphorylation of other site(s) overlay the effect of Tyr728 substitution. With regard to biological responses dependent on the intracellular regulation by c-Src and KSR1, different groups published some interesting findings. Kilkenny *et al.* (211) described a proliferation mechanism for MEF cells dependent on c-Src. MEFs expressing endogenous c-Src proliferate significantly faster upon FGF and EGF stimulation than cells lacking c-Src, while overexpression of c-Src diminished cell proliferation to the level of c-Src-deficient MEFs. Remarkably, the level of ERK activation was similar in cells with either endogenous expression or overexpression of c-Src. Furthermore, Sugimoto *et al.* (212) investigated the impact of KSR1 on Elk-1, a physiological substrate of ERK that is involved in the regulation of cell proliferation, differentiation, and apoptosis. They observed that KSR1 specifically blocks growth factor- as well as RAS-induced phosphorylation and activation of Elk-1 without affecting the overall

activation of ERK *per se*. Moreover, the integrity of the KSR1 kinase domain may be required, since a kinase-deficient mutant of KSR1 does not inhibit Elk-1, but even enhances both Elk-1 phosphorylation and transactivation activity in unstimulated cells. Previously published findings and the data obtained in the present study strongly suggest that KSR1-Tyr728 phosphorylation by LCK may be of major physiological relevance and not a simple artifact of transient transfection and/or overexpression.
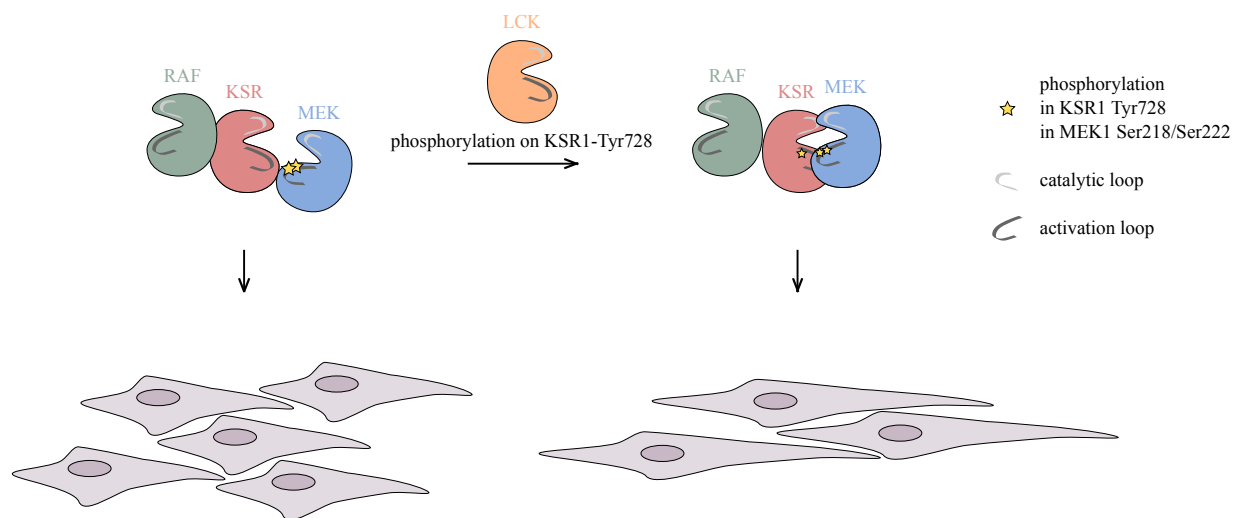

FIGURE 30: Hypothetic model of altered KSR1/RAF/MEK complex formation and cellular behavior caused by the LCK-induced Tyr728 phosphorylation in KSR1. Due to the phosphorylation of Tyr728 in the kinase domain of KSR1 by the Src kinase family member LCK, KSR1 binding to a regulatory RAF molecule is loosen, whereas KSR1/MEK interaction is tightened as a consequence of diminished RAF-dependent allosteric activation of KSR1. Intramolecular changes in KSR1, induced by Tyr728 phosphorylation, further limit the access of Ser218/222 in the activation segment of MEK by an altered KSR1/MEK interaction interface resulting in reduced MEK phosphorylation and activation. Consequently, due to the presumed downregulation of ERK activation upon KSR1-Tyr728 phosphorylation, cells change their morphology by developing much longer cell protrusions that leads to impaired motility. Moreover, cell proliferation is significantly diminished.

7.4 The effects of Tyr728 phosphorylation on the kinase activity of KSR1

Despite the high similarity between the protein sequence of KSR and RAF kinases (particularly with respect to their kinase domains), it has been debated for a long time whether KSR1 has a true kinase function or not (154, 156–158, 165, 167). As present in every known protein kinase, the catalytic and activation loop are important functional elements. On the one hand, the catalytic loop controls both the orientation of the ATP molecule inside the catalytic cleft and subsequent phosphate transfer. On the other hand, the activation loop regulates the

access of the substrate to the active site, which is usually displaced by phosphorylation of serine and/or threonine residues present in this segment, and then counteracts positive charged amino acid(s) in the catalytic loop. As discussed before, results from the present work suggest that phosphorylation of Tyr728 may have an impact on the activation segment in KSR1 due to conformational rearrangement and consequently alter both the MAPK signalosomes formation and activation (see Figs. 19, 20-22, 24, and 25). Structural modeling further revealed that Tyr728 is located in close proximity to the catalytic loop of the KSR1 kinase domain (as shown in Fig. 20*A*). This raises the question whether KSR1 has its own intrinsic catalytic activity, which might be regulated by Tyr728 phosphorylation.

7.4.1 The stabilizing effect of phospho-Tyr728 on Lys685 may enhance the catalytic activity of KSR1

Until recently, KSR was declared as an enzymatically inactive kinase or pseudokinase due to the substitution of the ATP-coordinating lysine residue in the subdomain II of the kinase domain of mammalian KSR by an arginine (Arg589 in mKSR1). Replacement of the invariant lysine by any other amino acid, including arginine, generally leads to a catalytically inactive kinase (158, 213). However, there are exceptions to this rule. For instance, when lysine at the position 274 in the atypical protein kinase C-ι (aPKCι), a residue essential for ATP binding and activity conserved in most protein kinases, was replaced by arginine (K274R mutant), this kinase retained its normal kinase activity. In contrast, replacement of Lys274 by tryptophan (K274W) completely abolished the kinase activity of aPKCι (214). These data suggest that in some cases replacement of the invariant lysine with arginine, but not with any other amino acid, can be tolerated with respect to catalytic activity of the respective kinase. In the case of KSR protein, the structural modeling of the kinase domain of KSR2 as well as KSR1 in complex with MEK1 indicates that KSR has the potential for catalytic activity (see (165) and Figs. 20 and 25). Additionally, it has been reported that KSR2 is the major kinase responsible for MEK1 phosphorylation at non-B-RAF sites, but KSR2 as well as KSR1 is also capable to phosphorylate MEK1 at Ser218 and Ser222 (B-RAF sites), however, with extremely low efficiency (163, 165). Furthermore, other groups also reported kinase activity for KSR1 and, additionally, towards different substrates, such as ceramide-activated protein (CAP) and C-RAF (156, 157, 161, 162).

Thus, a growing body of evidence supports the view that KSR proteins can indeed act as true kinases. Based on these facts and on the results from the present study, involvement of Tyr728 phosphorylation in regulation of the KSR1 catalytic activity is very likely. Notably, the conserved aspartic acid of the catalytic loop (Asp683 in KSR1, see Fig. 17*A* and *B*), which is located very close to Lys685, is supposed to act as a catalytic base to free up the hydroxyl oxygen on the substrate for nucleophilic attack (Figs. 20*B* and 25*A*). Additionally, the activation loop often contains a phosphorylation site that induces a conformational rearrangement of the loop upon phosphorylation allowing the substrate to bind to the protein kinase and positioning the conserved aspartate of the catalytic loop in the right place for the phosphate transfer reaction (13). Therefore, the close proximity of Tyr728 to these functional elements (Figs. 20*A* and *B* and 25*A*) indicates that Tyr728 phosphorylation may affect the potential catalytic competence of KSR1 kinase.

Lys685, a residue highly conserved in all protein kinases, is located within the catalytic loop generally coordinating the transfer reaction of the γ-phosphate of the ATP molecule onto the substrate. Structural modeling revealed the vicinity of Tyr728 to Lys685 (see Fig. 20*B*) giving a strong indication that Tyr728 phosphorylation may regulate KSR1 kinase activity via Lys685. Despite the fact that the KSR1 catalytic loop *per se* appears to be not significantly affected upon phosphorylation of Tyr728 (see MD simulations in Fig. 24*E*), the amino group of Lys685 seems to be conformationally fixed between the phosphate moiety of phospho-Tyr728 and the γ-phosphate group of the ATP molecule, such that it can ideally facilitate phosphate transfer from the ATP to an acceptor hydroxyl group in a substrate (Fig. 25*A* and *B*). Based on these observations KSR1 kinase activity might be induced by conformational rearrangements upon Tyr728 phosphorylation. Notably, it has been described for several tyrosine kinases that the phosphorylation of tyrosine residue(s) located in the activation loop is an essential early event that results in the catalytic activation of the protein, as shown for janus kinase 3 (JAK3), zeta-chain-associated protein kinase 70 (ZAP-70), the insulin receptor, and the fibroblast growth factor receptor 1 (FGFR1) (215, 216). For most of the members of receptor tyrosine kinases (RTKs, like insulin receptor and FGFR1), their so-called juxtaposition enhances autophosphorylation in *trans* of tyrosine residues, located in the activation loop or in the juxtamembrane region, inducing conformational rearrangements that consequently serve to stabilize the active state of the protein kinase (217). Despite similar disclosures, the activation

loop of the KSR1 kinase (aa 707-723) does not carry any tyrosine residue. However, Tyr728, which is located five residues ahead of the activation segment, is the tyrosine that is the closest in the linear sequence of amino acids giving a strong indication that Tyr728 and its phosphorylation have similar importance for the regulation of the KSR1 kinase activity.

7.4.2 Tyr728 may regulate the *cis*-autophosphorylation of KSR1 on Ser722

Ser722 is a part of the activation loop, located six residues ahead of Tyr728 in the linear sequence of amino acids (Figs. 17*A* and 20*A*). Additionally, Ser722 is localized in the vicinity of the catalytic site in the spatial model of the KSR1(KD) (see Fig. 20*A* and *C*). Remarkably, MS analysis of the present study further identified Ser722 as a novel phosphorylation site in KSR1 (Fig. 16). Phosphorylation of this residue was found in all replicates suggesting that Ser722 is one of the major sites for phosphorylation in murine KSR1. Based on its localization and phosphorylation level, Ser722 possibly affects the catalytic activity and/or the substrate specificity of KSR1. As shown in this work, Ser722 in KSR1 has almost no impact on the regulation of the KSR1/MEK interaction, but it controls the phosphorylation of Ser218 and Ser222 in the activation segment of MEK (see Fig. 26). Furthermore, Ser722 might be a linker between the ATP-coordinating catalytic loop and the activation loop in KSR1 to control the kinase activity of KSR1 and the access of the activation loop in MEK to the catalytic site in KSR1 for mediating the direct phosphorylation of MEK by KSR1.

Results of the present work together with the previously published data also suggest that KSR1-Ser722 might be autophosphorylated in *cis*. Goettel *et al.* (163) demonstrated that mammalian KSR1 is indeed capable of serine autophosphorylation, which likely occurs on a single or limited number of serine residues, since only a single migrating ^{32}P-labeled peptide was detected in 2D tryptic phosphopeptide mapping following *in vitro* kinase assay. Notably, autophosphorylation of a critical residue in the activation loop is an essential maturation event required for full enzyme activity of several protein kinases (218–220). Therefore, it seems very likely that Ser722 autophosphorylation is crucial for the activity of the KSR1 kinase. Additionally, Ser722 is invariant in KSR1 proteins of different species, but is substituted by a non-phosphorylatable amino acid (Gln835) in KSR2 (Fig. 17*A* and *B*). Consistently, no autophosphorylation of KSR2 has been reported so far.

Similar to the replacement of the serine (Ser722) in KSR1 to a glutamine (Gln835) in KSR2, the tyrosine (Tyr728) in KSR1 is also substituted by a non-phosphorylatable residue, histidine (His841), in KSR2 (Fig. 17*B*). The co-occurrence of these two amino acid exchanges in the course of KSR evolution supports the idea of a regulatory interrelation between the phosphorylation of Ser722 and Tyr728. In general, kinases that are autophosphorylated in *cis* are likely to have developed additional mechanisms to control their catalytic activity, including phosphorylation on other regions of the protein (220). Therefore, phosphorylated Tyr728 in KSR1 might be conceivable to regulate KSR1 kinase activity towards MEK depending on the phosphorylation level of Ser722. Moreover, loss of the autophosphorylation site Ser722 in KSR1(KD) would make the Tyr728-mediated regulation redundant, as it exists in mammalian KSR2. Of note, Ser722 does not regulate Tyr728 phosphorylation in KSR1 by LCK, as no significant differences in the phosphorylation level of Tyr728 between KSR1 wild type and Ser722 mutants were found (Fig. 27*C*). In line with published findings, this strongly supports the assumption that Tyr728 regulates Ser722 autophosphorylation possibly leading to full enzyme activity of the KSR1 kinase.

7.4.3 Tyr728 regulates the transition between the scaffolding and catalytic function of KSR1

Autophosphorylation of a critical residue in the activation loop of several protein kinases is an essential step needed for full catalytic activity. Lochhead *et al.* (220) revealed a molecular mechanism by which protein kinases phosphorylate their own activation loop. In detail, during maturation of the enzyme, a canonical kinase domain undergoes a transitory, functional intermediate form that may differ in residue and substrate specificity. As discussed before, the existence of such an intramolecular maturation mechanism is a *conditio sine qua non* for the LCK-induced phosphorylation of KSR1-Tyr728. LCK may phosphorylate the nascent KSR1 kinase passing through a transitory intermediate. Structural modeling and molecular dynamics simulations propose a local stabilization of the functional element in the mature kinase, involved in the catalytic reaction, by phospho-Tyr728 (Figs. 20, 24, and 25). Therefore, it is conceivable that phosphorylation of Tyr728 would increase the likelihood of the activating Ser722 autophosphorylation resulting in enhanced KSR1 kinase activity. Of note, the replacement of

tyrosine at the position 728 with histidine, whose uncharged form is isosterically analog to tyrosine, did not alter KSR1/MEK interaction (Fig. 22*A*). Hence, a histidine at the position 728 in KSR1 can be tolerated with respect to the interaction with MEK. In agreement with this, KSR2, which carries a histidine at the position homolog to Tyr728 in KSR1 (Fig. 17*B*), binds MEK as efficient as KSR1, but has very low intrinsic catalytic activity towards MEK (165).

Taken together, in the context of previously published data, the results of the present study support a model, in which Tyr728 phosphorylation may regulate the transition between the scaffold and the true kinase function of KSR1. Whereas autophosphorylation of Ser722 would enhance catalytic activity of KSR1, phosphorylation of KSR1-Tyr728 by LCK would *i*) facilitate the autophosphorylation of Ser722, *ii*) support the face-to-face binding of MEK to KSR1, and *iii*) counteract the side-to-side heterodimerization of KSR1 with regulatory RAF preventing the release of the MEK activation segment for its phosphorylation by a catalytic RAF molecule. The proposed regulatory mechanism may help KSR1 to serve as a control point used to fine-tune cellular responses by regulating the transition between its scaffolding and catalytic functions.

8 REFERENCES

1.   Kim, E. K., and Choi, E.-J. (2010) Pathological roles of MAPK signaling pathways in human diseases. *Biochim Biophys Acta* **1802**, 396–405

2.   Tidyman, W. E., and Rauen, K. A. (2009) The RASopathies: developmental syndromes of Ras/MAPK pathway dysregulation. *Curr Opin Genet Dev* **19**, 230–6

3.   Tanti, J.-F., and Jager, J. (2009) Cellular mechanisms of insulin resistance: role of stress-regulated serine kinases and insulin receptor substrates (IRS) serine phosphorylation. *Curr Opin Pharmacol* **9**, 753–62

4.   Chico, L. K., Van Eldik, L. J., and Watterson, D. M. (2009) Targeting protein kinases in central nervous system disorders. *Nat Rev Drug Discov* **8**, 892–909

5.   Muslin, A. J. (2008) MAPK signalling in cardiovascular health and disease: molecular mechanisms and therapeutic targets. *Clin Sci* **115**, 203–18

6.   Montagut, C., and Settleman, J. (2009) Targeting the RAF-MEK-ERK pathway in cancer therapy. *Cancer Lett* **283**, 125–34

7.   Hanahan, D., and Weinberg, R. A. (2000) The hallmarks of cancer. *Cell* **100**, 57–70

8.   Hanahan, D., and Weinberg, R. A. (2011) Hallmarks of cancer: the next generation. *Cell* **144**, 646–74

9.   Roskoski, R. (2010) RAF protein-serine/threonine kinases: structure and regulation. *Biochem Biophys Res Commun* **399**, 313–7

10.   Manning, G., Whyte, D. B., Martinez, R., Hunter, T., and Sudarsanam, S. (2002) The protein kinase complement of the human genome. *Science* **298**, 1912–34

11.   Alonso, A., Sasin, J., Bottini, N., Friedberg, I., Friedberg, I., Osterman, A., Godzik, A., Hunter, T., Dixon, J., and Mustelin, T. (2004) Protein tyrosine phosphatases in the human genome. *Cell* **117**, 699–711

12.   Bononi, A., Agnoletto, C., De Marchi, E., Marchi, S., Patergnani, S., Bonora, M., Giorgi, C., Missiroli, S., Poletti, F., Rimessi, A., and Pinton, P. (2011) Protein kinases and phosphatases in the control of cell fate. *Enzym Res* **2011**, 329098

13.   Hanks, S. K., and Hunter, T. (1995) Protein kinases 6. The eukaryotic protein kinase superfamily: kinase (catalytic) domain structure and classification. *FASEB J* **9**, 576–96

14.   Schulze, M., and Gohla, A. (2013) Kinases and phosphatases: key enzymes in targeted cancer therapy. *Dtsch Med Wochenschr* **138**, 437–40

15.   Seger, R., and Krebs, E. G. (1995) The MAPK signaling cascade. *FASEB J* **9**, 726–35

16.   Davis, R. J. (1994) MAPKs: new JNK expands the group. *Trends Biochem Sci* **19**, 470–3

17.   Pitzschke, A., Schikora, A., and Hirt, H. (2009) MAPK cascade signalling networks in plant defence. *Curr Opin Plant Biol* **12**, 421–6

18. Avruch, J. (2007) MAP kinase pathways: the first twenty years. *Biochim Biophys Acta* **1773**, 1150–60

19. Morrison, D. K. (2012) MAP kinase pathways. *Cold Spring Harb Perspect Biol* **4**

20. Zhang, W., and Liu, H. T. (2002) MAPK signal pathways in the regulation of cell proliferation in mammalian cells. *Cell Res* **12**, 9–18

21. Dhillon, A. S., Hagan, S., Rath, O., and Kolch, W. (2007) MAP kinase signalling pathways in cancer. *Oncogene* **26**, 3279–90

22. Rapp, U. R., Götz, R., and Albert, S. (2006) BuCy RAFs drive cells into MEK addiction. *Cancer Cell* **9**, 9–12

23. Wellbrock, C., Karasarides, M., and Marais, R. (2004) The RAF proteins take centre stage. *Nat Rev Mol Cell Biol* **5**, 875–85

24. McKay, M. M., and Morrison, D. K. (2007) Integrating signals from RTKs to ERK/MAPK. *Oncogene* **26**, 3113–21

25. Kim, H. J., and Bar-Sagi, D. (2004) Modulation of signalling by Sprouty: a developing story. *Nat Rev Mol Cell Biol* **5**, 441–50

26. Brown MD, S. D. (2009) Protein scaffolds in MAP kinase signalling. *Cell Signal* **21**, 462–9

27. Harvey, J. J. (1964) An unidentified virus which causes the rapid production of tumours in mice. *Nature* **204**, 1104–5

28. Quilliam, L. A., Khosravi-Far, R., Huff, S. Y., and Der, C. J. (1995) Guanine nucleotide exchange factors: activators of the Ras superfamily of proteins. *Bioessays* **17**, 395–404

29. Downward, J. (1996) Control of ras activation. *Cancer Surv* **27**, 87–100

30. Colicelli, J. (2004) Human RAS superfamily proteins and related GTPases. *Sci STKE* **2004**, RE13

31. Rajalingam, K., Schreck, R., Rapp, U. R., and Albert, S. (2007) Ras oncogenes and their downstream targets. *Biochim Biophys Acta* **1773**, 1177–95

32. Choy, E., Chiu, V. K., Silletti, J., Feoktistov, M., Morimoto, T., Michaelson, D., Ivanov, I. E., and Philips, M. R. (1999) Endomembrane trafficking of ras: the CAAX motif targets proteins to the ER and Golgi. *Cell* **98**, 69–80

33. Hancock, J. F., Paterson, H., and Marshall, C. J. (1990) A polybasic domain or palmitoylation is required in addition to the CAAX motif to localize p21ras to the plasma membrane. *Cell* **63**, 133–9

34. Fivaz, M., and Meyer, T. (2005) Reversible intracellular translocation of KRas but not HRas in hippocampal neurons regulated by Ca2+/calmodulin. *J Cell Biol* **170**, 429–41

35. Bivona, T. G., Quatela, S. E., Bodemann, B. O., Ahearn, I. M., Soskis, M. J., Mor, A., Miura, J., Wiener, H. H., Wright, L., Saba, S. G., Yim, D., Fein, A., Pérez de Castro, I., Li, C., Thompson, C. B., Cox, A. D., and Philips, M. R. (2006) PKC regulates a farnesyl-electrostatic switch on K-Ras that promotes its association with Bcl-XL on mitochondria and induces apoptosis. *Mol Cell* **21**, 481–93

36. Goodwin, J. S., Drake, K. R., Rogers, C., Wright, L., Lippincott-Schwartz, J., Philips, M. R., and Kenworthy, A. K. (2005) Depalmitoylated Ras traffics to and from the Golgi complex via a nonvesicular pathway. *J Cell Biol* **170**, 261–72

37. Rocks, O., Peyker, A., Kahms, M., Verveer, P. J., Koerner, C., Lumbierres, M., Kuhlmann, J., Waldmann, H., Wittinghofer, A., and Bastiaens, P. I. H. (2005) An acylation cycle regulates localization and activity of palmitoylated Ras isoforms. *Science* **307**, 1746–52

38. Malumbres, M., and Barbacid, M. (2003) RAS oncogenes: the first 30 years. *Nat Rev Cancer* **3**, 459–65

39. D Cox, A., and J Der, C. Ras family signaling: therapeutic targeting. *Cancer Biol Ther* **1**

40. Sebti, S. M., and Der, C. J. (2003) Opinion: Searching for the elusive targets of farnesyltransferase inhibitors. *Nat Rev Cancer* **3**, 945–51

41. Rowinsky, E. K. (2006) Lately, it occurs to me what a long, strange trip it's been for the farnesyltransferase inhibitors. *J Clin Oncol* **24**, 2981–4

42. Cheever, M. A., Greenberg, P. D., Irle, C., Thompson, J. A., Urdal, D. L., Mochizuki, D. Y., Henney, C. S., and Gillis, S. (1984) Interleukin 2 administered in vivo induces the growth of cultured T cells in vivo. *J Immunol* **132**, 2259–65

43. Pike, B. L., Raubitschek, A., and Nossal, G. J. (1984) Human interleukin 2 can promote the growth and differentiation of single hapten-specific B cells in the presence of specific antigen. *Proc Natl Acad Sci U S A* **81**, 7917–21

44. Thomas, S. M., and Brugge, J. S. (1997) Cellular functions regulated by Src family kinases. *Annu Rev Cell Dev Biol* **13**, 513–609

45. Brown, M. T., and Cooper, J. A. (1996) Regulation, substrates and functions of src. *Biochim Biophys Acta* **1287**, 121–49

46. Resh, M. D. (1994) Myristylation and palmitylation of Src family members: the fats of the matter. *Cell* **76**, 411–3

47. Superti-Furga, G., and Courtneidge, S. A. (1995) Structure-function relationships in Src family and related protein tyrosine kinases. *Bioessays* **17**, 321–30

48. Marth, J. D., Peet, R., Krebs, E. G., and Perlmutter, R. M. (1985) A lymphocyte-specific protein-tyrosine kinase gene is rearranged and overexpressed in the murine T cell lymphoma LSTRA. *Cell* **43**, 393–404

49. Talab, F., Allen, J. C., Thompson, V., Lin, K., and Slupsky, J. R. (2013) LCK is an important mediator of B-cell receptor signaling in chronic lymphocytic leukemia cells. *Mol Cancer Res* **11**, 541–54

50. Vivier, E., Nunès, J. A., and Vély, F. (2004) Natural killer cell signaling pathways. *Science* **306**, 1517–9

51. Cooper, J. A., and Howell, B. (1993) The when and how of Src regulation. *Cell* **73**, 1051–4

52. Palacios, E. H., and Weiss, A. (2004) Function of the Src-family kinases, Lck and Fyn, in T-cell development and activation. *Oncogene* **23**, 7990–8000

53. Hardwick, J. S., and Sefton, B. M. (1995) Activation of the Lck tyrosine protein kinase by hydrogen peroxide requires the phosphorylation of Tyr-394. *Proc Natl Acad Sci U S A* **92**, 4527–31

54. Sicheri, F., and Kuriyan, J. (1997) Structures of Src-family tyrosine kinases. *Curr Opin Struct Biol* **7**, 777–85

55. Eck, M. J., Atwell, S. K., Shoelson, S. E., and Harrison, S. C. (1994) Structure of the regulatory domains of the Src-family tyrosine kinase Lck. *Nature* **368**, 764–9

56. Hofmann, G., Schweimer, K., Kiessling, A., Hofinger, E., Bauer, F., Hoffmann, S., Rösch, P., Campbell, I. D., Werner, J. M., and Sticht, H. (2005) Binding, domain orientation, and dynamics of the Lck SH3-SH2 domain pair and comparison with other Src-family kinases. *Biochemistry* **44**, 13043–50

57. Veillette, A., Bookman, M. A., Horak, E. M., and Bolen, J. B. (1988) The CD4 and CD8 T cell surface antigens are associated with the internal membrane tyrosine-protein kinase p56lck. *Cell* **55**, 301–8

58. Nika, K., Soldani, C., Salek, M., Paster, W., Gray, A., Etzensperger, R., Fugger, L., Polzella, P., Cerundolo, V., Dushek, O., Höfer, T., Viola, A., and Acuto, O. (2010) Constitutively active Lck kinase in T cells drives antigen receptor signal transduction. *Immunity* **32**, 766–77

59. Mustelin, T., Vang, T., and Bottini, N. (2005) Protein tyrosine phosphatases and the immune response. *Nat Rev Immunol* **5**, 43–57

60. Courtneidge, S. A., Levinson, A. D., and Bishop, J. M. (1980) The protein encoded by the transforming gene of avian sarcoma virus (pp60src) and a homologous protein in normal cells (pp60proto-src) are associated with the plasma membrane. *Proc Natl Acad Sci U S A* **77**, 3783–7

61. Krueger, J. G., Garber, E. A., and Goldberg, A. R. (1983) Subcellular localization of pp60src in RSV-transformed cells. *Curr Top Microbiol Immunol* **107**, 51–124

62. Turner, J. M., Brodsky, M. H., Irving, B. A., Levin, S. D., Perlmutter, R. M., and Littman, D. R. (1990) Interaction of the unique N-terminal region of tyrosine kinase p56lck with cytoplasmic domains of CD4 and CD8 is mediated by cysteine motifs. *Cell* **60**, 755–65

63. Doyle, C., and Strominger, J. L. Interaction between CD4 and class II MHC molecules mediates cell adhesion. *Nature* **330**, 256–9

64. Norment, A. M., Salter, R. D., Parham, P., Engelhard, V. H., and Littman, D. R. (1988) Cell-cell adhesion mediated by CD8 and MHC class I molecules. *Nature* **336**, 79–81

65. Lin, J., and Weiss, A. (2001) T cell receptor signalling. *J Cell Sci* **114**, 243–4

66. Whitehurst, C. E., Boulton, T. G., Cobb, M. H., and Geppert, T. D. (1992) Extracellular signal-regulated kinases in T cells. Anti-CD3 and 4 beta-phorbol 12-myristate 13-acetate-induced phosphorylation and activation. *J Immunol* **148**, 3230–7

67. Won, J., Hur, Y.-G., Hur, E. M., Park, S.-H., Kang, M.-A., Choi, Y., Park, C., Lee, K.-H., and Yun, Y. (2003) Rosmarinic acid inhibits TCR-induced T cell activation and proliferation in an Lck-dependent manner. *Eur J Immunol* **33**, 870–9

68. Huang, S.-C., Tsai, H.-F., Tzeng, H.-T., Liao, H.-J., and Hsu, P.-N. (2011) Lipid raft assembly and Lck recruitment in TRAIL costimulation mediates NF-κB activation and T cell proliferation. *J Immunol* **186**, 931–9

69. Molina, T. J., Kishihara, K., Siderovski, D. P., van Ewijk, W., Narendran, A., Timms, E., Wakeham, A., Paige, C. J., Hartmann, K. U., and Veillette, A. (1992) Profound block in thymocyte development in mice lacking p56lck. *Nature* **357**, 161–4

70. Thompson, P. A., Ledbetter, J. A., Rapp, U. R., and Bolen, J. B. (1991) The Raf-1 serine-threonine kinase is a substrate for the p56lck protein tyrosine kinase in human T-cells. *Cell Growth Differ* **2**, 609–17

71. Li, M., Ong, S. S., Rajwa, B., Thieu, V. T., Geahlen, R. L., and Harrison, M. L. (2008) The SH3 domain of Lck modulates T-cell receptor-dependent activation of extracellular signal-regulated kinase through activation of Raf-1. *Mol Cell Biol* **28**, 630–41

72. Fabian, J. R., Daar, I. O., and Morrison, D. K. (1993) Critical tyrosine residues regulate the enzymatic and biological activity of Raf-1 kinase. *Mol Cell Biol* **13**, 7170–9

73. Tybulewicz, V. L. J., and Henderson, R. B. (2009) Rho family GTPases and their regulators in lymphocytes. *Nat Rev Immunol* **9**, 630–44

74. Rapp, U. R., Goldsborough, M. D., Mark, G. E., Bonner, T. I., Groffen, J., Reynolds, F. H., and Stephenson, J. R. (1983) Structure and biological activity of v-raf, a unique oncogene transduced by a retrovirus. *Proc Natl Acad Sci U S A* **80**, 4218–22

75. Kieber, J. J., Rothenberg, M., Roman, G., Feldmann, K. A., and Ecker, J. R. (1993) CTR1, a negative regulator of the ethylene response pathway in Arabidopsis, encodes a member of the raf family of protein kinases. *Cell* **72**, 427–41

76. Han, M., Golden, A., Han, Y., and Sternberg, P. W. (1993) C. elegans lin-45 raf gene participates in let-60 ras-stimulated vulval differentiation. *Nature* **363**, 133–40

77. Mark, G. E., MacIntyre, R. J., Digan, M. E., Ambrosio, L., and Perrimon, N. (1987) Drosophila melanogaster homologs of the raf oncogene. *Mol Cell Biol* **7**, 2134–40

78. Bonner, T. I., Kerby, S. B., Sutrave, P., Gunnell, M. A., Mark, G., and Rapp, U. R. (1985) Structure and biological activity of human homologs of the raf/mil oncogene. *Mol Cell Biol* **5**, 1400–7

79. Morrison, D. K., and Cutler, R. E. (1997) The complexity of Raf-1 regulation. *Curr Opin Cell Biol* **9**, 174–9

80. Light, Y., Paterson, H., and Marais, R. (2002) 14-3-3 Antagonizes Ras-Mediated Raf-1 Recruitment to the Plasma Membrane To Maintain Signaling Fidelity. *Mol Cell Biol* **22**, 4984–4996

81. Knighton, D. R., Zheng, J. H., Ten Eyck, L. F., Ashford, V. A., Xuong, N. H., Taylor, S. S., and Sowadski, J. M. (1991) Crystal structure of the catalytic subunit of cyclic adenosine monophosphate-dependent protein kinase. *Science* **253**, 407–14

82. Kolch, W. (2005) Coordinating ERK/MAPK signalling through scaffolds and inhibitors. *Nat Rev Mol Cell Biol* **6**, 827–37

83. Wan, P. T. C., Garnett, M. J., Roe, S. M., Lee, S., Niculescu-Duvaz, D., Good, V. M., Jones, C. M., Marshall, C. J., Springer, C. J., Barford, D., and Marais, R. (2004) Mechanism of activation of the RAF-ERK signaling pathway by oncogenic mutations of B-RAF. *Cell* **116**, 855–67

84. Wilhelm, S. M., Adnane, L., Newell, P., Villanueva, A., Llovet, J. M., and Lynch, M. (2008) Preclinical overview of sorafenib, a multikinase inhibitor that targets both Raf and VEGF and PDGF receptor tyrosine kinase signaling. *Mol Cancer Ther* **7**, 3129–40

85. Hekman, M., Fischer, A., Wennogle, L. P., Wang, Y. K., Campbell, S. L., and Rapp, U. R. (2005) Novel C-Raf phosphorylation sites: serine 296 and 301 participate in Raf regulation. *FEBS Lett* **579**, 464–8

86. Storm, S. M., Cleveland, J. L., and Rapp, U. R. (1990) Expression of raf family proto-oncogenes in normal mouse tissues. *Oncogene* **5**, 345–51

87. Marais, R., Light, Y., Paterson, H. F., Mason, C. S., and Marshall, C. J. (1997) Differential regulation of Raf-1, A-Raf, and B-Raf by oncogenic ras and tyrosine kinases. *J Biol Chem* **272**, 4378–83

88. Weber, C. K., Slupsky, J. R., Kalmes, H. A., and Rapp, U. R. (2001) Active Ras induces heterodimerization of cRaf and BRaf. *Cancer Res* **61**, 3595–8

89. Luo, Z., Tzivion, G., Belshaw, P. J., Vavvas, D., Marshall, M., and Avruch, J. (1996) Oligomerization activates c-Raf-1 through a Ras-dependent mechanism. *Nature* **383**, 181–5

90. Rushworth, L. K., Hindley, A. D., O'Neill, E., and Kolch, W. (2006) Regulation and role of Raf-1/B-Raf heterodimerization. *Mol Cell Biol* **26**, 2262–72

91. Davies, H., Bignell, G. R., Cox, C., Stephens, P., Edkins, S., Clegg, S., Teague, J., Woffendin, H., Garnett, M. J., Bottomley, W., Davis, N., Dicks, E., Ewing, R., Floyd, Y., Gray, K., Hall, S., Hawes, R., Hughes, J., Kosmidou, V., Menzies, A., Mould, C., Parker, A., Stevens, C., Watt, S., Hooper, S., Wilson, R., Jayatilake, H., Gusterson, B. A., Cooper, C., Shipley, J., Hargrave, D., Pritchard-Jones, K., Maitland, N., Chenevix-Trench, G., Riggins, G. J., Bigner, D. D., Palmieri, G., Cossu, A., Flanagan, A., Nicholson, A., Ho, J. W. C., Leung, S. Y., Yuen, S. T., Weber, B. L., Seigler, H. F., Darrow, T. L., Paterson, H., Marais, R., Marshall, C. J., Wooster, R., Stratton, M. R., and Futreal, P. A. (2002) Mutations of the BRAF gene in human cancer. *Nature* **417**, 949–54

92. Xu, S., Khoo, S., Dang, A., Witt, S., Do, V., Zhen, E., Schaefer, E. M., and Cobb, M. H. (1997) Differential regulation of mitogen-activated protein/ERK kinase (MEK)1 and MEK2 and activation by a Ras-independent mechanism. *Mol Endocrinol* **11**, 1618–25

93. Zheng, C. F., and Guan, K. L. (1993) Properties of MEKs, the kinases that phosphorylate and activate the extracellular signal-regulated kinases. *J Biol Chem* **268**, 23933–9

94. Jelinek, T., Catling, A. D., Reuter, C. W., Moodie, S. A., Wolfman, A., and Weber, M. J. (1994) RAS and RAF-1 form a signalling complex with MEK-1 but not MEK-2. *Mol Cell Biol* **14**, 8212–8

95. Giroux, S., Tremblay, M., Bernard, D., Cardin-Girard, J. F., Aubry, S., Larouche, L., Rousseau, S., Huot, J., Landry, J., Jeannotte, L., and Charron, J. (1999) Embryonic death

of Mek1-deficient mice reveals a role for this kinase in angiogenesis in the labyrinthine region of the placenta. *Curr Biol* **9**, 369–72

96. Bélanger, L.-F., Roy, S., Tremblay, M., Brott, B., Steff, A.-M., Mourad, W., Hugo, P., Erikson, R., and Charron, J. (2003) Mek2 is dispensable for mouse growth and development. *Mol Cell Biol* **23**, 4778–87

97. Roskoski, R. (2012) MEK1/2 dual-specificity protein kinases: structure and regulation. *Biochem Biophys Res Commun* **417**, 5–10

98. Kyriakis, J. M., App, H., Zhang, X. F., Banerjee, P., Brautigan, D. L., Rapp, U. R., and Avruch, J. (1992) Raf-1 activates MAP kinase-kinase. *Nature* **358**, 417–21

99. Zheng, C. F., and Guan, K. L. (1994) Activation of MEK family kinases requires phosphorylation of two conserved Ser/Thr residues. *EMBO J* **13**, 1123–31

100. Gopalbhai, K., Jansen, G., Beauregard, G., Whiteway, M., Dumas, F., Wu, C., and Meloche, S. (2003) Negative regulation of MAPKK by phosphorylation of a conserved serine residue equivalent to Ser212 of MEK1. *J Biol Chem* **278**, 8118–25

101. Rossomando, A. J., Dent, P., Sturgill, T. W., and Marshak, D. R. (1994) Mitogen-activated protein kinase kinase 1 (MKK1) is negatively regulated by threonine phosphorylation. *Mol Cell Biol* **14**, 1594–602

102. Eblen, S. T., Slack-Davis, J. K., Tarcsafalvi, A., Parsons, J. T., Weber, M. J., and Catling, A. D. (2004) Mitogen-activated protein kinase feedback phosphorylation regulates MEK1 complex formation and activation during cellular adhesion. *Mol Cell Biol* **24**, 2308–17

103. Matsuda, S., Gotoh, Y., and Nishida, E. (1993) Phosphorylation of Xenopus mitogen-activated protein (MAP) kinase kinase by MAP kinase kinase kinase and MAP kinase. *J Biol Chem* **268**, 3277–81

104. Brunet, A., Pagès, G., and Pouysségur, J. (1994) Growth factor-stimulated MAP kinase induces rapid retrophosphorylation and inhibition of MAP kinase kinase (MEK1). *FEBS Lett* **346**, 299–303

105. Crews, C. M., Alessandrini, A., and Erikson, R. L. (1992) The primary structure of MEK, a protein kinase that phosphorylates the ERK gene product. *Science* **258**, 478–80

106. Matsuda, S., Kosako, H., Takenaka, K., Moriyama, K., Sakai, H., Akiyama, T., Gotoh, Y., and Nishida, E. (1992) Xenopus MAP kinase activator: identification and function as a key intermediate in the phosphorylation cascade. *EMBO J* **11**, 973–82

107. Catalanotti, F., Reyes, G., Jesenberger, V., Galabova-Kovacs, G., de Matos Simoes, R., Carugo, O., and Baccarini, M. (2009) A Mek1-Mek2 heterodimer determines the strength and duration of the Erk signal. *Nat Struct Mol Biol* **16**, 294–303

108. Sontag, E., Fedorov, S., Kamibayashi, C., Robbins, D., Cobb, M., and Mumby, M. (1993) The interaction of SV40 small tumor antigen with protein phosphatase 2A stimulates the map kinase pathway and induces cell proliferation. *Cell* **75**, 887–97

109. Skarpen, E., Flinder, L. I., Rosseland, C. M., Orstavik, S., Wierød, L., Oksvold, M. P., Skålhegg, B. S., and Huitfeldt, H. S. (2008) MEK1 and MEK2 regulate distinct functions by sorting ERK2 to different intracellular compartments. *FASEB J* **22**, 466–76

110. Falchook, G. S., Lewis, K. D., Infante, J. R., Gordon, M. S., Vogelzang, N. J., DeMarini, D. J., Sun, P., Moy, C., Szabo, S. A., Roadcap, L. T., Peddareddigari, V. G. R., Lebowitz, P. F., Le, N. T., Burris, H. A., Messersmith, W. A., O'Dwyer, P. J., Kim, K. B., Flaherty, K., Bendell, J. C., Gonzalez, R., Kurzrock, R., and Fecher, L. A. (2012) Activity of the oral MEK inhibitor trametinib in patients with advanced melanoma: a phase 1 dose-escalation trial. *Lancet Oncol* **13**, 782–9

111. Flaherty, K. T., Robert, C., Hersey, P., Nathan, P., Garbe, C., Milhem, M., Demidov, L. V, Hassel, J. C., Rutkowski, P., Mohr, P., Dummer, R., Trefzer, U., Larkin, J. M. G., Utikal, J., Dreno, B., Nyakas, M., Middleton, M. R., Becker, J. C., Casey, M., Sherman, L. J., Wu, F. S., Ouellet, D., Martin, A.-M., Patel, K., and Schadendorf, D. (2012) Improved survival with MEK inhibition in BRAF-mutated melanoma. *N Engl J Med* **367**, 107–14

112. Voisin, L., Saba-El-Leil, M. K., Julien, C., Frémin, C., and Meloche, S. (2010) Genetic demonstration of a redundant role of extracellular signal-regulated kinase 1 (ERK1) and ERK2 mitogen-activated protein kinases in promoting fibroblast proliferation. *Mol Cell Biol* **30**, 2918–32

113. Lefloch, R., Pouysségur, J., and Lenormand, P. (2008) Single and combined silencing of ERK1 and ERK2 reveals their positive contribution to growth signaling depending on their expression levels. *Mol Cell Biol* **28**, 511–27

114. Boulton, T. G., Nye, S. H., Robbins, D. J., Ip, N. Y., Radziejewska, E., Morgenbesser, S. D., DePinho, R. A., Panayotatos, N., Cobb, M. H., and Yancopoulos, G. D. (1991) ERKs: a family of protein-serine/threonine kinases that are activated and tyrosine phosphorylated in response to insulin and NGF. *Cell* **65**, 663–75

115. Lefloch, R., Pouysségur, J., and Lenormand, P. (2009) Total ERK1/2 activity regulates cell proliferation. *Cell Cycle* **8**, 705–11

116. Hatano, N., Mori, Y., Oh-hora, M., Kosugi, A., Fujikawa, T., Nakai, N., Niwa, H., Miyazaki, J., Hamaoka, T., and Ogata, M. (2003) Essential role for ERK2 mitogen-activated protein kinase in placental development. *Genes Cells* **8**, 847–56

117. Yao, Y., Li, W., Wu, J., Germann, U. A., Su, M. S. S., Kuida, K., and Boucher, D. M. (2003) Extracellular signal-regulated kinase 2 is necessary for mesoderm differentiation. *Proc Natl Acad Sci U S A* **100**, 12759–64

118. Saba-El-Leil, M. K., Vella, F. D. J., Vernay, B., Voisin, L., Chen, L., Labrecque, N., Ang, S.-L., and Meloche, S. (2003) An essential function of the mitogen-activated protein kinase Erk2 in mouse trophoblast development. *EMBO Rep* **4**, 964–8

119. Nekrasova, T., Shive, C., Gao, Y., Kawamura, K., Guardia, R., Landreth, G., and Forsthuber, T. G. (2005) ERK1-deficient mice show normal T cell effector function and are highly susceptible to experimental autoimmune encephalomyelitis. *J Immunol* **175**, 2374–80

120. Pagès, G., Guérin, S., Grall, D., Bonino, F., Smith, A., Anjuere, F., Auberger, P., and Pouysségur, J. (1999) Defective thymocyte maturation in p44 MAP kinase (Erk 1) knockout mice. *Science* **286**, 1374–7

121. Roskoski, R. (2012) ERK1/2 MAP kinases: structure, function, and regulation. *Pharmacol Res* **66**, 105–43

122. Cobb, M. H., and Goldsmith, E. J. (2000) Dimerization in MAP-kinase signaling. *Trends Biochem Sci* **25**, 7–9

123. Khokhlatchev, A. V, Canagarajah, B., Wilsbacher, J., Robinson, M., Atkinson, M., Goldsmith, E., and Cobb, M. H. (1998) Phosphorylation of the MAP kinase ERK2 promotes its homodimerization and nuclear translocation. *Cell* **93**, 605–15

124. Casar, B., Pinto, A., and Crespo, P. (2008) Essential role of ERK dimers in the activation of cytoplasmic but not nuclear substrates by ERK-scaffold complexes. *Mol Cell* **31**, 708–21

125. Yoon, S., and Seger, R. (2006) The extracellular signal-regulated kinase: multiple substrates regulate diverse cellular functions. *Growth Factors* **24**, 21–44

126. Von Kriegsheim, A., Baiocchi, D., Birtwistle, M., Sumpton, D., Bienvenut, W., Morrice, N., Yamada, K., Lamond, A., Kalna, G., Orton, R., Gilbert, D., and Kolch, W. (2009) Cell fate decisions are specified by the dynamic ERK interactome. *Nat Cell Biol* **11**, 1458–64

127. Asano, E., Maeda, M., Hasegawa, H., Ito, S., Hyodo, T., Yuan, H., Takahashi, M., Hamaguchi, M., and Senga, T. (2011) Role of palladin phosphorylation by extracellular signal-regulated kinase in cell migration. *PLoS One* **6**, e29338

128. Roux, P. P., and Blenis, J. (2004) ERK and p38 MAPK-activated protein kinases: a family of protein kinases with diverse biological functions. *Microbiol Mol Biol Rev* **68**, 320–44

129. Lenormand, P., Sardet, C., Pagès, G., L'Allemain, G., Brunet, A., and Pouysségur, J. (1993) Growth factors induce nuclear translocation of MAP kinases (p42mapk and p44mapk) but not of their activator MAP kinase kinase (p45mapkk) in fibroblasts. *J Cell Biol* **122**, 1079–88

130. Hollenhorst, P. C., McIntosh, L. P., and Graves, B. J. (2011) Genomic and biochemical insights into the specificity of ETS transcription factors. *Annu Rev Biochem* **80**, 437–71

131. Buchwalter, G., Gross, C., and Wasylyk, B. (2004) Ets ternary complex transcription factors. *Gene* **324**, 1–14

132. Okazaki, K., and Sagata, N. (1995) The Mos/MAP kinase pathway stabilizes c-Fos by phosphorylation and augments its transforming activity in NIH 3T3 cells. *EMBO J* **14**, 5048–59

133. Murphy, L. O., Smith, S., Chen, R.-H., Fingar, D. C., and Blenis, J. (2002) Molecular interpretation of ERK signal duration by immediate early gene products. *Nat Cell Biol* **4**, 556–64

134. Morton, S., Davis, R. J., McLaren, A., and Cohen, P. (2003) A reinvestigation of the multisite phosphorylation of the transcription factor c-Jun. *EMBO J* **22**, 3876–86

135. Zimmermann, S., and Moelling, K. (1999) Phosphorylation and regulation of Raf by Akt (protein kinase B). *Science* **286**, 1741–4

136. Hekman, M., Wiese, S., Metz, R., Albert, S., Troppmair, J., Nickel, J., Sendtner, M., and Rapp, U. R. (2004) Dynamic changes in C-Raf phosphorylation and 14-3-3 protein binding in response to growth factor stimulation: differential roles of 14-3-3 protein binding sites. *J Biol Chem* **279**, 14074–86

137. Kornfeld, K., Hom, D. B., and Horvitz, H. R. (1995) The ksr-1 gene encodes a novel protein kinase involved in Ras-mediated signaling in C. elegans. *Cell* **83**, 903–13

138. Ritt, D. A., Daar, I. O., and Morrison, D. K. (2006) KSR regulation of the Raf-MEK-ERK cascade. *Methods Enzymol* **407**, 224–37

139. Clapéron, A., and Therrien, M. (2007) KSR and CNK: two scaffolds regulating RAS-mediated RAF activation. *Oncogene* **26**, 3143–58

140. Sundaram, M., and Han, M. (1995) The C. elegans ksr-1 gene encodes a novel Raf-related kinase involved in Ras-mediated signal transduction. *Cell* **83**, 889–901

141. Therrien, M., Chang, H. C., Solomon, N. M., Karim, F. D., Wassarman, D. A., and Rubin, G. M. (1995) KSR, a novel protein kinase required for RAS signal transduction. *Cell* **83**, 879–88

142. Morrison, D. K. (2001) KSR: a MAPK scaffold of the Ras pathway? *J Cell Sci* **114**, 1609–12

143. Ohmachi, M., Rocheleau, C. E., Church, D., Lambie, E., Schedl, T., and Sundaram, M. V (2002) C. elegans ksr-1 and ksr-2 have both unique and redundant functions and are required for MPK-1 ERK phosphorylation. *Curr Biol* **12**, 427–33

144. Channavajhala, P. L., Wu, L., Cuozzo, J. W., Hall, J. P., Liu, W., Lin, L.-L., and Zhang, Y. (2003) Identification of a novel human kinase supporter of Ras (hKSR-2) that functions as a negative regulator of Cot (Tpl2) signaling. *J Biol Chem* **278**, 47089–97

145. Dougherty, M. K., Ritt, D. A., Zhou, M., Specht, S. I., Monson, D. M., Veenstra, T. D., and Morrison, D. K. (2009) KSR2 is a calcineurin substrate that promotes ERK cascade activation in response to calcium signals. *Mol Cell* **34**, 652–62

146. Van Blitterswijk, W. J. (1998) Hypothesis: ceramide conditionally activates atypical protein kinases C, Raf-1 and KSR through binding to their cysteine-rich domains. *Biochem J* **331**, 679–80

147. Zhou, M., Horita, D. A., Waugh, D. S., Byrd, R. A., and Morrison, D. K. (2002) Solution structure and functional analysis of the cysteine-rich C1 domain of kinase suppressor of Ras (KSR). *J Mol Biol* **315**, 435–46

148. Colongonzalez, F., and Kazanietz, M. (2006) C1 domains exposed: From diacylglycerol binding to protein–protein interactions. *Biochim Biophys Acta - Mol Cell Biol Lipids* **1761**, 827–837

149. Cacace, A. M., Michaud, N. R., Therrien, M., Mathes, K., Copeland, T., Rubin, G. M., and Morrison, D. K. (1999) Identification of constitutive and ras-inducible phosphorylation sites of KSR: implications for 14-3-3 binding, mitogen-activated protein kinase binding, and KSR overexpression. *Mol Cell Biol* **19**, 229–40

150. Xing, H., Kornfeld, K., and Muslin, A. J. (1997) The protein kinase KSR interacts with 14-3-3 protein and Raf. *Curr Biol* **7**, 294–300

151. Müller, J., Ory, S., Copeland, T., Piwnica-Worms, H., and Morrison, D. K. (2001) C-TAK1 regulates Ras signaling by phosphorylating the MAPK scaffold, KSR1. *Mol Cell* **8**, 983–93

152. Bell, B., Xing, H., Yan, K., Gautam, N., and Muslin, A. J. (1999) KSR-1 binds to G-protein betagamma subunits and inhibits beta gamma-induced mitogen-activated protein kinase activation. *J Biol Chem* **274**, 7982–6

153. Müller, J., Ritt, D. A., Copeland, T. D., and Morrison, D. K. (2003) Functional analysis of C-TAK1 substrate binding and identification of PKP2 as a new C-TAK1 substrate. *EMBO J* **22**, 4431–42

154. Michaud, N. R., Therrien, M., Cacace, A., Edsall, L. C., Spiegel, S., Rubin, G. M., and Morrison, D. K. (1997) KSR stimulates Raf-1 activity in a kinase-independent manner. *Proc Natl Acad Sci U S A* **94**, 12792–6

155. Jacobs, D., Glossip, D., Xing, H., Muslin, A. J., and Kornfeld, K. (1999) Multiple docking sites on substrate proteins form a modular system that mediates recognition by ERK MAP kinase. *Genes Dev* **13**, 163–75

156. Zhang, Y., Yao, B., Delikat, S., Bayoumy, S., Lin, X. H., Basu, S., McGinley, M., Chan-Hui, P. Y., Lichenstein, H., and Kolesnick, R. (1997) Kinase suppressor of Ras is ceramide-activated protein kinase. *Cell* **89**, 63–72

157. Yan, F., and Polk, D. B. (2001) Kinase suppressor of ras is necessary for tumor necrosis factor alpha activation of extracellular signal-regulated kinase/mitogen-activated protein kinase in intestinal epithelial cells. *Cancer Res* **61**, 963–9

158. Stewart, S., Sundaram, M., Zhang, Y., Lee, J., Han, M., and Guan, K. L. (1999) Kinase suppressor of Ras forms a multiprotein signaling complex and modulates MEK localization. *Mol Cell Biol* **19**, 5523–34

159. Boudeau, J., Miranda-Saavedra, D., Barton, G. J., and Alessi, D. R. (2006) Emerging roles of pseudokinases. *Trends Cell Biol* **16**, 443–52

160. Dar, A. C. (2013) A pickup in pseudokinase activity. *Biochem Soc Trans* **41**, 987–94

161. Zafrullah, M., Yin, X., Haimovitz-Friedman, A., Fuks, Z., and Kolesnick, R. (2009) Kinase suppressor of Ras transphosphorylates c-Raf-1. *Biochem Biophys Res Commun* **390**, 434–40

162. Xing HR, K. R. (2001) Kinase suppressor of Ras signals through Thr269 of c-Raf-1. *J Biol Chem* **276**, 9733–41

163. Goettel, J. A., Liang, D., Hilliard, V. C., Edelblum, K. L., Broadus, M. R., Gould, K. L., Hanks, S. K., and Polk, D. B. (2011) KSR1 is a functional protein kinase capable of serine autophosphorylation and direct phosphorylation of MEK1. *Exp Cell Res* **317**, 452–63

164. Hu, J., Yu, H., Kornev, A. P., Zhao, J., Filbert, E. L., Taylor, S. S., and Shaw, A. S. (2011) Mutation that blocks ATP binding creates a pseudokinase stabilizing the scaffolding function of kinase suppressor of Ras, CRAF and BRAF. *Proc Natl Acad Sci U S A* **108**, 6067–72

165. Brennan, D. F., Dar, A. C., Hertz, N. T., Chao, W. C. H., Burlingame, A. L., Shokat, K. M., and Barford, D. (2011) A Raf-induced allosteric transition of KSR stimulates phosphorylation of MEK. *Nature* **472**, 366–9

166. Roy, F., and Therrien, M. (2002) MAP kinase module: the Ksr connection. *Curr Biol* **12**, R325–7

167. Denouel-Galy, A., Douville, E. M., Warne, P. H., Papin, C., Laugier, D., Calothy, G., Downward, J., and Eychène, A. (1998) Murine Ksr interacts with MEK and inhibits Ras-induced transformation. *Curr Biol* **8**, 46–55

168. Yu, W., Fantl, W. J., Harrowe, G., and Williams, L. T. (1998) Regulation of the MAP kinase pathway by mammalian Ksr through direct interaction with MEK and ERK. *Curr Biol* **8**, 56–64

169. Nguyen, A., Burack, W. R., Stock, J. L., Kortum, R., Chaika, O. V, Afkarian, M., Muller, W. J., Murphy, K. M., Morrison, D. K., Lewis, R. E., McNeish, J., and Shaw, A. S. (2002) Kinase suppressor of Ras (KSR) is a scaffold which facilitates mitogen-activated protein kinase activation in vivo. *Mol Cell Biol* **22**, 3035–45

170. Yasuda, J., Whitmarsh, A. J., Cavanagh, J., Sharma, M., and Davis, R. J. (1999) The JIP group of mitogen-activated protein kinase scaffold proteins. *Mol Cell Biol* **19**, 7245–54

171. Liu, L., Channavajhala, P. L., Rao, V. R., Moutsatsos, I., Wu, L., Zhang, Y., Lin, L.-L., and Qiu, Y. (2009) Proteomic characterization of the dynamic KSR-2 interactome, a signaling scaffold complex in MAPK pathway. *Biochim Biophys Acta* **1794**, 1485–95

172. Aitken, A. (2006) 14-3-3 proteins: a historic overview. *Semin Cancer Biol* **16**, 162–72

173. Ory, S., Zhou, M., Conrads, T. P., Veenstra, T. D., and Morrison, D. K. (2003) Protein phosphatase 2A positively regulates Ras signaling by dephosphorylating KSR1 and Raf-1 on critical 14-3-3 binding sites. *Curr Biol* **13**, 1356–64

174. Raabe, T., and Rapp, U. R. (2003) Ras signaling: PP2A puts Ksr and Raf in the right place. *Curr Biol* **13**, R635–7

175. Ritt, D. A., Zhou, M., Conrads, T. P., Veenstra, T. D., Copeland, T. D., and Morrison, D. K. (2007) CK2 Is a component of the KSR1 scaffold complex that contributes to Raf kinase activation. *Curr Biol* **17**, 179–84

176. Volle, D. J., Fulton, J. A., Chaika, O. V, McDermott, K., Huang, H., Steinke, L. A., and Lewis, R. E. (1999) Phosphorylation of the kinase suppressor of ras by associated kinases. *Biochemistry* **38**, 5130–7

177. Matheny, S. A., Chen, C., Kortum, R. L., Razidlo, G. L., Lewis, R. E., and White, M. A. (2004) Ras regulates assembly of mitogenic signalling complexes through the effector protein IMP. *Nature* **427**, 256–60

178. Chen, C., Lewis, R. E., and White, M. A. (2008) IMP modulates KSR1-dependent multivalent complex formation to specify ERK1/2 pathway activation and response thresholds. *J Biol Chem* **283**, 12789–96

179. McKay, M. M., Ritt, D. A., and Morrison, D. K. (2009) Signaling dynamics of the KSR1 scaffold complex. *Proc Natl Acad Sci U S A* **106**, 11022–7

180. McKay, M. M., and Morrison, D. K. (2007) Caspase-dependent cleavage disrupts the ERK cascade scaffolding function of KSR1. *J Biol Chem* **282**, 26225–34

181. Brennan, J. A., Volle, D. J., Chaika, O. V, and Lewis, R. E. (2002) Phosphorylation regulates the nucleocytoplasmic distribution of kinase suppressor of Ras. *J Biol Chem* **277**, 5369–77

182. Yan, F., John, S. K., Wilson, G., Jones, D. S., Washington, M. K., and Polk, D. B. (2004) Kinase suppressor of Ras-1 protects intestinal epithelium from cytokine-mediated apoptosis during inflammation. *J Clin Invest* **114**, 1272–80

183. Fusello, A. M., Mandik-Nayak, L., Shih, F., Lewis, R. E., Allen, P. M., and Shaw, A. S. (2006) The MAPK scaffold kinase suppressor of Ras is involved in ERK activation by stress and proinflammatory cytokines and induction of arthritis. *J Immunol* **177**, 6152–8

184. Lozano, J., Xing, R., Cai, Z., Jensen, H. L., Trempus, C., Mark, W., Cannon, R., and Kolesnick, R. (2003) Deficiency of kinase suppressor of Ras1 prevents oncogenic ras signaling in mice. *Cancer Res* **63**, 4232–8

185. Xing, H. R., Cordon-Cardo, C., Deng, X., Tong, W., Campodonico, L., Fuks, Z., and Kolesnick, R. (2003) Pharmacologic inactivation of kinase suppressor of ras-1 abrogates Ras-mediated pancreatic cancer. *Nat Med* **9**, 1266–8

186. Sibilski, C., Mueller, T., Kollipara, L., Zahedi, R. P., Rapp, U. R., Rudel, T., and Baljuls, A. (2013) Tyr728 in the kinase domain of the murine kinase suppressor of RAS 1 regulates binding and activation of the mitogen-activated protein kinase kinase. *J Biol Chem* **288**, 35237–52

187. Baljuls, A., Mueller, T., Drexler, H. C. A., Hekman, M., and Rapp, U. R. (2007) Unique N-region determines low basal activity and limited inducibility of A-RAF kinase: the role of N-region in the evolutionary divergence of RAF kinase function in vertebrates. *J Biol Chem* **282**, 26575–90

188. Yurchak, L. K., and Sefton, B. M. (1995) Palmitoylation of either Cys-3 or Cys-5 is required for the biological activity of the Lck tyrosine protein kinase. *Mol Cell Biol* **15**, 6914–22

189. Harrison, R. E., Sikorski, B. A., and Jongstra, J. (2004) Leukocyte-specific protein 1 targets the ERK/MAP kinase scaffold protein KSR and MEK1 and ERK2 to the actin cytoskeleton. *J Cell Sci* **117**, 2151–7

190. Winkler, D. G., Park, I., Kim, T., Payne, N. S., Walsh, C. T., Strominger, J. L., and Shin, J. (1993) Phosphorylation of Ser-42 and Ser-59 in the N-terminal region of the tyrosine kinase p56lck. *Proc Natl Acad Sci U S A* **90**, 5176–80

191. Watts, J. D., Sanghera, J. S., Pelech, S. L., and Aebersold, R. (1993) Phosphorylation of serine 59 of p56lck in activated T cells. *J Biol Chem* **268**, 23275–82

192. Watts, J. D., Welham, M. J., Kalt, L., Schrader, J. W., and Aebersold, R. (1993) IL-2 stimulation of T lymphocytes induces sequential activation of mitogen-activated protein kinases and phosphorylation of p56lck at serine-59. *J Immunol* **151**, 6862–71

193. Xia, F., Li, J., Hickey, G. W., Tsurumi, A., Larson, K., Guo, D., Yan, S.-J., Silver-Morse, L., and Li, W. X. (2008) Raf activation is regulated by tyrosine 510 phosphorylation in Drosophila. *PLoS Biol* **6**, e128

194. Kortum, R. L., and Lewis, R. E. (2004) The molecular scaffold KSR1 regulates the proliferative and oncogenic potential of cells. *Mol Cell Biol* **24**, 4407–16

195. Cabeza-Arvelaiz, Y., and Schiestl, R. H. (2012) Transcriptome analysis of a rotenone model of parkinsonism reveals complex I-tied and -untied toxicity mechanisms common to neurodegenerative diseases. *PLoS One* **7**, e44700

196. Flaswinkel, H., Barner, M., and Reth, M. (1995) The tyrosine activation motif as a target of protein tyrosine kinases and SH2 domains. *Semin Immunol* **7**, 21–7

197. Stefanová, I., Hemmer, B., Vergelli, M., Martin, R., Biddison, W. E., and Germain, R. N. (2003) TCR ligand discrimination is enforced by competing ERK positive and SHP-1 negative feedback pathways. *Nat Immunol* **4**, 248–54

198. Joung, I., Kim, T., Stolz, L. A., Payne, G., Winkler, D. G., Walsh, C. T., Strominger, J. L., and Shin, J. (1995) Modification of Ser59 in the unique N-terminal region of tyrosine kinase p56lck regulates specificity of its Src homology 2 domain. *Proc Natl Acad Sci U S A* **92**, 5778–82

199. Berry, R. (2011) The role of L(u)ck in T cell triggering. *Sci Signal* **4**, jc2

200. Chiang, G. G., and Sefton, B. M. (2001) Specific dephosphorylation of the Lck tyrosine protein kinase at Tyr-394 by the SHP-1 protein-tyrosine phosphatase. *J Biol Chem* **276**, 23173–8

201. Hu, J., Stites, E. C., Yu, H., Germino, E. A., Meharena, H. S., Stork, P. J. S., Kornev, A. P., Taylor, S. S., and Shaw, A. S. (2013) Allosteric activation of functionally asymmetric RAF kinase dimers. *Cell* **154**, 1036–46

202. Fraser, J. S., Clarkson, M. W., Degnan, S. C., Erion, R., Kern, D., and Alber, T. (2009) Hidden alternative structures of proline isomerase essential for catalysis. *Nature* **462**, 669–73

203. Bu, Z., and Callaway, D. J. E. (2011) Proteins move! Protein dynamics and long-range allostery in cell signaling. *Adv Protein Chem Struct Biol* **83**, 163–221

204. Jiménez, J. L., Hegemann, B., Hutchins, J. R. A., Peters, J.-M., and Durbin, R. (2007) A systematic comparative and structural analysis of protein phosphorylation sites based on the mtcPTM database. *Genome Biol* **8**, R90

205. Baljuls, A., Kholodenko, B. N., and Kolch, W. (2013) It takes two to tango--signalling by dimeric Raf kinases. *Mol Biosyst* **9**, 551–8

206. Xing, H. R., Campodonico, L., and Kolesnick, R. (2004) The kinase activity of kinase suppressor of Ras1 (KSR1) is independent of bound MEK. *J Biol Chem* **279**, 26210–4

207. Dougherty, D. A. (2007) Cation-{pi} Interactions Involving Aromatic Amino Acids. *J Nutr* **137**, 1504S–1508

208. Xie, H., Pallero, M. A., Gupta, K., Chang, P., Ware, M. F., Witke, W., Kwiatkowski, D. J., Lauffenburger, D. A., Murphy-Ullrich, J. E., and Wells, A. (1998) EGF receptor regulation of cell motility: EGF induces disassembly of focal adhesions independently of the motility-associated PLCgamma signaling pathway. *J Cell Sci* **111**, 615–24

209. Boehm, M. B. (2008) Regulation of Cellular Metabolism and Cell Motility by KSR. *Dissertation*, 1–207

210. Lin, J., Harding, A., Giurisato, E., and Shaw, A. S. (2009) KSR1 modulates the sensitivity of mitogen-activated protein kinase pathway activation in T cells without altering fundamental system outputs. *Mol Cell Biol* **29**, 2082–91

211. Kilkenny, D. M., Rocheleau, J. V, Price, J., Reich, M. B., and Miller, G. G. (2003) c-Src regulation of fibroblast growth factor-induced proliferation in murine embryonic fibroblasts. *J Biol Chem* **278**, 17448–54

212. Sugimoto, T., Stewart, S., Han, M., and Guan, K. L. (1998) The kinase suppressor of Ras (KSR) modulates growth factor and Ras signaling by uncoupling Elk-1 phosphorylation from MAP kinase activation. *EMBO J* **17**, 1717–27

213. Roy, F., Laberge, G., Douziech, M., Ferland-McCollough, D., and Therrien, M. (2002) KSR is a scaffold required for activation of the ERK/MAPK module. *Genes Dev* **16**, 427–38

214. Spitaler, M., Villunger, A., Grunicke, H., and Uberall, F. (2000) Unique structural and functional properties of the ATP-binding domain of atypical protein kinase C-iota. *J Biol Chem* **275**, 33289–96

215. Furdui, C. M., Lew, E. D., Schlessinger, J., and Anderson, K. S. (2006) Autophosphorylation of FGFR1 kinase is mediated by a sequential and precisely ordered reaction. *Mol Cell* **21**, 711–7

216. Hubbard, S. R. (1997) Crystal structure of the activated insulin receptor tyrosine kinase in complex with peptide substrate and ATP analog. *EMBO J* **16**, 5572–81

217. Hubbard, S. R. (2004) Juxtamembrane autoinhibition in receptor tyrosine kinases. *Nat Rev Mol Cell Biol* **5**, 464–71

218. Abe, M. K., Kahle, K. T., Saelzler, M. P., Orth, K., Dixon, J. E., and Rosner, M. R. (2001) ERK7 is an autoactivated member of the MAPK family. *J Biol Chem* **276**, 21272–9

219. Cole, A., Frame, S., and Cohen, P. (2004) Further evidence that the tyrosine phosphorylation of glycogen synthase kinase-3 (GSK3) in mammalian cells is an autophosphorylation event. *Biochem J* **377**, 249–55

220. Lochhead, P. A., Sibbet, G., Morrice, N., and Cleghon, V. (2005) Activation-loop autophosphorylation is mediated by a novel transitional intermediate form of DYRKs. *Cell* **121**, 925–36

9 APPENDIX

LIST OF ABBREVIATIONS

^{32}P	Phosphorus-32
2D	two-dimensional
3D	three-dimensional
°C	degree(s) Celsius
%	percent
∞	infinite
$(NH_4)_2SO_4$	ammonium sulfate
α	anti or alpha
Å	Ångström
aa	amino acid
ADP	adenosine diphosphate
Ala (A)	alanine
APS	ammonium peroxydisulfate
Arg (R)	arginine
AS-ODN	antisense oligonucleotide
Asp (D)	aspartic acid
ATP	adenosine triphosphate
β	beta
bp	base pair(s)
BSA	bovine serum albumin
γ	gamma
C-lobe, C-terminal	carboxy-lobe, carboxy-terminal
C-TAK1	Cdc25C-associated kinase 1
Cα-atom	backbone (carbon) atom
CA1, 2, 3, 4, and 5	conserved area 1, 2, 3, 4, and 5
$CaCl_2$	calcium chloride
CIAP	calf intestine alkaline phosphatase
CK2	casein kinase 2
cm	centimeter
CO_2	carbon dioxide
$γPO_4$	gamma-phosphate
CR1, 2, and 3	conserved region 1, 2, and 3
CRD	cysteine-rich domain
CSYLAPE	cysteine-serine-tyrosine-leucine-alanine-proline-glutamic acid
Cys (C)	cysteine
ddH_2O	double distilled water
DEF motif	docking site for ERK, FxFP motif
DFG motif	aspartate-phenylalanine-glycine motif
DMEM	Dulbecco's modified eagle medium
DMSO	dimethyl sulfoxide
DNA	deoxyribonucleic acid
dNTP	deoxyribonucleoside triphosphate

DPBS	Dulbecco's phosphate-buffered saline
DTT	dithiothreitol
e.g.	*exempli gratia* ("for example")
ECL	enhanced chemiluminescence
EDTA	ethylenediaminetetraacetic acid-disodium salt
EGF	epidermal growth factor
EGFR	EGF receptor
ER	endoplasmic reticulum
ERK	extracellular signal-regulated protein kinase
et al.	*et alii* ("and others")
ζ	zeta
F	farad
FACS	fluorescence-activated cell sorting
FBS	fetal bovine serum
FGF	fibroblast growth factor
FGFR1	FGF receptor 1
Fig.	figure
for	forward
FTI	cytosolic farnesyltransferase inhibitor
FxFP motif	phenylalanine-(variable amino acid)-phenylalanine-proline motif
g	gram or gravity
GDP	guanosine diphosphate
GFP	green fluorescent protein
GGTaseI	geranylgeranyltransferase I
Gln (Q)	glutamine
Glu (E)	glutamic acid
Gly (G)	glycine
Grb2	growth-factor-receptor-binding protein 2
GST	glutathione S-transferase
GTP	guanosine-5'-triphosphate
h	hour(s) or human
H_2O	water, hydrate
HBS	HEPES-buffered saline
HCl	hydrochloride
HEK 293T	human embryonic kidney 293T
HEPES	4-(2-hydroxyethyl)-1-piperazineethanesulfonic acid
His (H)	histidine
HRD motif	histidine-arginine-aspartic acid motif
HSP90, 70, and 68	heat-shock protein 90, 70, and 68
HVR	hypervariable region
IB	immunoblot
IMP	impedes mitogenic signal propagation
IRES	internal ribosome entry site
ITAM	immunoreceptor tyrosine-based activation motif
k	kilo

K	potassium
kb	kilobase
KCl	potassium chloride
KD	kinase domain
KDEL	lysine-aspartic acid-glutamic acid-leucine
KH_2PO_4	monopotassium phosphate
KSR	kinase suppressor of RAS
KSR1$^{-/-}$	KSR1-deficient
λ	lambda
l	liter
LB	Luria-Bertani
LC-MS	liquid chromatography-mass spectrometry
LCK	lymphocyte-specific protein tyrosine kinase
Lys (K)	lysine
μ	micro
m	milli or meter or murine/mouse
M	molar
M2PK	pyruvate kinase isoenzyme type M2
MAP2K	MAPK kinase
MAP3K	MAPK kinase kinase
MAPK	mitogen-activated protein kinase
MD	molecular dynamics
MEF	mouse embryonic fibroblast
MEK	mitogen-activated protein/ERK kinase
MEM	minimum essential medium
Met (M)	methionine
Mg, Mg^{2+}	magnesium (ion)
$MgCl_2$	magnesium chloride
$MgSO_4$	magnesium sulfate
MHC	major histocompatibility complex
min	minute(s)
mRNA	messenger ribonucleic acid
MS	mass spectrometry
MSZ	Institut für Medizinische Strahlenkunde und Zellforschung (Institute for Medical Radiation and Cell Research)
n	nano
N-lobe, N-terminal	amino-lobe, amino-terminal
Na_2HPO_4	disodium phosphate
Na_3VO_4	sodium orthovanadate
$Na_4P_2O_7$	sodium pyrophosphate
NaCl	sodium chloride
NaF	sodium fluoride
NaOH	sodium hydroxide
NCBI	National Center for Biotechnology Information
NEAA	non-essential amino acids

NP-40	Nonidet P-40
OD	optical density
π	pi
p	pico or phospho
P value	significance
PARP	poly ADP ribose polymerase
PBS	phosphate-buffered saline
PCR	polymerase chain reaction
PD	GST pull-down
PDT	population doubling time
PEI	polyethylenimine
Phe (F)	phenylalanine
PP2A	protein phosphatase 2A
Pro (P)	proline
PVDF	polyvinylidene fluoride
r	rabbit
r.m.s.	root-mean-square
RAF (isoforms A, B, C, and D)	(A-, B-, C-, and *Drosophila*-) rapidly growing fibrosarcoma
RAS	rat sarcoma
RBD	RAS-binding domain
rev	reverse
rpm	rotations per minute
RSK	ribosomal S6 kinase
RTK	receptor tyrosine kinase
SD	standard deviation
SDS	sodium dodecyl sulfate
SDS-PAGE	SDS polyacrylamide gel electrophoresis
sec, s	second(s)
Ser (S)	serine
SFK	Src family kinase
SH1, 2, 3, and 4	Src homology 1, 2, 3, and 4
SOS	son of sevenless
Src (c-Src)	sarcoma (cellular Src)
TBE	Tris-borate-EDTA
TBS	Tris-buffered saline
TBST	Tween 20-containing TBS
TCR	T cell receptor
TEMED	N,N,N',N'-Tetramethylethylenediamine
Thr (T)	threonine
T_m	melting temperature
TNF(-α)	tumor necrosis factor (alpha)
Tris	Tris-(hydroxymethyl)-aminomethane, Trometamol
Trp (W)	tryptophan
Tyr (Y)	tyrosine
UV/Vis	ultraviolet visible

v	viral
V	volt
v/v	volume/volume
VAIK motif	valine-alanine-isoleucine-lysine motif
Val (V)	valine
W	watt
w/v	weight/volume
WT	wild type
ψ	Psi
Y728-OH	non-phosphorylated Tyr728
Y728-PO$_4$	phosphorylated Tyr728

ACKNOWLEDGEMENTS

CURRICULUM VITAE

PERSONAL DETAILS

Name	**Claudia Sibilski**
Date and place of birth	August 2nd, 1984 in Rudolstadt
Nationality	German

ACADEMIC AND SCHOOL EDUCATION

Desired qualification	**Dr. rer. nat.**
Educational institution	Department of Microbiology Julius Maximilians University of Würzburg, Germany
Specification	Biology (with the focus on protein biochemistry)
Period of time	2009 – present time
Qualification	**Diploma in Biology Univ.**
Educational institution	Julius Maximilians University of Würzburg, Germany
Specification	Biochemistry (major), cell and developmental biology (minor), microbiology (minor)
Period of time	2003 – 2009
Diploma thesis	*Mechanism of oncogene addiction in B-RAF-V600E-transformed cells*
Educational institution	Institute for Medical Radiation and Cell Research Julius Maximilians University of Würzburg, Germany
Specification	Protein biochemistry
Period of time	2008 – 2009
Qualification	**A-Level**
Educational institution	Friedrich Fröbel Gymnasium of Bad Blankenburg and Staatliche Grundschule of Schwarza, Germany
Specification	Mathematics, biology
Period of time	1991 – 2003

LIST OF PUBLICATIONS

Sibilski, C., Müller, T., Kollipara, L., Zahedi, R. P., Rapp, U. R., Rudel, T., and Baljuls, A. (2013) Tyr728 in the Kinase Domain of the Murine Kinase Suppressor of RAS 1 regulates Binding and Activation of the Mitogen-activated Protein Kinase Kinase. *J Biol Chem* 288, 35237–52

Sibilski, C., Zahedi, R. P., Müller, T., Sickmann, A., Rapp, U. R., and Baljuls, A. (2011) LCK-induced tyrosine phosphorylation of KSR stabilizes its structure leading to altered MEK activation. *Poster presentation during the international symposium of SFB487*

Fischer, A., Baljuls, A., Reinders, J., Nekhoroshkova, E., **Sibilski, C.**, Metz, R., Albert, S., Rajalingam, K., Hekman, M., and Rapp, U. R. (2009) Regulation of RAF Activity by 14-3-3 Proteins: RAF kinases associate functionally with both homo- and heterodimeric forms of 14-3-3 proteins. *J Biol Chem* 284, 3183–94

_____   _____
Place, date   Signature (Claudia Sibilski)

EIDESSTATTLICHE ERKLÄRUNG

gemäß der Promotionsordnung der Fakultät für Biologie
(Julius-Maximilians-Universität Würzburg)

Hiermit erkläre ich ehrenwörtlich, dass ich die vorliegende Dissertation eigenständig, d.h. selbstständig und ohne Hilfe einer kommerziellen Promotionsberatung, angefertigt und keine anderen als die angegebenen Quellen oder Hilfsmittel benutzt habe.

Weiterhin versichere ich, dass ich die Gelegenheit zum Promotionsvorhaben nicht kommerziell vermittelt bekommen und insbesondere nicht eine Person oder Organisation eingeschaltet habe, welche gegen Entgelt Betreuer bzw. Betreuerinnen für die Anfertigung von Dissertation sucht.

Außerdem habe ich die Regeln der Universität Würzburg über gute wissenschaftliche Praxis eingehalten.

Ich erkläre, dass diese Dissertation noch in keinem anderen Prüfungsverfahren in gleicher oder ähnlicher Form vorgelegen hat.

Ebenfalls habe ich keine weiteren akademischen Grade erworben oder versucht zu erwerben, außer den mit dem Zulassungsgesuch urkundlich vorgelegten Graden.

_____   _____
Ort, Datum   Unterschrift (Claudia Sibilski)